UNIVERSIDADE FEDERAL DE SÃO CARLOS
CENTRO DE CIÊNCIAS EXATAS E TECNOLOGIA
PROGRAMA DE PÓS-GRADUAÇÃO EM ENGENHARIA QUÍMICA

Letícia Pereira Almeida

APLICAÇÃO DO ARRASTE GASOSO ASSOCIADO AO VÁCUO EM FERMENTAÇÕES EXTRATIVAS UTILIZANDO MATÉRIAS-PRIMAS SACARINA E AMILÁCEA

SÃO CARLOS – SP

2025

UNIVERSIDADE FEDERAL DE SÃO CARLOS
CENTRO DE CIÊNCIAS EXATAS E TECNOLOGIA
PROGRAMA DE PÓS-GRADUAÇÃO EM ENGENHARIA QUÍMICA

APLICAÇÃO DO ARRASTE GASOSO ASSOCIADO AO VÁCUO EM FERMENTAÇÕES EXTRATIVAS UTILIZANDO MATÉRIAS-PRIMAS SACARINA E AMILÁCEA

Letícia Pereira Almeida

Tese apresentada como parte dos requisitos para obtenção do título de Doutora em Engenharia Química, área de concentração em Pesquisa e Desenvolvimento de processos Químicos.

Orientador: Prof. Dr. Alberto Colli Badino Junior
Coorientador: Prof. Dr. Mateus Nordi Esperança

SÃO CARLOS – SP

2025

FEDERAL UNIVERSITY OF SÃO CARLOS
CENTER FOR EXACT SCIENCES AND TECHNOLOGY
GRADUATE PROGRAM IN CHEMICAL ENGINEERING

APPLICATION OF VACUUM-ASSISTED GAS STRIPPING IN EXTRACTIVE FERMENTATIONS USING SACCHARINE AND STARCHY FEEDSTOCKS

Letícia Pereira Almeida

Thesis presented as part of the requirements to obtain Ph.D degree in Chemical Engineering, concentration area: Research and Development of Chemical Processes.

Advisor: Prof. Dr. Alberto Colli Badino Junior
Co-advisor: Prof. Dr. Mateus Nordi Esperança

SÃO CARLOS – SP

2025

UNIVERSIDADE FEDERAL DE SÃO CARLOS

Centro de Ciências Exatas e de Tecnologia
Programa de Pós-Graduação em Engenharia Química

Folha de Aprovação

Defesa de Tese de Doutorado da candidata Letícia Pereira Almeida, realizada em 29/07/2025.

Comissão Julgadora:

Prof. Dr. Alberto Colli Badino Junior (UFSCar)

Prof. Dr. Antonio Jose Gonçalves da Cruz (UFSCar)

Prof. Dr. Diego Andrade Lemos (UFSCar)

Prof. Dr. Jorge Luiz Silveira Sonego (UFPE)

Profa. Dra. Mariane Molina Buffo (SENAI)

O Relatório de Defesa assinado pelos membros da Comissão Julgadora encontra-se arquivado junto ao Programa de Pós-Graduação em Engenharia Química.

DEDICATÓRIA

Aos meus pais, Antônio e Lúcia, e
ao meu esposo, Izaque.

AGRADECIMENTOS

Agradeço, primeiramente a Deus, a vida e por sua presença constante ao longo da minha jornada.

Ao meu esposo, Izaque, por todo o amor, companheirismo, pela paciência e apoio incondicional ao longo de todos esses anos, você foi imprescindível para a conclusão deste ciclo.

À minha família, principalmente aos meus pais, Lúcia e Antônio, e aos meus irmãos, Larissa e Vinícius, por todo amor e apoio constante ao longo da minha vida.

Aos meus orientadores, professores Alberto e Mateus, por todo conhecimento, incentivo, paciência e confiança dessa jornada que foi o doutorado.

À minha avó Fátima, meu avô Odenil e à minha tia Lucila, por sempre acreditarem e torcerem por mim. Obrigada, vó, por sempre me colocar em suas orações.

Ao professor Mark e à Kansas State University, pelo suporte e pela infraestrutura que tornaram possível a realização da minha experiência de intercâmbio.

Aos colegas e amigos de laboratório, pela amizade, apoio, cafés e ótimos momentos compartilhados, em especial Mariane, Natalia, Marina, Rauber, Ivan e Brenda.

Aos meus alunos de Iniciação Científica, Matheus, Rebeca e Giancarlo, pela dedicação e pelos trabalhos realizados, que tanto contribuíram para meu crescimento como líder e orientadora.

Aos membros da banca examinadora, por aceitarem meu convite e pela generosidade em dedicar seu tempo e conhecimento para enriquecer este trabalho.

Aos técnicos Natália, Thais, Eudoro e Oscar, pelo suporte e ajuda cedida no desenvolvimento deste trabalho.

Agradeço ao Programa de Pós-Graduação em Engenharia Química da UFSCar, pela oportunidade e infraestrutura para realização deste trabalho.

Muito obrigada!

APOIO FINANCEIRO

O presente trabalho foi realizado com apoio da Coordenação de Aperfeiçoamento de Pessoal deNível Superior - Brasil (CAPES) - Código de Financiamento 001, da Agência Nacional do Petróleo, Gás Natural e Biocombustíveis (ANP), da Fundação de Amparo à Pesquisa do Estado de São Paulo (FAPESP, Projeto nº 2024/10494-5) e do Ministério da Ciência, Tecnologia e Inovação (MCTI), por meio da bolsa de doutorado concedida pelo programa PRH 39.1 DEQ/UFSCar.

“A verdadeira viagem de descobrimento não consiste em procurar novas paisagens, mas em ter novos olhos”.

Marcel Proust

RESUMO

Apesar de consolidada industrialmente, a fermentação alcoólica possui como limitação o efeito tóxico do etanol na levedura, levando a obtenção de vinhos com baixo teor alcoólico (10–15% v v^{-1}). Técnicas de remoção de etanol podem ser empregadas para mitigar o efeito inibitório desse produto e aumentar a produtividade do processo. Nesse sentido, o presente trabalho avaliou a fermentação alcoólica extrativa utilizando o arraste gasoso associado ao vácuo. Inicialmente, investigou-se a remoção de etanol de soluções hidroalcoólicas em diferentes configurações operacionais de vazão específica de CO_2, temperatura e pressão, com o objetivo de identificar aquela que proporcionaria a maior remoção de etanol da fase líquida, bem como a maior concentração na fase gasosa. Em seguida, fermentações extrativas utilizando matéria-prima sacarina foram avaliadas através das técnicas de arraste gasoso convencional e associado ao vácuo, bem como a análise energética de ambos os processos. Por fim, foram conduzidas fermentações extrativas utilizando matéria-prima amilácea, avaliando os processos de hidrólise e fermentação separada (HFS) e sacarificação e fermentação simultânea (SFS). Foram desenvolvidos modelos para descrever os processos, baseando-se nas equações de balanço de massa e cinéticas das etapas de hidrólise, fermentação e remoção de etanol e água. Os resultados da remoção de etanol em soluções hidroalcoólicas mostraram que todas as três variáveis operacionais apresentaram efeito significativo dentro da faixa experimental avaliada. A aplicação da técnica promoveu a concentração do etanol na fase gasosa em até 6 vezes. Nas fermentações extrativas a partir de fonte sacarina, observou-se que tanto o arraste gasoso associado ao vácuo quanto o arraste gasoso convencional aumentaram em até 14,3% a produtividade em etanol. A análise energética indicou que a técnica integrada reduziu em 31,3% a energia requerida em comparação ao arraste gasoso convencional. Por fim, a fermentação extrativa de matéria-prima amilácea aumentou a produtividade em etanol em até 60% em relação à fermentação convencional. A modelagem matemática descreveu adequadamente o processo fermentativo. O arraste gasoso associado ao vácuo demonstrou ser uma técnica promissora, com potencial para melhorar a produtividade em etanol e reduzir os custos nas etapas de recuperação e concentração do etanol removido.

Palavras-chaves: etanol, hidrólise e fermentação simultâneas, fermentação extrativa, arraste gasoso, vácuo, integração de processos.

ABSTRACT

Despite being well-established industrially, ethanol fermentation is limited by the toxic effect of ethanol on yeast, resulting in wines with low alcohol content (10–15% v v^{-1}). Ethanol removal techniques can be applied to mitigate the inhibitory effect of the product and increase process productivity. In this context, the present work evaluated extractive ethanol fermentation using vacuum-assisted gas stripping. Initially, ethanol removal from hydroalcoholic solutions was investigated under different operational configurations of CO_2 specific flow rate, temperature, and pressure, with the aim of identifying the conditions that provided the highest ethanol removal from the liquid phase and the highest concentration in the gas phase. Subsequently, extractive fermentations with saccharine feedstock were assessed using both conventional and vacuum-assisted gas stripping, and the energy requirements of both processes were analyzed. Finally, extractive fermentations with starchy feedstock were conducted in separate hydrolysis and fermentation (SHF) and simultaneous saccharification and fermentation (SSF) processes. Mathematical models were developed to describe the processes, based on mass balance equations and incorporating the kinetics of hydrolysis, fermentation, and ethanol and water removal. The results of ethanol removal from hydroalcoholic solutions showed that all three operational variables significantly affected the process within the evaluated experimental range. The application of the technique increased the ethanol concentration in the gas phase by up to six times. In extractive fermentations with saccharine feedstock, both vacuum-assisted and conventional gas stripping increased ethanol productivity by up to 14.3%. The energy analysis indicated that the integrated technique reduced energy demand by 31.3% compared to conventional gas stripping. Finally, extractive fermentation of starchy feedstock increased ethanol productivity by 60% compared to conventional fermentation. The mathematical model adequately described the fermentation process. Vacuum-assisted gas stripping demonstrated potential as a promising technique, with the capacity to enhance ethanol productivity and lower the costs associated with the recovery and concentration of the removed ethanol.

Keywords: ethanol, simultaneous hydrolysis and fermentation, extractive fermentation, gas stripping, vacuum, process integration.

LIST OF FIGURES

LIST OF TABLES

SUMMARY

CHAPTER 1

1. INTRODUCTION

In recent decades, rising fossil fuel consumption and the resulting greenhouse gas (GHG) emissions have caused severe environmental degradation, public health issues, and accelerated global warming. By 2024, energy-related CO_2 emissions reached a record 37.6 Gt, pushing atmospheric CO_2 concentrations to unprecedented levels. The transportation sector alone accounts for over 28% of global energy consumption, emitting roughly 8 Gt of CO_2 annually, equivalent to 15% of total GHG emissions (International Energy Agency, 2024).

Petroleum-based liquid fuels currently supply 95% of the transportation sector's energy demand, with global consumption exceeding 4.8 billion gallons of diesel and gasoline per day (Khan et al., 2023). Transitioning to bio-based alternatives, such as biodiesel and, more prominently, bioethanol, could significantly curb GHG emissions. Ethanol, the world's most widely adopted liquid biofuel, is used both in low-emission gasoline blends (compatible with conventional engines) and as pure ethanol (E100). The latter is especially prevalent in markets like Brazil, where ethanol infrastructure is well-established (Ghazali and Mustafa, 2025; Shekhar et al., 2025).

Bioethanol is produced via sugar fermentation and categorized into three generations based on feedstock: first-generation (1G, conventional crops), second-generation (2G, lignocellulosic biomass), and third-generation (3G, algae). Among these, 1G ethanol dominates global production due to its mature technology, lower processing costs, and widespread availability of food-based feedstocks like sugarcane, corn, sorghum, and wheat (Agarwal and Kumar, 2018; Naik et al., 2010). Despite being a well-established process, ethanol fermentation faces a critical limitation: the inhibitory effect of ethanol on yeast cells restricts final concentrations to 10–15% v v^{-1}. This not only reduces productivity but also escalates energy demands during recovery, as distillation requires up to 2.5 kg of steam per liter of ethanol (Ensinas et al., 2007; Fan et al., 2019; Maiorella et al., 1983).

Addressing these challenges, substantial research efforts focused on developing strategies to overcome ethanol inhibition. Biological approaches have shown particular promise, including evolutionary adaptation techniques that employ selective pressure to develop ethanol-tolerant yeast strains (Mavrommati et al., 2023; Yang and Tavazoie, 2020), and advanced genetic engineering methods that modify key metabolic pathways to enhance ethanol

tolerance(Alper et al., 2006; Varize et al., 2022; Wan et al., 2024). Process-based approaches have also been explored, including lowering the fermentation temperature (Deed et al., 2015; Veloso et al., 2019) and removing ethanol from the broth while it is being produced using extractive techniques such as liquid–liquid extraction, pervaporation, vacuum, and gas stripping (Fan et al., 2016; Lemos et al., 2020; Pereira et al., 2024; Rodrigues et al., 2018; Sonego et al., 2018). Among these approaches, vacuum and gas stripping have gained significant attention as promising technologies due to their operational simplicity and high selectivity for volatile compounds.

Vacuum extractive fermentation has been extensively studied as an innovative approach to alleviate ethanol inhibition in *S. cerevisiae* fermentations, and achieve complete sugar conversion in high-solids (>30% w w^{-1}) fermentation systems (Huang et al., 2015; Kumar et al., 2018; Shihadeh et al., 2014). In these studies, the intermittent or continuous application of vacuum, typically at absolute pressures around 6–7 kPa, maintained the ethanol concentration in the broth below critical inhibition levels, resulting in lower residual glucose concentrations and improved ethanol productivity compared to conventional fermentation (Kumar et al., 2018; Nguyen et al., 2009). Despite these advantages, the substantial energy requirements for maintaining vacuum conditions, particularly in industrial-scale fermenters, pose a major challenge to the economic viability of this technique (Tavares et al., 2019). Energy demands scale non-linearly with reactor volume, with vacuum systems accounting for 40-60% of total process energy consumption in pilot-scale studies.

Regarding gas stripping, both experimental and modeling studies have explored this extractive fermentation strategy to increase substrate concentration in the feed (180–300 g L^{-1}) and achieve higher ethanol levels (up to 17.2 v v^{-1}) (Rodrigues et al., 2018; Sonego et al., 2018). The technique has been evaluated under different conditions of temperature, CO_2 flow rate, and initial ethanol concentration (Martins et al., 2020; Silva et al., 2015; Sonego et al., 2014). In addition to improving ethanol productivity, gas stripping has also been shown to lower broth temperature and reduce cooling water consumption, contributing to process sustainability (Almeida et al., 2021; Campos et al., 2025; Silva et al., 2015). Despite its potential, gas stripping faces technical and economic challenges, particularly in terms of scaling up the process. As highlighted by Sonego et al. (2014), a specific flow rate of 2.5 vvm is necessary to achieve optimal ethanol removal rate, which presents a significant obstacle to industrial application.

In this context, exploring different configurations and techniques for ethanol removal is considered a promising approach to enhance the efficiency of established processes (Andlar et

al., 2018; Si et al., 2018). While the advantages of vacuum and gas stripping have been reported separately, their integration for removing ethanol from fermentation broths remains underexplored, particularly concerning process optimization. Therefore, this thesis explores the potential application of vacuum-assisted gas stripping as a strategy for in situ ethanol removal during extractive fermentations using saccharine and starchy feedstocks.

1.1. Goals

This thesis aimed to investigate the use of vacuum-assisted gas stripping for *in situ* ethanol removal during extractive fermentations. To achieve the proposed goal, the following specific goals were established:

- ✓ To evaluate the effects of operational variables, including temperature, specific CO_2 flow rate, and pressure, on ethanol removal efficiency via vacuum-assisted gas stripping;
- ✓ To compare ethanol removal performance based on power input and energy requirements;
- ✓ To characterize the gas phase composition during ethanol removal from both ethanol solutions and fermentation broth using mid-infrared spectroscopy;
- ✓ To assess the application of vacuum-assisted gas stripping in extractive fermentations of both saccharine and starchy feedstocks;
- ✓ To develop and validate models of ethanol production from sorghum in both extractive separate hydrolysis and fermentation (ESHF) and extractive simultaneous saccharification and fermentation (ESSF) processes.

1.2. Chapter overview

To outline the steps taken to accomplish the objectives of this thesis, the work is structured into six chapters. A brief description of each chapter is provided below:

Chapter 2. *Theoretical basis and state of the art*. This chapter outlines the key theoretical concepts that support the relevance and development of the research. It also provides an overview of existing studies on the ethanol extractive fermentations.

Chapter 3. *Ethanol removal by vacuum-assisted gas stripping: Influence of operating conditions*. This chapter investigates the effects of key operating parameters - temperature, CO_2

flow rate, and system pressure - on ethanol removal efficiency using vacuum-assisted gas stripping. The research presented in this chapter was published in 2024 in "Chemical Engineering and Processing - Process Intensification" journal.

Chapter 4. *Extractive ethanol fermentation using vacuum-assisted gas stripping: gas-phase monitoring*. This chapter examines extractive fermentations using a saccharine feedstock, employing both conventional and vacuum-assisted gas stripping, with gas-phase ethanol monitoring via mid-infrared spectroscopy.

Chapter 5. *Bioethanol production from sorghum via extractive fermentation with vacuum-assisted gas stripping: Experimental and modeling*. This chapter presents the development and validation of mathematical models describing ethanol production in both separate hydrolysis and fermentation (SHF) and simultaneous saccharification and fermentation (SSF) processes integrated with vacuum-assisted gas stripping for ethanol removal. The research presented in this chapter is currently under review in "Renewable Energy" journal.

Chapter 6. *Final considerations and future perspectives.* This chapter presents the main conclusions of this thesis and suggestions for future work.

CHAPTER 2

2. THEORETICAL BASIS AND STATE OF THE ART

2.1. Ethanol and biofuels

Biofuels have emerged as a promising alternative to fossil fuels, primarily due to their potential to reduce greenhouse gas (GHG) emissions (Khanna et al., 2011). Among them, ethanol is the most widely used liquid biofuel for transportation, either as a standalone fuel or as a gasoline additive to enhance octane ratings (Prasad et al., 2007). Global ethanol production has grown substantially in recent decades. Brazil is the world's second-largest bioethanol producer, accounting for 28% of global output (118 billion liters) in the 2024 harvest (Renewable Fuels Association, 2024). Figure 2.1 illustrates the evolution of global ethanol production since 2010 and the historical production in Brazil.

Figure 2.1 – Evolution of ethanol production presented as (a) global trends since 2010 and (b) historical data for Brazil.

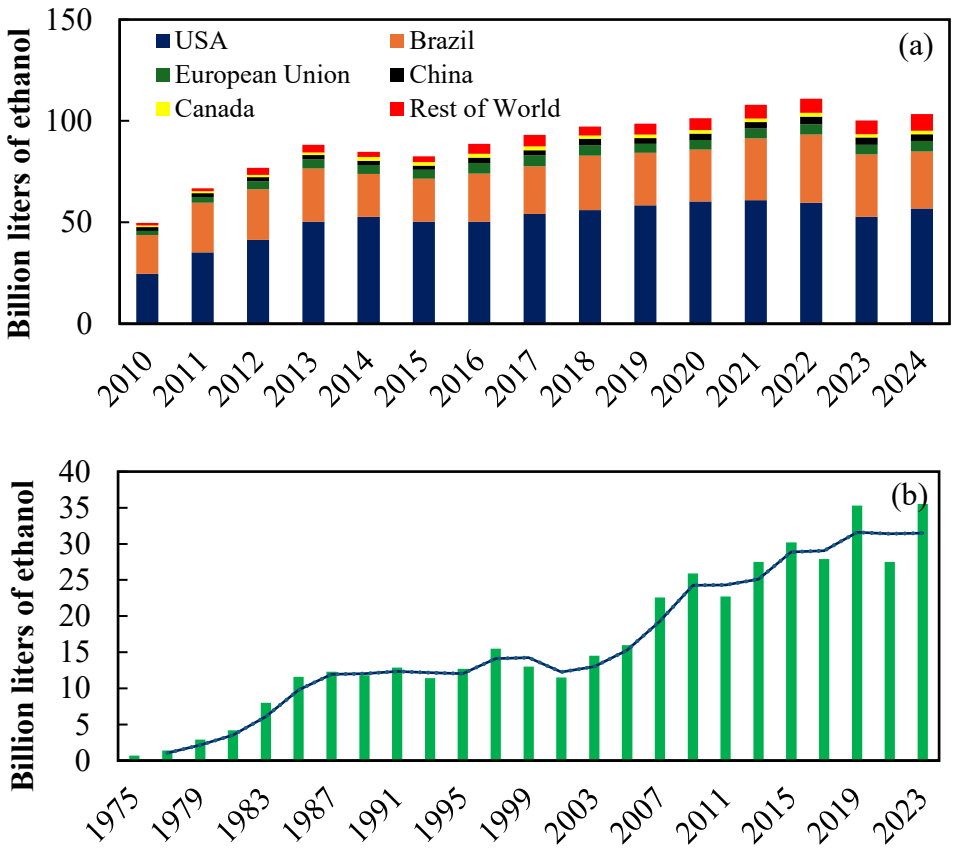

Source: Author's personal archive based on data from the Brazilian National Agency of Petroleum, Natural Gas and Biofuels (ANP, 2021) and U.S. Department of Energy (2024).

Ethanol is produced via sugar fermentation utilizing feedstocks such as corn, sugarcane, wheat, sorghum, and sugar beets, as well as cellulosic materials and algal biomass. The complexity of ethanol production (Figure 2.2) varies significantly depending on the feedstock, ranging from straightforward sugar fermentation to multi-stage biomass conversion processes (Sánchez and Cardona, 2008). Based on the type of feedstock used, ethanol is classified into three generations. The most prevalent form is first-generation (1G) ethanol, which is produced by fermenting sugar- or starch-based crops using conventional yeast strains (Joyia et al., 2024).

Figure 2.2 – Schematic representation of the production routes for first-, second-, and third-generation ethanol.

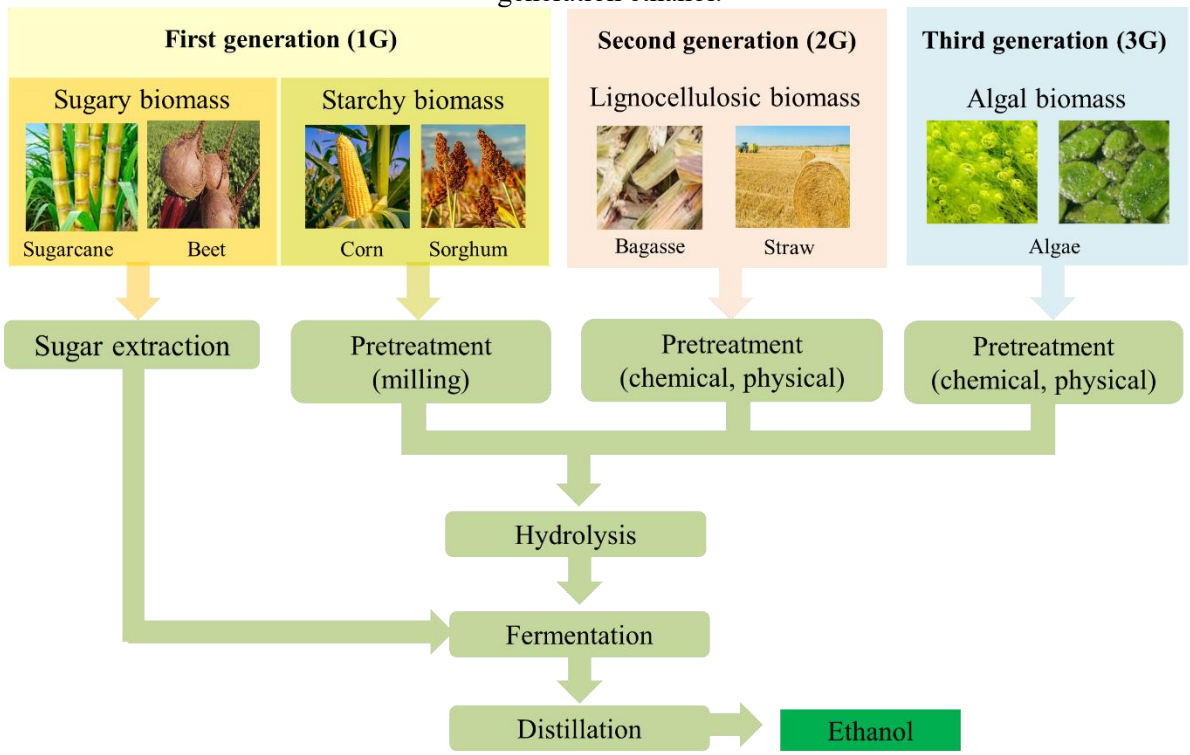

Source: Author's personal archive

2.2. Ethanol production processes

2.2.1. Ethanol production process from sugarcane

In Brazil, sugarcane serves as the primary feedstock for ethanol production, accounting for 87% of the total output during the 2024/2025 harvest (CONAB, 2025). The production process begins with harvested sugarcane undergoing washing, cutting, and milling, yielding sugarcane juice (for fermentation) and bagasse (a lignocellulosic byproduct). Most Brazilian distilleries operate as annexed units to sugar mills, creating integrated facilities capable of co-

producing sugar and ethanol. This model represents approximately 70% of industrial plants, while the remaining 30% are autonomous distilleries dedicated solely to ethanol production (Basso et al., 2011).

In integrated facilities, the molasses produced during sugar crystallization is diluted with either sugarcane juice or water to adjust the total reducing sugars (TRS) concentration in the fermentation mash to optimal levels. In contrast, autonomous distilleries heat the sugarcane juice to reduce bacterial contamination, followed by decantation and, in most cases, evaporative concentration before fermentation. Beyond sugar and ethanol, the sugarcane industry has expanded its product portfolio to include electricity cogenerated from sugarcane bagasse (Wheals et al., 1999).

In Brazil, sugarcane-based ethanol plants predominantly utilize the Melle-Boinot process, a fed-batch fermentation system with cell recycling (Figure 2.3). The process employs three to four tanks in parallel fermentation, operated with staggered feeding times. Initiation involves inoculating the tank with yeast suspension, comprising approximately 30% yeast cells (wet basis) and 25 to 30% of the total fermentation volume. The fermentation must (18 to 22% w w^{-1} TRS) is fed gradually over 4 to 6 hours into three or four parallel tanks operating with staggered initiation times. During this feeding phase, sucrose undergoes rapid enzymatic hydrolysis via yeast-derived invertase (β-fructofuranosidase, EC 3.2.1.26), cleaving each sucrose molecule into equimolar amounts of glucose and fructose. These TRS (Total Reducing Sugars) are then fermented, yielding ethanol and carbon dioxide (CO_2). The fermentation proceeds until complete sugar depletion, typically within 6-10 hours, achieving ethanol concentrations of 8-12% (v v^{-1}). Throughout the process, the temperature is monitored and maintained below 35 °C (Basso et al., 2011; Pereira et al., 2018).

At the end of fermentation, centrifugation separates the yeast cream from the wine. The yeast cream is acid-treated with sulfuric acid and recycled into subsequent fermentation cycles (Pereira et al., 2018). The clarified wine is then distilled, yielding hydrous ethanol with a concentration of approximately 95.6% (v v^{-1}). This concentration corresponds to the ethanol–water azeotrope, which cannot be separated further by conventional distillation. To produce anhydrous ethanol, additional dehydration steps are required, as heterogeneous azeotropic distillation (using solvents like cyclohexane), extractive distillation (with monoethylene glycol), or adsorption on molecular sieves (Dias et al., 2015; Gil et al., 2012).

Figure 2.3 – Block-flow diagram of sugarcane-based bioethanol production.

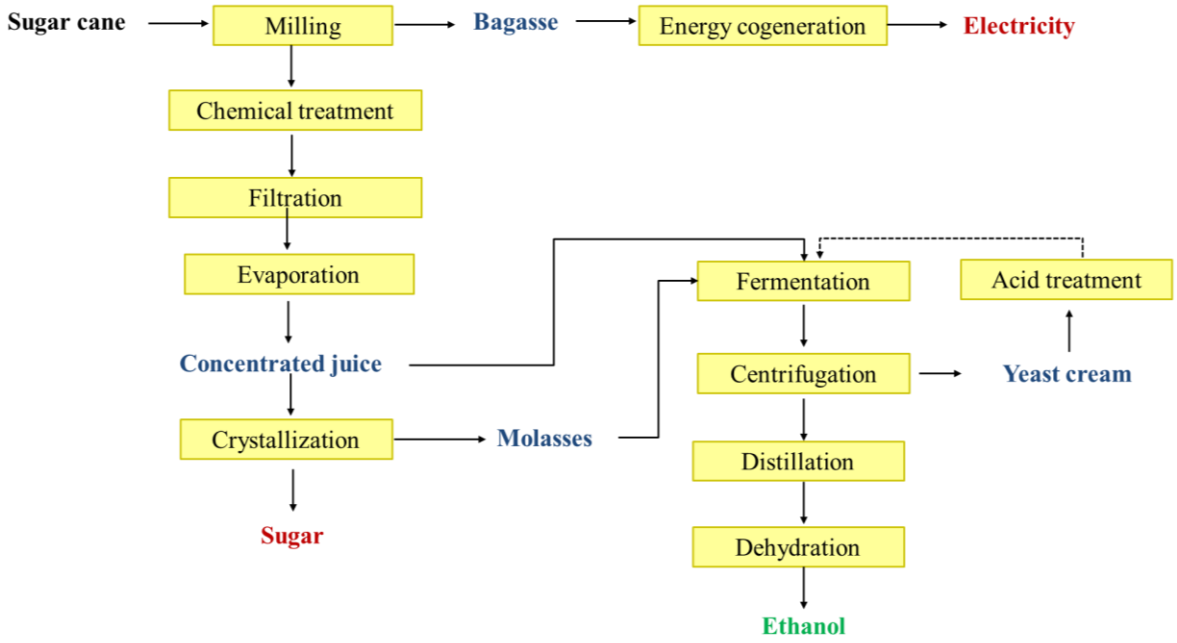

Source: Author's personal archive

2.2.2. Ethanol production process from starchy biomass

The following section focuses on corn ethanol production via dry milling - a method analogous to that used for grain sorghum. Corn processing typically employs two distinct approaches: dry milling and wet milling. The key distinction between these methods lies in their resource allocation: dry milling prioritizes simplicity and cost-effectiveness, whereas wet milling maximizes byproduct valorization.

Although wet milling generates multiple profitable co-products (e.g., corn oil, protein feed), its adoption is limited by higher capital/operating costs, driven largely by elevated energy demands compared to dry milling. In dry milling plants, the primary objective is to maximize capital return per liter of ethanol produced. In contrast, wet milling facilities enable separation of high-value grain components (e.g., germ, fiber, gluten) prior to fermentation (Bothast and Schlicher, 2005).

Ethanol production via dry milling consists of five stages: grinding, cooking, liquefaction, saccharification, and fermentation. This process generates a co-product known as distillers' dried grains with solubles (DDGS), which is used as animal feed (Sánchez and Cardona, 2008). In the dry milling process for ethanol production, whole grain kernels are mechanically reduced to coarse flour through hammer milling.

This flour is mixed with water to form a mash containing 25-32% solids (Bothast and Schlicher, 2005). Prior to thermal treatment, the corn mash pH is adjusted to optimize α-amylase activity. Next, the mash is heated to a high temperature of 80–85 °C, followed by high-pressure cooking in a jet cooker at temperatures ranging from 104 to 107 °C (Kwiatkowski et al., 2006). The resulting mixture, called mash, contains gelatinized starch. To break down this starch into short-chain saccharides (dextrins), the mash undergoes liquefaction using α-amylase enzymes. This step not only produces dextrins but also reduces viscosity - critical for efficient mixing and pumping in subsequent processing stages. Some facilities avoid steam injection, opting instead for extended liquefaction at 85 °C (Kumar and Singh, 2019).

The next step, saccharification, involves converting dextrins into glucose through the enzymatic action of glucoamylase. During this stage, the long-chain dextrins, produced in liquefaction, are hydrolyzed into fermentable sugars. The resulting glucose is then fermented into ethanol by yeast, either in separate steps (Separate Hydrolysis and Fermentation, or SHF) or simultaneously with saccharification (Simultaneous Saccharification and Fermentation, or SSF). Fermentation typically runs for 48 to 72 hours, yielding a final ethanol concentration of 14–20% v v^{-1}. The SSF process is the most widely applied at the industrial scale due to its advantages, as it reduces the risk of microbial contamination, lowers the initial osmotic stress on the yeast by avoiding a highly concentrated glucose solution, and is generally more energy-efficient. After fermentation, ethanol is concentrated through a combination of distillation and dehydration processes. The residual solids from distillation are dried to produce distillers' dried grains with solubles (DDGS), valuable animal feed supplement (Bothast and Schlicher, 2005; Kumar and Singh, 2019). The complete process flow is presented schematically in Figure 2.4.

Figure 2.4 – Block-flow diagram of the starchy biomass-to-bioethanol production process.

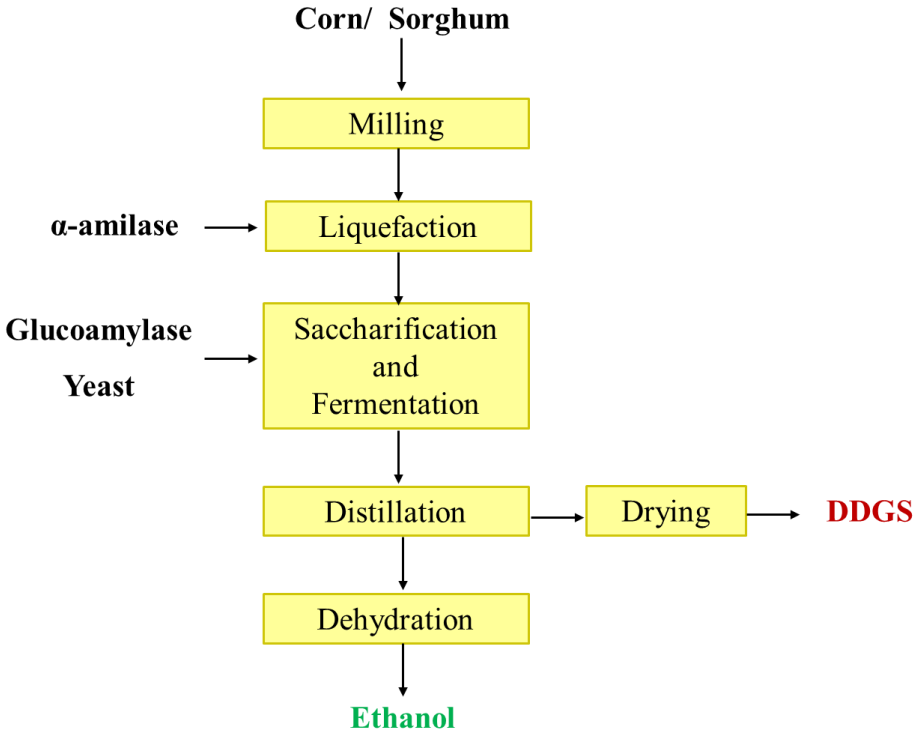

Source: Author's personal archive

2.3. Metabolic pathway of ethanol fermentation

Under anaerobic conditions, the yeast *Saccharomyces cerevisiae* converts fermentable sugars into ethanol and CO_2 through a sequence of reactions inside the cell, as illustrated in the simplified pathway of ethanol fermentation in Figure 2.5. First, sugars are broken down into pyruvate during glycolysis. Then, pyruvate is converted into ethanol and CO_2. The theoretical yields are 0.511 g of ethanol and 0.489 g of CO_2 per gram of glucose consumed.

In addition to ethanol and CO_2, the fermentation also produces by-products. Glycerol, the main by-product, accumulates up to 1.0% (w v^{-1}) in most fermentations. Smaller amounts of organic acids and higher alcohols are also formed. The synthesis of these by-products, as well as the growth of yeast cells, directs some glycolytic intermediates to the corresponding metabolic pathways, decreasing the ethanol yield. Therefore, the ethanol fermentation efficiency, defined as the ratio between the real (experimental) and theoretical yields, typically ranges from 90 to 93% (Bai et al., 2008).

Figure 2.5 – Metabolic pathway of ethanol fermentation in *S. cerevisiae*.

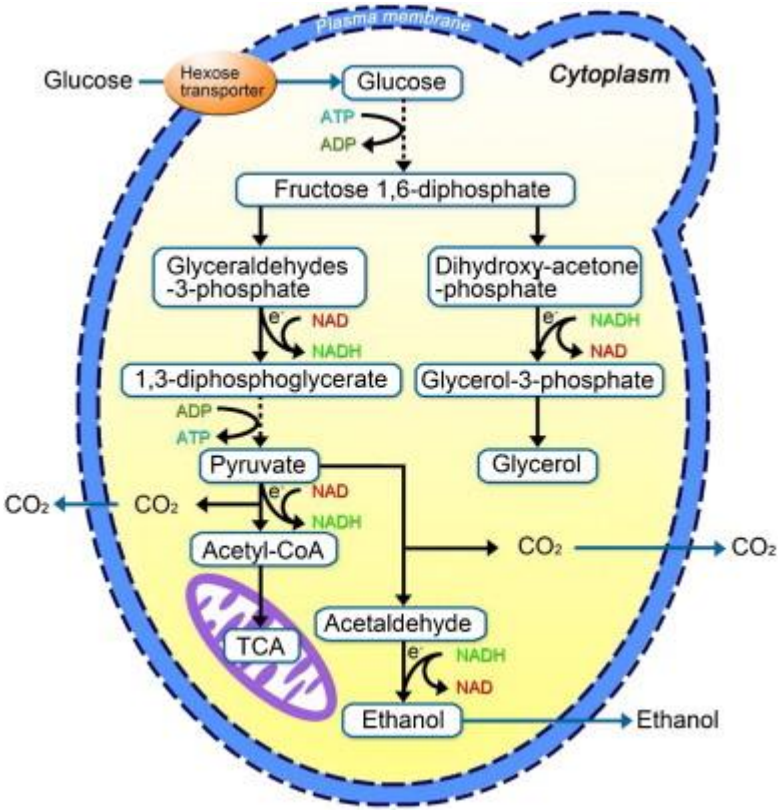

Source: Liu et al. (2013).

During ethanol fermentation, yeast cells face both environmental stresses, such as nutrient limitation, pH fluctuations, high temperatures, and contamination, as well as metabolic stresses. The later includes osmotic stress from high substrate concentrations and ethanol accumulation, which inhibits growth and reduces ethanol production (as discussed later). Figure 2.6 summarizes these factors, which often act synergistically to impair cell viability and ethanol productivity.

Figure 2.6 – Potential stress factors on *S. cerevisiae* during ethanol fermentation.

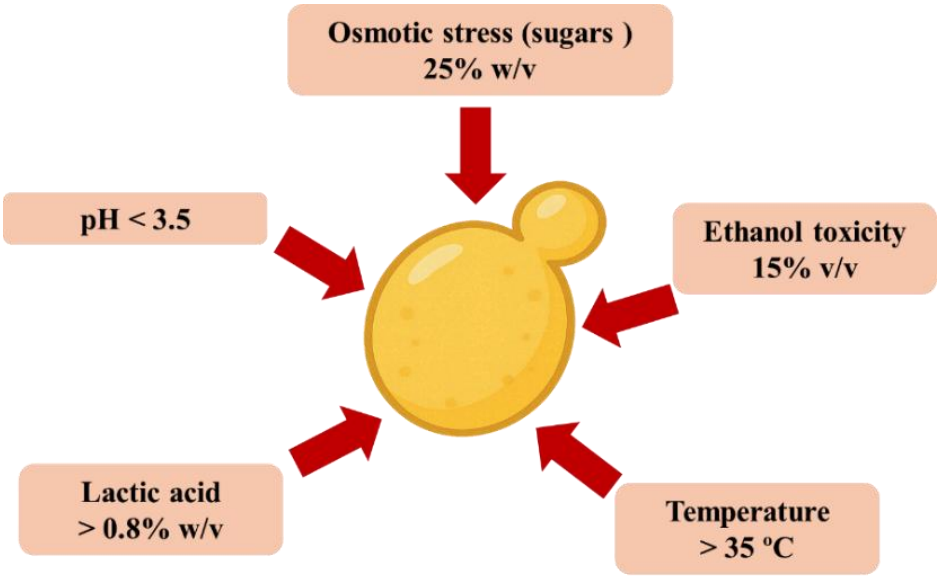

Source: Author's personal archive

2.4. Fermentation kinetics

Fermentation kinetics are evaluated by monitoring substrate consumption, microbial cell growth, and product formation, which define characteristic profiles and can be described by mathematical models integrating bioprocess stoichiometry with reaction rate expressions (Badino and Cruz, 2012). Such kinetic models serve as powerful tools for predicting bioethanol production performance, reducing experimental work, lowering costs, and accelerating process optimization (Nosrati-Ghods et al., 2020).

Cell growth represents an autocatalytic reaction where the growth rate is directly proportional to the cell concentration (Shuler and Kargi, 2002). In batch fermentation systems, the cell growth rate is determined by the specific growth rate (μ), as shown in Eq. (2.1). The specific rates of substrate consumption (μ_S) and product formation (μ_P) are similarly defined by Eqs. (2.2) and (2.3).

$$\frac{dC_X}{dt} = \mu \cdot C_X \tag{2.1}$$

$$\frac{dC_S}{dt} = -\mu_S \cdot C_S \tag{2.2}$$

$$\frac{dC_P}{dt} = \mu_P \cdot C_P \tag{2.3}$$

where C_X, C_S, and C_P represent the concentrations of cells, substrate, and product, respectively.

The fundamental kinetic behavior of alcoholic fermentation can be described by the Monod saturation model, where the specific cell growth rate (μ) is expressed by Eq. (2.4).

$$\mu = \mu_{max} \cdot \frac{C_S}{C_S + K_S} \tag{2.4}$$

where μ_{max} is the maximum specific cell growth rate (h^{-1}), and K_S is the saturation constant.

The Monod model describes microbial growth kinetics as a function of substrate concentration, where the specific growth rate (μ) increases hyperbolically with substrate availability until reaching a maximum value (μ_{max}) at saturating concentrations. However, this model is only valid under ideal conditions, where no significant inhibition occurs. In ethanol fermentation, high concentrations of substrate, product (ethanol), or biomass can inhibit microbial growth (Han and Levenspiel, 1988).

Several studies have investigated the growth kinetics of ethanologenic microorganisms, with particular attention to inhibition phenomena. Among these, the hybrid Andrews-Levenspiel model (Andrews, 1968; Levenspiel, 1980) has proven particularly effective for alcoholic fermentation systems, as it takes into account both substrate and product inhibition, Eq. (2.5).

$$\mu = \mu_{max} \cdot \frac{C_S}{K_S + C_S + \frac{C_S^2}{K_{IS}}} \cdot \left(1 - \frac{C_E}{C_{Emax}}\right)^n \tag{2.5}$$

where K_{IS} is the substrate inhibition constant ($g \cdot L^{-1}$), C_{Emax} is the ethanol concentration for complete growth inhibition ($g \cdot L^{-1}$).

2.5. Product inhibition in ethanol fermentation

Ethanol is well known to inhibit both yeast cell growth and ethanol production. Moreover, ethanol is a primary metabolite whose production is closely linked to yeast cell growth (Bai et al., 2008). In one of the earliest kinetic studies, Aiba et al. (1968) operated a chemostat fermentation system with media containing initial glucose concentrations of 10 and 20 g L^{-1}, fed at different dilution rates. Because the ethanol produced at these glucose levels was too low to exert an inhibitory effect, ethanol was externally added to the fermenter to achieve the desired concentrations and investigate its effects on yeast growth and ethanol production. According to the authors, ethanol concentrations above 40 g·L^{-1} can reduce both the yeast growth rate and ethanol production rate, thereby resulting in lower productivities.

While some researchers have reported that externally added ethanol is less toxic than ethanol produced by yeast cells during fermentation (Loureiro and Ferreira, 1983; Nagodawithana and Steinkraus, 1976), other studies suggest that the inhibitory effect of ethanol, regardless of its source, is the same due to the high permeability of yeast cell membranes to ethanol (Guijarro and Lagunas, 1984). The increase in ethanol concentration in the medium alters the fluidity and composition of the plasma membrane, disrupting ionic balance and compromising its rigidity. These changes negatively impact cell viability, membrane integrity, and metabolic capacity by interfering with endocytosis and impairing the synthesis of stress proteins (Moon et al., 2012). Moreover, the stress caused by ethanol on yeast can be intensified by excessive acidity and high temperatures in the fermentation tanks (Amorim, 2005).

The inhibitory effect of ethanol limits the alcohol content in the fermentation process, as fermentor productivity drops significantly at ethanol concentrations above 15% v v^{-1} (Taylor et al., 2010). As a result, large volumes of water are required, which increases the size of the equipment and energy consumption for distillation (up to 2.5 kg of steam per liter of ethanol) (Ensinas et al, 2007).

2.6. Ethanol separation techniques

To mitigate ethanol toxicity during fermentation, various process engineering approaches, including in situ recovery strategies, have been employed. The main in situ ethanol recovery techniques employed during ethanol fermentation are liquid-liquid extraction, pervaporation, vacuum, and gas stripping.

2.6.1. Liquid-liquid extraction

Liquid-liquid extraction (LLE) is a separation technique used to remove ethanol during the fermentation process. In this process, two insoluble phases are brought into contact, and the ethanol is extracted from the broth into the organic phase (Kollerup and Daugulis, 1985). The contact between the fermentation broth and solvent can occur directly, in which the cells are exposed to the organic phase, or indirectly, using a cell-free portion of the broth (Grundtvig et al., 2018; Offeman et al., 2010). Ethanol removed by the extractant can be recovered in a regeneration unit, while the solvent is regenerated and can be reused in a subsequent extraction (Cai et al., 2022).

Several factors must be considered when selecting an extraction solvent, including its ability to achieve good performance in partitioning the product between the aqueous and organic phases (high distribution coefficient), high selectivity, low solubility in the aqueous phase, and it must be biocompatible and non-toxic. Other characteristics, such as non-flammability and chemical stability under fermentation conditions, should be considered. In addition, an inexpensive and recyclable solvent is desirable (Bokhary et al., 2021; Huang et al., 2008; Weilnhammer and Blass, 1994).

Among the solvents, oleic acid has been used as an extractant in various processes and configurations, particularly due to its relative ethanol distribution coefficient and low toxicity to microorganisms. Lemos et al. (2018) conducted liquid–liquid extractive fed-batch fermentations using a drop column bioreactor with oleic acid recirculation. The results showed that it was possible to achieve ethanol productivities of 11.27–12.98 g L^{-1} h^{-1}, corresponding to an increase of 12.7–29.8% when compared with the control assays without ethanol removal. In another work, Lemos et al. (2020) also performed fed-batch extractive fermentations with in situ ethanol removal by oleic acid. At the feed of must containing 306.6 g L^{-1} sucrose, the total ethanol concentration reached 100.3–139.8 g L^{-1}, a value 19.9–67.2% higher than the value obtained in conventional fed-batch fermentation.

Although LLE offers advantages such as operational simplicity and the potential to enhance yields and productivity, some challenges still need to be addressed. High volumes of solvent are often required due to the low ethanol concentration in the broth and the moderate distribution coefficient of many extractants. As a result, relatively large amounts of solvent are necessary to achieve effective recovery.

2.6.2. Pervaporation

Among various *in situ* product separation methods, pervaporation, a membrane-based technique, has emerged as an appealing choice for *in situ* ethanol separation (Van der Bruggen and Luis, 2014; Fan et al., 2016; Samanta and Ray, 2015). In the pervaporation process, the selective permeation of target molecules through a membrane is elucidated by the sorption-diffusion theory, a fundamental framework in membrane separation science. This theory delineates the intricate transport mechanism of target molecules through the membrane, characterized by a three-stage process: molecule sorption from the upstream flow into the membrane surface, molecule diffusion through the membrane thickness and molecule desorption to the vapor phase of the downstream flow (Kamelian et al., 2019).

The performance of a pervaporation system is primarily governed by two parameters of the membrane: the separation factor and the permeation flux. These, in turn, are affected by several operational and material factors, such as the type of membrane material, its thickness, the level of vacuum or sweep gas applied, as well as the temperature and composition of the feed solution (Bharathiraja et al., 2017). The membrane material is chosen based on the nature of the desired component. Hydrophobic membranes tend to favor the passage of organic compounds over water, which are then recovered in the permeate (Zentou et al., 2019). Among hydrophobic polymeric membranes, polydimethylsiloxane (PDMS) is the most used for ethanol recovery due to its combination of high selectivity and excellent stability (Fan et al., 2019; Wei et al., 2011; Xiangli et al., 2007).

Ding et al. (2012) developed a continuous ethanol fermentation system combining a cell-immobilized bed fermentor with pervaporation using a composite PDMS membrane in a closed-circulation configuration. For batch fermentation without membrane pervaporation, glucose and ethanol concentrations in the broth were, respectively, 20.4 g L^{-1} and 28.6 g L^{-1} after 24 h, yielding a volumetric productivity of 3.21 g L^{-1} h^{-1}. In contrast, the extractive continuous fermentation system maintained stable operation for 250 hours, achieving an ethanol productivity of 9.6 g L^{-1} h^{-1}, representing a 200% increase over batch operation. The PDMS membrane demonstrated consistent selectivity for ethanol, with separation factors ranging from 5.0 to 7.2 relative to water.

Many studies on membrane-based pervaporation have highlighted its high selectivity and effective separation performance (Ding et al., 2012; Fan et al., 2019; O'Brien et al., 2000; Xue et al., 2016). Nevertheless, fouling remains a critical drawback, as it reduces membrane efficiency, decreases productivity, and increases maintenance costs. The accumulation of

bacterial cells on the membrane surface also raises concerns about contamination, challenging the process's long-term stability (Zentou et al., 2019).

2.6.3. Vacuum

The vacuum technique enhances ethanol removal from the fermentation broth through pressure reduction, which depresses the boiling point of the ethanol–water mixture and enables vaporization at the fermentation temperatures. This process selectively fractionates and extracts ethanol and water vapors, thereby reducing ethanol concentration in the broth and mitigating its inhibitory effects on yeast metabolism (Nguyen et al., 2009; Tavares et al., 2019). The thermodynamic equilibrium can be calculated using Raoult's Law modified for liquid-vapor systems, as indicated in Eq. (2.6).

$$y_i \cdot P = x_i \cdot \gamma_i \cdot P_{sat,i} \tag{2.6}$$

where y_i is the molar fraction of specie “i” in the gas phase in equilibrium to the liquid phase (-), P is the operating pressure (Pa), γ_i is the activity coefficient of specie “i” estimated by the UNIQUAC model, x_i is molar fraction of specie “i” in the liquid phase, and $P_{sat,i}$ is vapor pressure of specie “i” calculated by Antoine’s Equation (Pa).

The extractive fermentation using vacuum was first described by Cysewski and Wilke (1977) and has been successfully employed in various studies (Huang et al., 2015; Mariano et al., 2012; Nguyen et al., 2009; Shihadeh et al., 2014; Tavares et al., 2019). Nguyen et al. (2009) evaluated a continuous fermentation system integrated with a separation process, operating under both atmospheric and vacuum pressures for 140 hours. At atmospheric pressure, the system stabilized with only 30% glucose conversion, resulting in ethanol production of 55 g L^{-1}. Under vacuum conditions (47 mmHg), 52% of the glucose was converted, resulting in an ethanol concentration of 44.2 g L^{-1} in the fermentation broth. Moreover, the ethanol productivity reached 5.8 g L^{-1} h^{-1}, around 60% higher than the control.

Shihadeh et al. (2014) investigated vacuum application to corn fermentations with solids contents of 30, 40, and 45 % (w v^{-1}). Extractive fermentation exhibited ethanol efficiencies of 75.6, 62.8, and 39.0% at these solids concentrations, comparable to conventional fermentation performance. However, by optimizing enzyme dosage and yeast inoculum size, the vacuum

fermentation efficiency at 40% (w v^{-1}) solids increased to 77%, representing 23.6% improvement over conventional processing at equivalent solids loading. Kumar et al. (2018) assessed the vacuum fermentation of corn mash at 30, 40, and 42% solids concentrations. At 40% solids, 1 hour vacuum cycles applied at 12, 24, 36, and 48 hours achieved complete substrate utilization and enhanced ethanol yield by 65% compared to conventional fermentation. At 42% solids, extended of 1.5 hour vacuum cycles reduced residual glucose to 0.17% while boosting ethanol yield by 88%. At 32% solids, vacuum operation halved the fermentation time (32 hours *vs* 72 hours in controls) while maintaining complete substrate consumption.

Volodko et al. (2020) conducted the fermentation of sweet sorghum syrup under vacuum conditions, resulting in a 55% increase in ethanol productivity compared to conventional fermentation. Farias and Maugeri-Filho (2021) performed a sequential fed-batch extractive fermentation with cell recycling for bioethanol production from hemicellulosic hydrolysate and sugarcane molasses. To promote ethanol removal, the bioreactor vessel was coupled to a flash tank operated under vacuum conditions (100–150 mmHg). Ethanol productivity reached 9.5 g L^{-1} h^{-1}, ten times higher than conventional processes, with a yield of 0.482 $g_{ethanol}$ $gs_{substrate}^{-1}$ and an ethanol efficiency of 94.3% during the second recycle.

Despite these promising findings, the integrated vacuum fermentation approach faces several practical challenges that limit its industrial scalability. Two key constraints include substantial energy requirements for auatained vacuum operation, and the need for large fermentation volumes to achieve economic viability. Therefore, further efforts are necessary on process optimization to improve energy efficiency and reduce capital costs, thereby enhancing the commercial feasibility of this technology.

2.6.4. Gas stripping

Gas stripping is an in situ product recovery technique that involves sparging an inert gas through the fermentation broth (Cai et al., 2024; Qureshi, 2014). This operation promotes the transfer of volatile compounds, such as ethanol, from the liquid phase to the gas phase, driven by the vapor–liquid equilibrium (Atasoy et al., 2018). Compared to alternative separation techniques, gas stripping presents distinct advantages, including operational simplicity and cost-effectiveness. These benefits are further amplified by the ability to recycle carbon dioxide (CO_2) generated during ethanol fermentation, which significantly reduces dependence on

external gas inputs (Sonego et al., 2014).

The removal of solvents from aqueous solutions via gas stripping follows first-order kinetics, as described by Truong and Blackburn (1984) model (Eq (2.7)). This kinetic framework has been successfully applied to analyze gas stripping performance in different fermentation systems (Ezeji et al., 2003; Sonego et al., 2014; de Vrije et al., 2013).

$$\dot{r} = -\frac{dC}{dt} = k_s a \cdot C \tag{2.7}$$

where $\dot{r}$ is the velocity of solvent removal from the liquid phase to gas phase (g L^{-1} h^{-1}) C is the solvent concentration in the liquid phase (g L^{-1}), and $k_s a$ is the constant of solvent removal (h^{-1}).

The constant of solvent removal ($k_s a$) is a kinetic coefficient and regards both effects of thermodynamic and mechanical entrainments. Mechanical entrainment is a phenomenon characteristic of systems in which liquids and gases are in relative motion, commonly observed in chemical processes involving aeration, boiling, evaporation, and distillation. When bubbles of a gas are injected at the bottom of a liquid column, they rise to the free surface. The liquid film surrounding these bubbles eventually breaks, resulting in the formation of droplets that the ascending gas phase can carry away (Zhang et al., 2012). The second mechanism, known as thermodynamic entrainment, involves the removal of ethanol as a vapor, constrained by the saturation of the gas phase (thermodynamic equilibrium). As the gas stream passes through the liquid phase, the volatile components of the medium, including ethanol and water, extract energy from the liquid to vaporize.

Gas stripping has been shown to be an effective strategy for ethanol removal during fermentation, with several studies reporting its successful application, especially in corn-based processes. Taylor et al. (1995) achieved high glucose conversions (90–100%) using high substrate concentrations (200–600 g L^{-1}) in continuous extractive fermentations with CO_2. The system consisted of a 2 L continuous fermentor coupled to a 10 cm diameter packed stripping column. Fouling of the column packing due to yeast cell attachment was observed, partially blocking the gas flow and reducing column performance. Nevertheless, stable operation was maintained for 150 days, and the process demonstrated the potential for reducing ethanol inhibition. In a subsequent study, Taylor et al. (1996) employed larger reactors and proposed

periodic washing of the packed column to address the fouling problem, thereby significantly improving system performance. The authors reported complete conversion of 600 g L^{-1} of substrate and high productivity of 15 g L^{-1} h^{-1}.

Later, Taylor et al. (1998) investigated ethanol stripping in a packed column using air as the stripping gas, coupled with a 30 L continuous fermentor operated for 185 days. The broth was circulated through the stripping column and returned to the fermentor. The authors reported a high ethanol yield (~0.50 $g_{ethanol}$ $gs_{ubstrate}^{-1}$) and noted that ethanol significantly reduced cell yield, while glucose consumption remained largely unaffected at ethanol levels up to 65 g L^{-1}. More recently, Taylor et al. (2010) evaluated the performance of a 70 L continuous fermentor fed with high-solids corn starch syrup, integrated with a CO_2 stripping column for ethanol removal. The system operated stably for 60 days, achieving 95% starch conversion and an ethanol yield equal to 88% of the theoretical maximum.

Recent studies have explored the application of gas stripping to fermentation processes for ethanol production from sugarcane sucrose. Sonego et al. (2014) investigated ethanol production from sucrose by extractive batch fermentation using CO_2 as the stripping gas in a 5 L bubble column bioreactor. Initially, the authors examined the influence of specific CO_2 flow rate and solution temperature on ethanol and water removal, using hydroalcoholic solutions containing 80.0 g L^{-1}. The condition of 2.0 vvm at 34 °C yielded the best ethanol removal. In extractive fermentation, productivity was 25% higher compared to conventional fermentation. In a subsequent study, Sonego et al. (2016) investigated ethanol production via extractive fed-batch fermentation with CO_2 stripping, evaluating different substrate concentrations in the feed, filling times, and ethanol stripping start times. Their results demonstrated that a filling time of 5 h, combined with ethanol removal starting after 3 h of fermentation, minimized substrate and ethanol inhibition on the yeast. This approach enable the use of a high substrate concentration (240 g L^{-1}) in the feed. Complete sugar consumption was achieved within 12 h of fermentation, yielding a 33% higher total ethanol concentration compared to conventional process.

In another study, Sonego et al. (2018) optimized extractive fed-batch ethanol fermentation with CO_2 stripping at 34 °C, employing a high substrate concentration (428.6 g L^{-1}) in the must. Despite a lower volumetric productivity (8.6 g L^{-1} h^{-1}) compared to conventional fermentation (10.4 g L^{-1} h^{-1}), complete substrate conversion was achieved, yielding an ethanol concentration of 136.9 g L^{-1} (17.2 °GL), 65% higher than the control.

More recently, Rodrigues et al. (2025) investigated an extractive fermentation with ethanol recovery via absorption, comparing open and closed systems with and without CO_2

recirculation from fermentation. The recovery system utilized two serially connected absorbers with monoethylene glycol (MEG) as the absorbent. In the extractive fermentation without CO_2 recirculation, complete conversion of 300.0 g L^{-1} substrate yielded 135.2 g L^{-1} ethanol, a 68% increase over conventional fermentation.

Additional studies have demonstrated that gas stripping in extractive fermentation can serve a dual purpose, cooling the fermentation vessel while simultaneously reducing cooling water requirements (Almeida et al., 2021; Campos et al., 2025, 2022; Veloso et al., 2023). Almeida et al. (2021) demonstrated the cooling benefits of gas stripping in both batch (10 L) and fed-batch (100 L) extractive fermentations at 34 °C using a CO_2 flow rate of 1.0 vvm, achieving up to 63% reduction in cooling water consumption. Building on this concept, Campos et al. (2025) developed an innovative temperature control strategy for fed-batch extractive ethanol fermentation that completely eliminated cooling water requirements. Their system relied exclusively on the evaporative cooling effect generated by CO_2-induced vaporization of ethanol and water, successfully maintaining the fermentation temperature at 34°C. This approach not only proved the feasibility of CO_2 as a sole cooling medium but also represented a significant advancement in process intensification and sustainable bioprocessing.

Although gas stripping has demonstrated significant potential for enhancing fermentation performance and sustainability, its industrial-scale implementation faces considerable challenges. The ethanol removal rates reported in laboratory studies (Sonego et al., 2018; Veloso et al., 2023), require high specific flow rates (2.5 vvm), which become economically and technically impractical in large-scale bioreactors. This limitation has prompted investigation of vacuum-assisted gas stripping as a promising alternative. By operating at reduced pressure, this approach enables effective ethanol removal at significantly lower gas flow rates, addressing a critical barrier to industrial adoption.

CHAPTER 3

3. ETHANOL REMOVAL BY VACUUM-ASSISTED GAS STRIPPING: INFLUENCE OF OPERATING CONDITIONS

Abstract

One way to overcome the inhibitory effects caused by ethanol on yeast cell growth is the use of extractive fermentation, whereby ethanol is removed from the fermentation broth as it is produced. The present work investigates ethanol removal from solution by vacuum-assisted gas stripping, which is a promising method for enhancing performance, compared to conventional gas stripping. Evaluation was made of the effects of carbon dioxide flow rate (ϕ_{CO2}), temperature (T), and pressure (P) on ethanol removal performance. Bench-scale assays were performed using a 2-L bubble column containing 10% v v^{-1} ethanol solution, with monitoring of the gas and liquid phases by FT-MIR spectroscopy. The ethanol entrainment factor (F_E) increased with ϕ_{CO2} and temperature, but decreased at higher pressure. Only ϕ_{CO2} had significant and positive effects on the concentration factor (F_C) and selectivity ($\alpha_{E/W}$), within the operating ranges of the variables studied. An ethanol removal model was obtained that provided an accurate description of the process behavior, with good agreement between the experimental and simulated data. In addition, the energy requirement for ethanol removal by vacuum-assisted gas stripping in the bioreactor was lower than for the conventional stripping process.

Keywords: Ethanol separation; gas stripping; vacuum; integrated process.

3.1. Introduction

Brazil is the world's second largest ethanol producer, accounting for 27% of global production (103 billion liters) in the 2021 harvest (Renewable Fuels Association, 2022). Alcoholic fermentation is a well-established process in Brazilian distilleries, where the sugar cane sugars are converted into ethanol by the yeast *Saccharomyces cerevisiae*. At the end of the process, the fermentation yield is around 90–92% of the theoretical value (0.511 $g_{ethanol}\ g_{substrate}^{-1}$) (Amorim et al., 2011). However, this fermentation process has some limitations. In particular, the ethanol accumulated in the broth inhibits yeast cell growth, with the cell growth rate

decreasing at ethanol concentrations above 40.0 g L^{-1} and completely ceasing when the concentration is close to 95.0 g L^{-1}, resulting in a low ethanol concentration in the final wine (~10 % v v^{-1}) (Maiorella et al., 1983). As a consequence, there are high energy costs for the recovery of ethanol in the distillation process, which has a steam requirement of approximately 2.2 kg_{steam} $kg_{ethanol}^{-1}$(Dias et al., 2015).

To overcome the inhibitory effects of ethanol on the yeast, several techniques have been investigated for recovery of the product from the broth while it is being produced, including liquid-liquid extraction, pervaporation, gas stripping, and application of vacuum (Abdehagh et al., 2014; Campos et al., 2022; Desai and Zimmerman, 2023; Van Hecke et al., 2014; Kujawska et al., 2015; Lemos et al., 2020, 2017). The performance parameters that have been evaluated for these separation techniques include the removal rate and product selectivity. In liquid-liquid extraction, the effectiveness of ethanol removal is related to the partition coefficient, but a difficulty is that most extractants with good partition coefficients can be toxic to the yeast (Xue et al., 2014b). In the case of pervaporation, this technique is efficient in separating organic compounds from aqueous solutions, as well as liquid mixtures with similar boiling points (Nagasawa and Tsuru, 2017). However, it has been reported that fouling decreases the separation factor and the flux through the membrane, consequently reducing performance (Kujawska et al., 2015). On the other hand, gas stripping and vacuum fermentation have attracted great interest, since their advantages include simple operation and selective removal of volatile compounds (Huang et al., 2015; Outram et al., 2017).

In vacuum fermentation, ethanol is extracted from the fermentation broth under reduced pressure, which lowers the boiling point of the ethanol-water mixture and increases vaporization at the optimum fermentation temperature (30–35 ºC). Kumar et al. (2018) evaluated simultaneous saccharification and vacuum-assisted fermentation for high solids media, using corn slurry as carbon source in a bioreactor operated with vacuum cycles (6.7 kPa). It was reported that the extractive fermentation enabled complete conversion of high solids slurries, with ethanol productivity 88% higher than for the conventional process.

In the gas stripping method, volatile compounds are removed by a gas stream from a liquid broth (Abdulrazzaq et al., 2016a; Desai et al., 2022; Gilmour and Zimmerman, 2020; Silva et al., 2015). This technique has been evaluated under different operating conditions, considering the effects of variables including temperature, CO_2 flow rate, and initial ethanol concentration (Abdulrazzaq et al., 2016b; Martins et al., 2020; Rodrigues et al., 2018; Silva et al., 2015; Sonego et al., 2014). In a recent study, Almeida et al. (2021) used CO_2 as the stripping

gas during extractive ethanol fermentation, leading to ethanol productivity of 21.7 g L^{-1} h^{-1}, which was 27% higher than in conventional fermentation. The authors also reported that the application of the stripping process resulted in an approximately 63% lower demand for cooling water in the fermentation vat heat exchangers. In fact, gas stripping has also been widely evaluated as an effective technique for ethanol removal in fermentation processes by thermophilic bacteria at high temperatures (Calverley et al., 2021, 2020). Calverley et al. (2021) performed stripping assays using heated microbubbles to ethanol removal from model solutions in the continuous mode, the ethanol concentration was maintained below the inhibitory level (2% v v^{-1}) for thermophilic bacteria.

Although the benefits of vacuum and gas stripping during ethanol fermentation have been reported separately in the literature, there have been no previous studies concerning the integration of these separation techniques for the removal of ethanol from hydroalcoholic solutions or fermentation broths. Specifically, there is a lack of studies focusing on monitoring both the liquid and gaseous phases to improve understanding of the ethanol removal process. Therefore, the aim of the present work was to study the use of vacuum-assisted gas stripping for ethanol removal from a model solution. Fourier transform mid-infrared spectroscopy (FT-MIR) was employed to monitor the compositions of the liquid and gas phases. Firstly, analysis was made of the effects of CO_2 flow rate, temperature, and pressure (under vacuum conditions).

The experimental results were compared to those obtained from a mathematical model based on thermodynamic equilibrium, allowing for the identification of the experimental conditions under which the system achieved the best performance in terms of ethanol removal, ethanol concentration factor, and ethanol/water selectivity. Finally, a comparative evaluation of ethanol removal was performed, considering power input and energy requirements.

3.2. Materials and Methods

3.2.1. Experimental procedure

Figure 3.1 illustrates the experimental setup employed in this work. The experiments were performed using a 2–L working volume bubble column pneumatic bioreactor (9.7 cm internal diameter, 33.8 cm liquid height, and 56.2 cm total height) containing a solution of ethanol at an initial concentration of 80 g L^{-1} (10% v v^{-1}). The stripping gas was commercial carbon dioxide (CO_2) from a cylinder (99.8% purity). The CO_2 was injected through a crosshead sparger at the base of the bioreactor, with the gas flow rate measured and regulated using a mass

flow controller (GFC 371, Aalborg). The temperature of the solution was kept constant by recirculating water from a thermostatic bath through the bioreactor jacket. The vacuum pressure of the system was maintained by a vacuum pump. Each experiment lasted 6 h. Every hour, the volume of the liquid phase (V) was measured and samples were collected for quantification of the ethanol concentration.

Figure 3.1 – Schematic illustration of the equipment used in the vacuum-assisted stripping experiments: (1) mass flow controller, (2) CO_2 cylinder, (3) bioreactor, (4) vacuum pump, (5) thermostatic bath, (6) gas sampling chamber, (7) spectrometer, and (8) data acquisition.

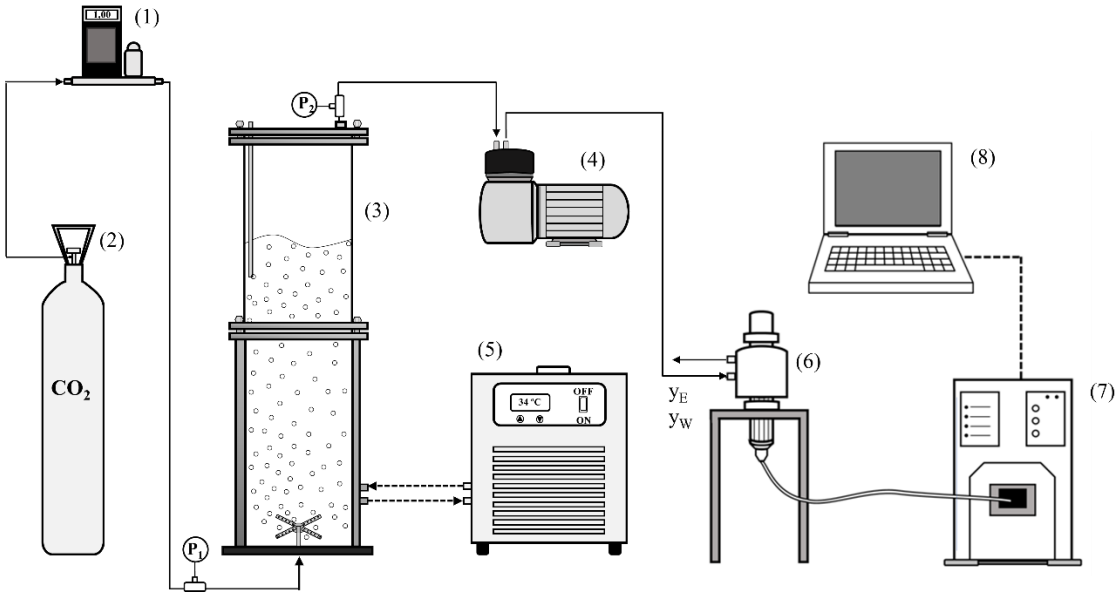

3.2.2. Experimental design and statistical analysis

A 2^3 factorial design was employed to assess the effects of the CO_2 flow rate (ϕ_{CO2}), solution temperature (T), and pressure in the reactor head (P) on the ethanol removal performance of the vacuum-stripping process. Table 3.1 shows the coded and original values for the independent variables. The CO_2 flow rate and solution temperature were selected based on previous studies (Rodrigues et al., 2018; Silva et al., 2015), and the pressure range was chosen from a preliminary investigation. Statistica v. 7.0 software was used for analysis of the experimental data.

Table 3.1 – Coded and original values of the independent variables: solution temperature (T), pressure in the reactor head (P), and specific CO_2 flow rate (ϕ_{CO2}).

Variable	Code	Levels		
		-1	0	1
T (ºC)	x_1	28	31	34
P (kPa)*	x_2	41.31	54.64	67.97
ϕ_{CO2} (vvm)	x_3	0.2	0.6	1.0

*The pressure in the reactor head (P) corresponds to P_2.

3.2.3. Performance parameters

The response variables selected to evaluate the performance of the vacuum-assisted gas stripping operation were the entrainment factor (F_E), concentration factor (F_C), and ethanol/water selectivity ($\alpha_{E/W}$), obtained using Eqs. (3.1), (3.2), and (3.3), respectively.

$$F_E\,(\%) = \frac{C_{E0}\cdot V_0 - C_{EF}\cdot V_F}{C_{E0}\cdot V_0}\times 100 \tag{3.1}$$

$$F_C\,(-) = \frac{y_E^*}{x_E^*} \tag{3.2}$$

$$\alpha_{E/W}\,(-) = \frac{y_E^*/y_W^*}{x_E^*/x_W^*} \tag{3.3}$$

where, C_{E0} is the initial ethanol concentration in the solution (g L^{-1}), C_{EF} is the final ethanol concentration in the solution (g L^{-1}), V_0 is the initial solution volume (L), V_F is the final solution volume (L), x_E^* and x_W^* are the ethanol and water mass fractions in the liquid phase, and y_E^* and y_W^* are the ethanol and water mass fractions in the gas phase.

3.2.4. FT-MIR spectroscopy

Fourier transform mid-infrared spectroscopy (FT-MIR) was used to determine the molar fractions of ethanol (y_E) and water (y_W) in the gas phase and the ethanol concentration in the liquid phase, according to the methods described by Rodrigues et al. (2018) and Santos et al. (2022), respectively. Liquid phase measurements were performed after each assay, using a fiber-optic attenuated total reflectance (ATR) probe coupled to a spectrometer (ReactIR 45m, Mettler-Toledo AutoChem, Inc.) equipped with a liquid nitrogen-cooled mercury cadmium telluride (MCT) detector. Gas phase data were acquired online, using a gas cell (DST Fiber to Gas Cell, Mettler-Toledo) connected to a spectrometer. A purge system employing nitrogen gas was used to remove CO_2 and water from the compartment. Spectra were collected in the range from 3335 to 15411 nm, at resolution of 4.2 nm, with 256 scans per sample.

3.2.5. Vacuum-assisted gas stripping modeling

The mathematical model developed to describe the process employed equations for the molar balances of ethanol and water, according to the principles of vapor-liquid equilibrium. The modeling assumed that the carbon dioxide bubbles leaving the liquid phase were saturated with ethanol and water. According to Ezeji et al. (2005), saturation of a stripping gas with volatile organic solvents occurs in milliseconds.

3.2.6. Molar balance

Modeling of the vacuum-assisted gas stripping operation employed the ethanol and water molar balances (Eqs. (3.4) and (3.5)), assuming the liquid phase as the control volume (Silva et al., 2015).

$$\frac{dn_E}{dt} = -\left(\dot{n}_{CO_2} + \dot{n}_E + \dot{n}_W\right)\cdot y_E \tag{3.4}$$

$$\frac{dn_W}{dt} = -\left(\dot{n}_{CO_2} + \dot{n}_E + \dot{n}_W.\right)\cdot y_W \tag{3.5}$$

where, $\dot{n}_{CO_2}$ is the carbon dioxide molar flow rate (mol h^{-1}), $\dot{n}_E$ is the ethanol molar flow rate (mol.h^{-1}), $\dot{n}_W$ is the water molar flow rate (mol h^{-1}), and t is the time (h).

The carbon dioxide molar flow rate was calculated according to the ideal gas law (Eq. (3.6)).

$$\dot{n}_{CO_2} = \frac{P \cdot Q_{CO_2}}{R \cdot T} \tag{3.6}$$

where, P is the system pressure (Pa), Q_{CO_2} (L h^{-1}) is the carbon dioxide volumetric flow rate, and R is the ideal gas constant (8.3145 kPa L $mol^{-1}.K^{-1}$).

3.2.6.1. Gas-liquid equilibrium

The molar fractions of ethanol (y_E) and water (y_W) in the gas phase were determined using thermodynamic assumptions for gas-liquid equilibrium, employing the modified Raoult law (SMITH et al., 2005), described by Eqs.(3. 7) and (3.8).

$$y_E = \frac{x_E \cdot \gamma_E \cdot P_{sat,E}}{P} \tag{3.7}$$

$$y_W = \frac{x_W \cdot \gamma_W \cdot P_{sat,W}}{P} \tag{3.8}$$

where, $P_{sat,E}$ and $P_{sat,W}$ are the ethanol and water saturation vapor pressures (atm), x_E and x_W are the ethanol and water molar fractions in the liquid phase, and γ_E and γ_W are the ethanol and water activity coefficients.

The molar fractions of ethanol and water in the liquid phase were determined using Eqs. (3.9) and (3.10).

$$x_E = \frac{n_E}{n_E + n_W + n_{CO_2}} \tag{3.9}$$

$$x_W = \frac{n_W}{n_E + n_W + n_{CO_2}} \tag{3.10}$$

where, n_E, n_W, and n_{CO_2} are the number of mols of ethanol, water, and carbon dioxide in the liquid phase, respectively.

The gas-liquid equilibrium for carbon dioxide and the ethanol solution was predicted using Henry's Law (SMITH et al., 2005), given by Eq. 11. The Henry constant (H_e, in atm) was determined using a correlation (Eq. (3.12)) obtained from data available in the literature (Dalmolin et al., 2006). Since the assays were performed with ethanol molar fractions of around 0.03, the H_e values for the water-CO_2 binary system were assumed.

$$y_{CO_2} = \frac{x_{CO_2} \cdot H_e}{P} \tag{3.11}$$

$$H_e = 4.665 \cdot T + 482.360 \tag{3.12}$$

where, y_{CO_2} is the CO_2 molar fraction in the gas phase, x_{CO_2} is the CO_2 molar fraction in the liquid phase, and T is the temperature (ºC).

The sums of the molar fractions for the species in the gas and liquid phases were determined using Eqs. (3.13) and (3.14), respectively.

$$x_E + x_W + x_{CO_2} = 1 \tag{3.13}$$

$$y_E + y_W + y_{CO_2} = 1 \tag{3.14}$$

The saturation vapor pressure (P_{sat}) of component "i" was determined using the Antoine equation (Eq. (3.15)).

$$P_{sat,\,i} = \frac{1}{760} \cdot e^{A_i - \frac{B_i}{T - C_i}} \tag{3.15}$$

where, A_i, B_i, and C_i are the Antoine equation constants, and T is the temperature (ºC). For the temperature range evaluated in this study, the Antoine equation constant values for ethanol are $A_E = 18.91$, $B_E = 3803.98$, and $C_E = -41.68$. For water, the values are $A_W = 18.30$, $B_W = 3816.44$,

and C_W = -46.1 (REID et al., 1987).

The UNIQUAC model (Abrams and Prausnitz, 1975) was applied to calculate the activity coefficients for ethanol (E) and water (W). The binary parameters of UNIQUAC are r_E = 2.1055, q_E = 1.9720, r_W = 0.9200, q_W = 1.4000, a_{EW} = 2.0046, a_{WE} = -2.4936, b_{EW} = -728.9705 K, and b_{WE} = 756.9477 K (Perry et al., 1997).

The mathematical model in this work was implemented using Scilab v. 6.0.1software. The Runge-Kutta algorithm was employed for numerical solution of the differential equations system. The prediction quality of the model was assessed using the residual standard deviation (RSD) statistical criterion proposed by Cleran et al. (1991), defined by Eq. (3.16).

$$\text{RSD}\ (\%) = \frac{\sqrt{\frac{1}{N_p}\sum_{j=1}^{N_p}\left(n_{exp}(t_j)-n_{sim}(t_j)\right)^2}}{\bar{n}_{exp}}\cdot 100 \tag{3.16}$$

where, n_{exp} (t_j) is the experimental number of mols of ethanol or water in the alcoholic solution at time t_j, n_{sim} (t_j) is the number of mols predicted by the model at time t_j, $\bar{n}_{exp}$ is the average of the experimental number of mols, and N_p is the number of experimental points.

3.2.7. Energy analysis

The energy balance in the system can be used to calculate the energy requirement for stripping under atmospheric or vacuum conditions. Using the flow work definition (Himmelblau and Riggs, 2012), Chisti (1989) calculated the gassed power input due to the isothermal gas expansion of the bubbles rising through the liquid column in pneumatic bioreactors (P_{IE}), according to Eqs. (3.17)-(3.19).

$$P_{IE} = Q_m \cdot R \cdot T \cdot \ln\left(\frac{P_b}{P_h}\right) \tag{3.17}$$

$$P_b = P_t + \rho_L \cdot g \cdot h_L \tag{3.18}$$

$$P_{IE} = Q_m \cdot R \cdot T \cdot \ln\left(1 + \frac{\rho_L \cdot g \cdot h_L}{P_t}\right) \quad (3.19)$$

where, P_{IE} is the power input due to isothermal gas expansion (W), Q_m is the molar gas flow rate (kmol.s^{-1}), R is the gas constant (8314 J kmol^{-1} K^{-1}), P_b is the pressure at the bottom of the bioreactor (Pa), P_t is the pressure at the head of the bioreactor (Pa), ρ_L is the liquid density (kg.m^{-3}), g is the gravitational acceleration (m.s^{-2}), and h_L is the liquid height (m).

The total power input, or flow work, in the system under stripping and vacuum-stripping conditions was calculated using Eq.(3.20), considering the bioreactor inlet (1) and outlet (2) gas streams (Figure 3.1).

$$P_T = Q_m \cdot R \cdot T \cdot \ln\left(\frac{P_1}{P_2}\right) \quad (3.20)$$

where, P_T (W ≡ J s^{-1}) is the total power input, P_1 (Pa) is the pressure in the inlet gas stream, and P_2 (Pa) is the pressure in the outlet gas stream, which was considered equal to the pressure at the head of the bioreactor (P_h=P_2).

Performance comparison of conventional stripping and vacuum-assisted gas stripping considered the energy requirement for ethanol removal, calculated as the ratio between the total power input and the ethanol removal rate (Eq. (3.21)).

$$E_{EtOH} = \frac{P_T}{R_{EtOH}} \quad (3.21)$$

where E_{EtOH} is the energy requirement (kJ kg$_E^{-1}$) and R_{EtOH} is the ethanol removal rate (kg$_E$.s^{-1}).

3.3. Results and discussion

3.3.1. Experimental design for effective factors

3.3.1.1. Factorial design

Eleven experiments for ethanol removal by vacuum-assisted gas stripping were performed randomly, using a factorial design with the independent variables temperature (T), pressure (P), and CO_2 flow rate (ϕ_{CO2}). The results for the entrainment factor (F_E), concentration factor (F_C), and ethanol/water selectivity ($\alpha_{E/W}$) are shown in Table 3.2. The highest F_E value (35.64%) was obtained in run 6, suggesting that ethanol was preferentially entrained under conditions of reduced pressure, high temperature, and high specific CO_2 flow rate. The lowest F_E value was found for run 3, as expected because it had the lowest levels for ϕ_{CO2} and T, as well as the highest level for P. Sonego et al. (2014) performed ethanol removal by CO_2 stripping in a 2-L working volume bubble column bioreactor, obtaining F_E of 21.0% using ϕ_{CO2} and T of 2.0 vvm and 34 °C, respectively. Therefore, the integrated process strategy employed in the present work provided effective removal of ethanol from the hydroalcoholic solution, since the F_E values were higher than those reported in the literature.

The values of concentration factor (F_C) and ethanol/water selectivity ($\alpha_{E/W}$) were obtained from an average of the data acquired throughout the entire assays. The highest F_C values were obtained in runs 6, 10, and 11 (Table 2), with a gas stream approximately 6 times more concentrated in ethanol compared to the liquid phase. Therefore, if only the water and ethanol fractions of the exit gas stream were considered, it would contain 60% v v^{-1} ethanol. These values exceed those typically found in the phlegm stream (40-50 %v v^{-1}) obtained from distillation columns. As a result, the ethanol present in the stream leaving the bioreactor could be directed to the rectification column after a simple condensation process, for example. This possibility would enable a reduction in the energy requirements in the downstream process.

The ethanol/water selectivity ($\alpha_{E/W}$), defined as the ratio between the ethanol and water contents in the gas and liquid phases, represents the ability to preferentially remove ethanol, compared to water. High selectivity values (up to 11) were achieved in the assays performed, due to the higher volatility of ethanol than water (Perry et al., 1997) .

Table 3.2 – Entrainment factor (F_E), concentration factor (F_C), and ethanol/water selectivity ($\alpha_{E/W}$) values obtained in the vacuum-assisted gas stripping and conventional gas stripping assays.

Vacuum-assisted gas stripping (factorial design)						
	Independent variables – coded: real			**Responses**		
Run	**x_1: T (°C)**	**x_2: P (kPa)**	**x_3: ϕ_{CO2} (vvm)**	**F_E (%)**	**F_C (-)**	**$\alpha_{E/W}$ (-)**
1	-1 (28)	-1 (41.31)	-1 (0.2)	7.67	4.68	6.83
2	1 (34)	-1 (41.31)	-1 (0.2)	13.87	5.67	9.50
3	-1 (28)	1 (67.97)	-1 (0.2)	4.20	3.09	3.81
4	1 (34)	1 (67.97)	-1 (0.2)	8.23	3.41	4.29
5	-1 (28)	-1 (41.31)	1 (1.0)	28.23	5.83	9.95
6	1 (34)	-1 (41.31)	1 (1.0)	35.64	6.03	11.00
7	-1 (28)	1 (67.97)	1 (1.0)	16.85	5.14	7.95
8	1 (34)	1 (67.97)	1 (1.0)	24.94	5.91	10.49
9	0 (31)	0 (54.64)	0 (0.6)	18.19	5.47	9.15
10	0 (31)	0 (54.64)	0 (0.6)	15.96	6.08	11.19
11	0 (31)	0 (54.64)	0 (0.6)	16.11	6.33	10.86
Conventional gas stripping						
12	34	101.32	1.0	17.08	5.97	10.52
13	34	101.32	2.5	36.66	6.04	11.07

3.3.1.2. Effect of operating conditions on performance parameters

The data in Table 3.2 were used to generate a Pareto chart (Figure 3.2) for identification of the most influential variables (at a 90% confidence level). As shown in Figure 3.2(a), the variables temperature (T), pressure (P), and CO_2 flow rate (ϕ_{CO2}) were important for the F_E response. The most significant variable was ϕ_{CO2}, with a 22.24% contribution and a positive effect on F_E. A higher ϕ_{CO2} increases the contribution of liquid entrainment to ethanol removal. When the gas bubbles leaving the liquid burst at the liquid-gas interface, droplets are formed that can become entrained in the gas stream leaving the bioreactor, especially at higher gas flow

rates (Bagul et al., 2013; Zhang et al., 2012).

The solution temperature (T) had a positive effect on F_E, with ethanol removal increasing at higher temperatures. The ethanol removal by gas stripping is a complex and dynamic phenomenon: initially, CO_2 bubbles exhibit no ethanol content, and as the gas phase is sparged, ethanol (and water) is transferred from the liquid to the gas phase until carbon dioxide bubbles become ethanol-saturated. Then, an equilibrium condition is achieved and ethanol (and water) content in bubbles is subjected to thermodynamic effects. The temperature of solution (T) had a positive effect on F_E, with ethanol removal increasing at higher temperatures. As the temperature increases, ethanol vapor pressure increases, and according to the gamma-phi formulation (VLE), ethanol fraction in the gas phase also increases. This effect was also demonstrated by Xue et al., (2014a), who studied the separation of butanol from solutions at temperatures from 25 to 60 ºC, where the butanol removal rate increased at higher temperatures.

Finally, as shown in Figure 3.2(a), increase of the pressure led to lower F_E, demonstrating that ethanol removal increased under reduced pressure (vacuum). The mass transfer of ethanol between the liquid and gas phases is limited by thermodynamic equilibrium, since the driving force for mass transfer across the interface is proportional to the concentration difference and depends on the gas phase composition, which is determined by liquid-gas equilibrium (Cussler, 2009). Hence, higher vacuum led to greater mass transfer of ethanol and water from the liquid phase to the gas phase, due to the greater driving forces provided by the increases of the molar fractions of ethanol and water in the gas phase at saturation, resulting in greater vaporization of ethanol and water.

As shown in the Pareto chart (Figure 3.2(b)), the concentration factor (F_C) was only influenced by the specific CO_2 flow rate (ϕ_{CO2}), which had a positive effect, indicating that higher ϕ_{CO2} favored F_C. In previous studies, Martins et al. (2020) and Silva et al. (2015) investigated ethanol removal by gas stripping at atmospheric pressure, where it was found that higher ϕ_{CO2} led to lower F_C, due to greater liquid entrainment, resulting in a diluted output gas stream. The difference between the results obtained here and in the previous studies, concerning the effect of ϕ_{CO2} on F_C, could be attributed to the operating conditions. In the present work, it was observed that an increase in the CO_2 flow rate increased the removal of ethanol by vaporization and droplet entrainment. Furthermore, a higher molar composition of ethanol and water at gas-liquid equilibrium was obtained under vacuum conditions. Therefore, the amount of ethanol removed by vaporization was higher, relative to the ethanol removed in liquid

droplets, resulting in an ethanol-enriched gas stream. This outcome demonstrated an advantage of the vacuum-assisted gas stripping process, compared to the conventional stripping operation.

Figure 3.2 – Pareto charts for a 90% confidence level: (a) entrainment factor (F_E), (b) concentration factor (F_C), and c) ethanol/water selectivity ($\alpha_{E/W}$).

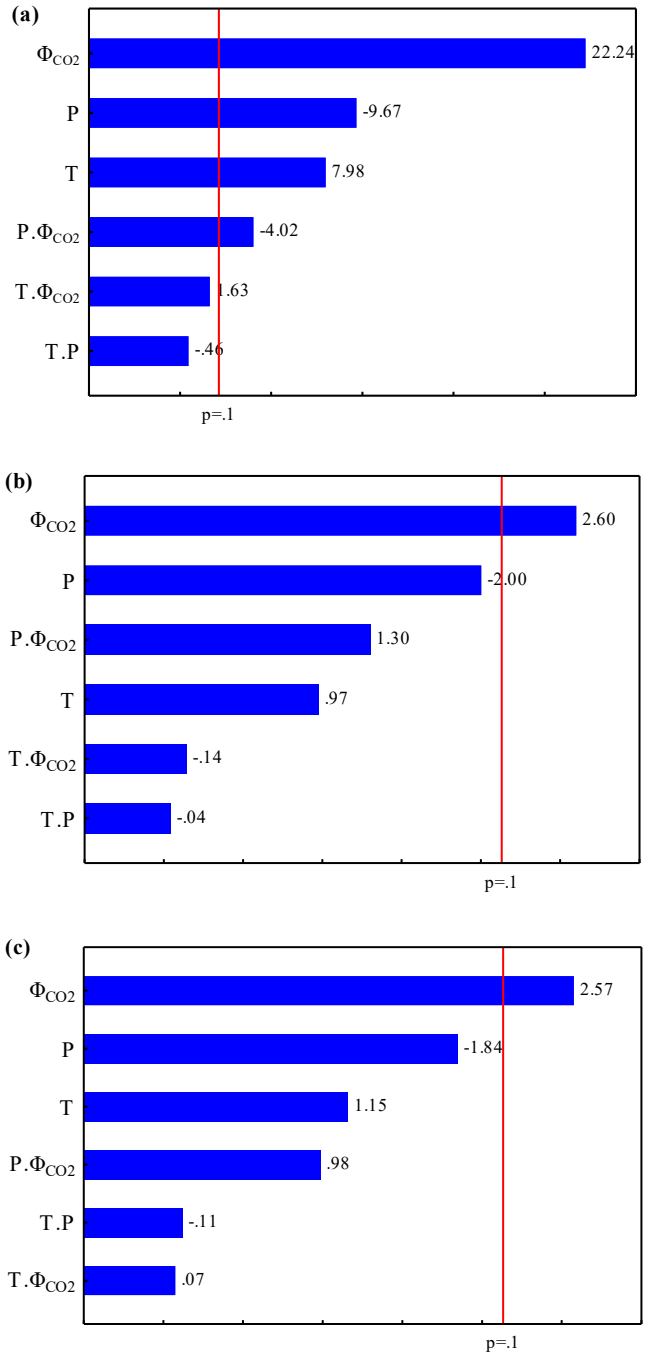

The ethanol/water selectivity ($\alpha_{E/W}$) (Figure 3.2(c)) was also positively influenced by ϕ_{CO2}, with increase of the CO_2 flow rate resulting in preferential removal of ethanol, relative to

water. This could be explained by the fact that higher ϕ_{CO2} acted to increase the height of the gas-liquid dispersion (gas hold-up), resulting in a decrease of the headspace height. It is important to note that the bioreactor was not completely enclosed by the jacket. Consequently, the temperature at the top of the bioreactor (headspace) could not be controlled, resulting in the condensation of ethanol and water vapors when the gas contacted the wall at a lower temperature. It is therefore likely that the decrease of the headspace height, due to the ϕ_{CO2} increase, could have reduced the vapor condensation. Hence, a greater amount of ethanol was removed by vaporization in the gas stream, which increased the ethanol/water selectivity.

The optimal operating condition for maximization of the responses F_E and F_C was determined by application of the desirability function (DF), in the final step of the experimental design (Figure 3.3). The DF is a useful criterion for obtaining the best value corresponding to each factor, providing the global optimum point, considering the different experimental responses.

Figure 3.3 – Desirability function results for the entrainment factor (F_E) and concentration factor (F_C) responses.

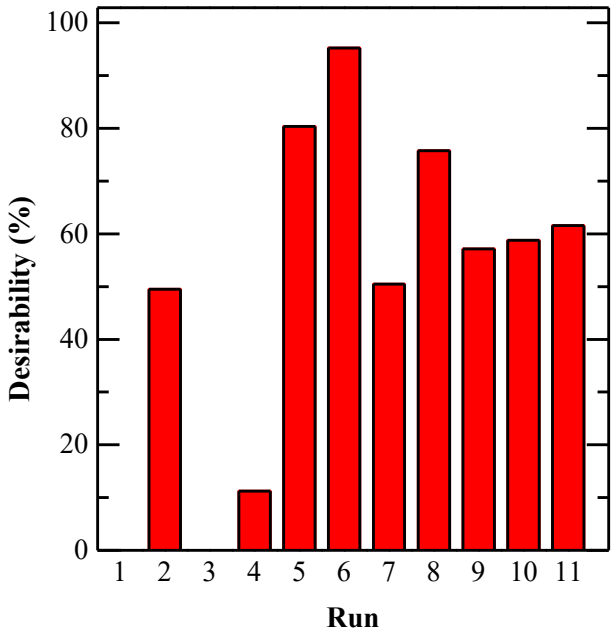

The DF values were obtained using the methodology described by Liu and Tang (2010). The same weight was assigned to the response variables F_E and F_C, according to the desired

goal. As shown in Figure 3.3, the optimum condition for maximization of F_E and F_C corresponded to run 6 (34 ºC, 41.31 kPa, and 1.0 vvm), obtaining F_E and F_C values of 35.64% and 6.03 (-), respectively. A high desirability value of 0.9526 was achieved at the optimum point for the process. However, the experiments revealed additional operating conditions that could be of interest for ethanol removal during fermentation on an industrial scale, such as the central point condition (runs 9 to 11), where the operational parameters (especially the vacuum pressure and the CO_2 flow rate) were milder.

3.3.2. Performance comparison of vacuum-assisted gas stripping and conventional stripping

Figure 3.4 shows the profiles of F_E as a function of ϕ_{CO2}, at 34 ºC, for different pressures. In the case of ethanol removal at 34 ºC and atmospheric pressure, the highest F_E value (36.66%) was obtained with a specific CO_2 flow rate of 2.5 vvm. Similar performances were found for the assays under vacuum pressure, with F_E of 35.66% at 67.97 kPa and 1.5 vvm, and F_E of 35.64% at 41.31 kPa and 1.0 vvm (Table 3.2). The results showed that the best F_E value obtained under atmospheric conditions could be achieved using vacuum-assisted gas stripping with the CO_2 flow rate reduced by 1.7 and 2.5 times, at pressures of 67.97 and 41.34 kPa, respectively. Furthermore, an F_E value close to the value of around 23.6% obtained under atmospheric conditions and 1.5 vvm could be achieved at 41.31 kPa, with a 3-fold reduction of ϕ_{CO2}. The highest F_E value, within the range of experimental conditions studied, was achieved at 41.31 kPa and 1.5 vvm, which resulted in removal of approximately 50% of the ethanol initially present in the bioreactor.

Figure 3.4 – Entrainment factor (F_E) values obtained in the experiments at 34 ºC, under different vacuum pressures (41.31 kPa (squares) and 67.97 kPa (circles)) and at atmospheric pressure (101.32 kPa (triangles)). Error bars correspond to the standard deviation.

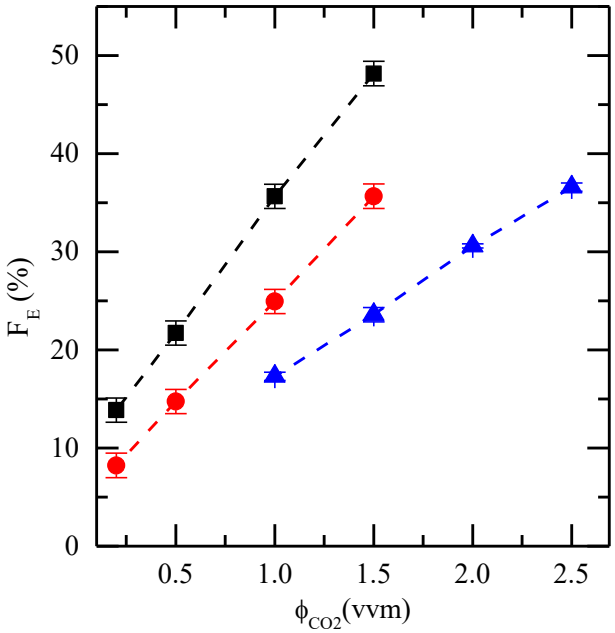

3.3.3. Gas stream ethanol content

The molar fraction of ethanol (y_E) in the gas stream was analyzed using FT-MIR spectroscopy, comparing the results with the thermodynamic equilibrium calculated from the data for the liquid phase (Eq. (3.7)). For evaluation of saturation of ethanol and water in the CO_2 bubbles, analysis of the gas stream was performed with the reactor headspace maintained at the temperature of the liquid phase, using a silicone rubber heater and thermal insulation between the headspace and the MIR spectrometer. As shown in Figure 3.5, the CO_2 bubbles left the bioreactor saturated in all the assays carried out with controlled headspace temperature, since the y_E values reached the gas phase ethanol molar fraction predicted by thermodynamic equilibrium ($y_{E,eq}$).

Figure 3.5 – Molar fractions of ethanol predicted by thermodynamic equilibrium ($y_{E,eq}$, triangles) and measured by FT-MIR spectroscopy in the outlet gas stream, with the reactor headspace maintained at the liquid phase temperature (y_E, circles) and without temperature control (y_E, squares). Error bars correspond to the standard deviation.

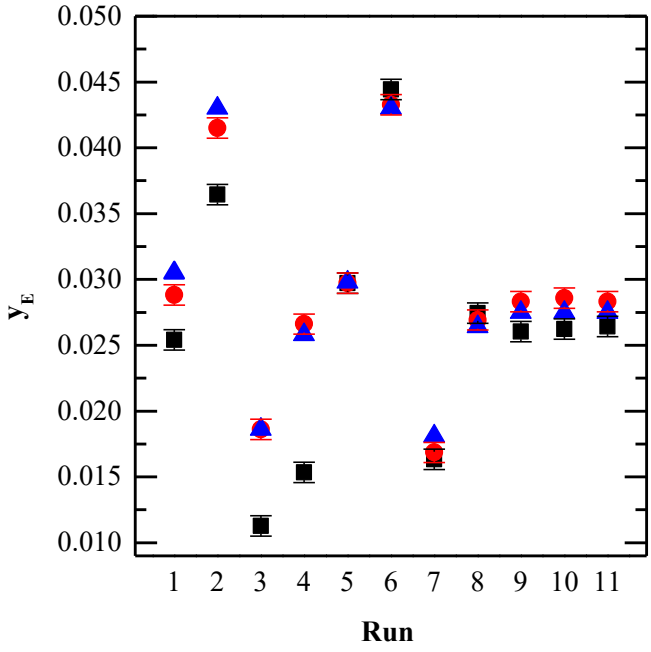

Ezeji et al. (2005) developed a mass balance model showing that larger gas bubbles (diameter of 5.0 mm) should become 95% saturated with butanol in only 0.14 s, when the bubbles rise through a butanol solution. This was consistent with the data obtained here, since saturation was reached in the CO_2 bubbles sparged into the ethanol solution. During the assays, the velocity of the rising bubbles was determined by video analysis, employing Tracker open-access software (https://physlets.org/tracker/), enabling estimation of the time taken by the bubbles to rise through the liquid column. The bubble rising velocities ranged from 0.133±0.017 to 0.198±0.038 m s^{-1}, with a shortest CO_2 bubble rising time of 2.401±0.682 s. Therefore, the CO_2 bubbles had sufficient time to reach ethanol and water saturation during the vacuum-stripping experiments.

For the assays without headspace temperature control (the condition used for the stripping experiments), it was observed (Figure 3.5) that for ϕ_{CO2} of 0.2 vvm (runs 1-4), the composition of the gas leaving the bioreactor was below ethanol saturation. This suggested that the increase of the headspace height caused by the lower CO_2 flow rate led to lower y_E in the outlet gas stream. Calverley et al. (2020) performed ethanol stripping using heated microbubbles, where it was observed that increase of the headspace height was associated with

increased condensation of ethanol and water on the reactor wall. Similar behavior was reported by Martins et al. (2023), who studied the effect of the headspace in ethanol stripping. These findings provided further support for the results obtained for the concentration factor and the ethanol/water selectivity.

3.3.4. Process modeling

Figure 3.6(a) shows the RSD values for all the experiments, which were in the ranges 0.43-2.78% and 0.40-1.04% for the mols of ethanol and water, respectively. Since the RSD represents the standard deviation of the model in comparison to a data set, the low values indicated that the model given by Eqs. (3.4) and (3.5) had good predictive robustness for vacuum-assisted gas stripping performed under different input conditions.

Figure 3.6(b) compares the experimental and simulated data for the mols of ethanol (n_E) and water (n_W) in the liquid phase, according to time, in the assay performed at 28.0 ºC, 0.2 vvm, and 67.97 kPa (run 3, Table 3.2). The model described the decrease in mols of ethanol and water during the vacuum-assisted gas stripping operation, with the behavior being the same as observed for the other conditions studied (data not shown). The results showed that for all the assays, the prediction model provided excellent agreement between the simulated and experimental results, satisfactorily describing the behavior of the process. Hence, it was possible to extend the model previously reported by Silva et al. (2015) to vacuum conditions. The application of a mathematical model can enable description of the entire process, providing analysis and enabling possible economic improvements by the optimization of operating conditions (Mayank et al., 2013; Ivan I.K. Veloso et al., 2023).

Figure 3.6 – Modeling accuracy for the vacuum-assisted gas stripping: (a) RSD values obtained for the model predictions. (b) Simulated (line) and experimental data for mols of ethanol (n_E, squares) and water (n_W, circles), for the stripping assay with specific CO_2 flow rate of 0.2 vvm, temperature of 28.0 ºC, and pressure of 67.97 kPa (run 3).

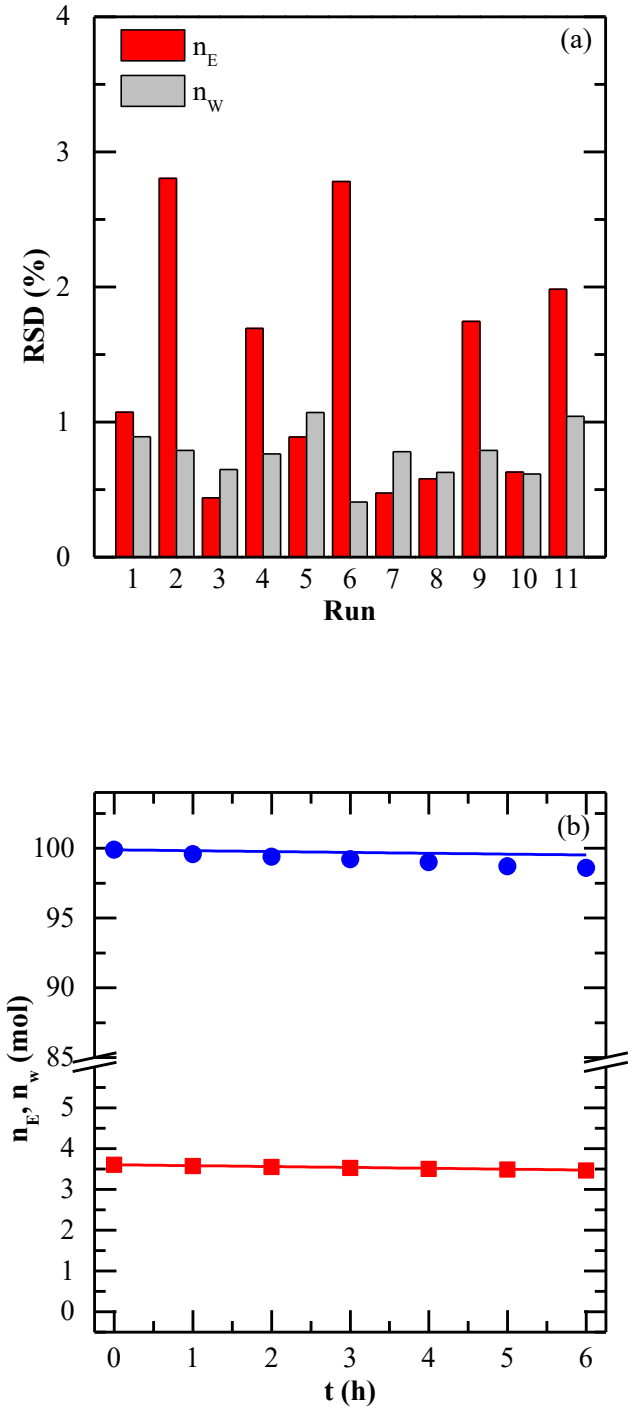

3.3.5. Energy analyses for the vacuum-assisted gas stripping process

Figure 3.7 shows the total power input (P_T), the power input due to isothermal gas expansion (P_{IE}), and the energy requirement (E_{EtOH}), as a function of ϕ_{CO2} and P. The P_T values ranged from 0.14 to 0.39 W, increasing with the increase of ϕ_{CO2} (Figure 7(a)). These results were consistent with data previously reported by Fadavi and Chisti (2007). The measured bioreactor P_T values were linked to the amount of ethanol removed from the liquid phase, since the increase of ϕ_{CO2} led to higher P_T and a higher ethanol removal rate. Furthermore, the superficial velocity of the CO_2 bubbles increased, promoting greater ethanol removal.

The values obtained for the power input due to isothermal expansion (P_{IE}) were in the range from 0.11 to 0.17 W. P_{IE} made the greatest contribution to P_T, accounting for between 71.0 and 81.2% of the total bioreactor power input. The energy requirement (E_{EtOH}) values ranged from 106.7 to 142.6 kJ kg_E^{-1}. Although higher ϕ_{CO2} led to a higher ethanol removal rate, the increase of P_T due to ϕ_{CO2} resulted in a higher energy requirement for ethanol removal in the experiments performed using conventional gas stripping.

The total power input values were 0.27, 0.19, and 0.14 W for the experiments performed at ϕ_{CO2} =1.0 vvm and pressures (P_2) of 41.31, 67.97, and 101.32 kPa, respectively (Figure 7(b)). Increase of the vacuum, resulting in a decrease of the absolute pressure, led to higher P_T. This behavior could be attributed to the change in the ratio between the pressures of the inlet and outlet gas streams (P_1/P_2, in Eq. 3.20), with values of 1.07, 1.05, and 1.03 obtained, respectively. The difference between P_1 and P_2 was due to the pressure drop in the sparger holes, isothermal gas expansion, and the pressure drop at the reactor outlet. For P_{IE}, values of 0.26, 0.16, and 0.11 W were obtained, contributing between 81.1 and 95.3% to P_T.

Figure 3.7 – Values of total power input (PT), power input due to isothermal expansion (P_{IE}), and energy requirement (E_{EtOH}) for (a) different values of ϕ_{CO2} at atmospheric pressure and (b) different pressure conditions at ϕ_{CO2} = 1.0 vvm.

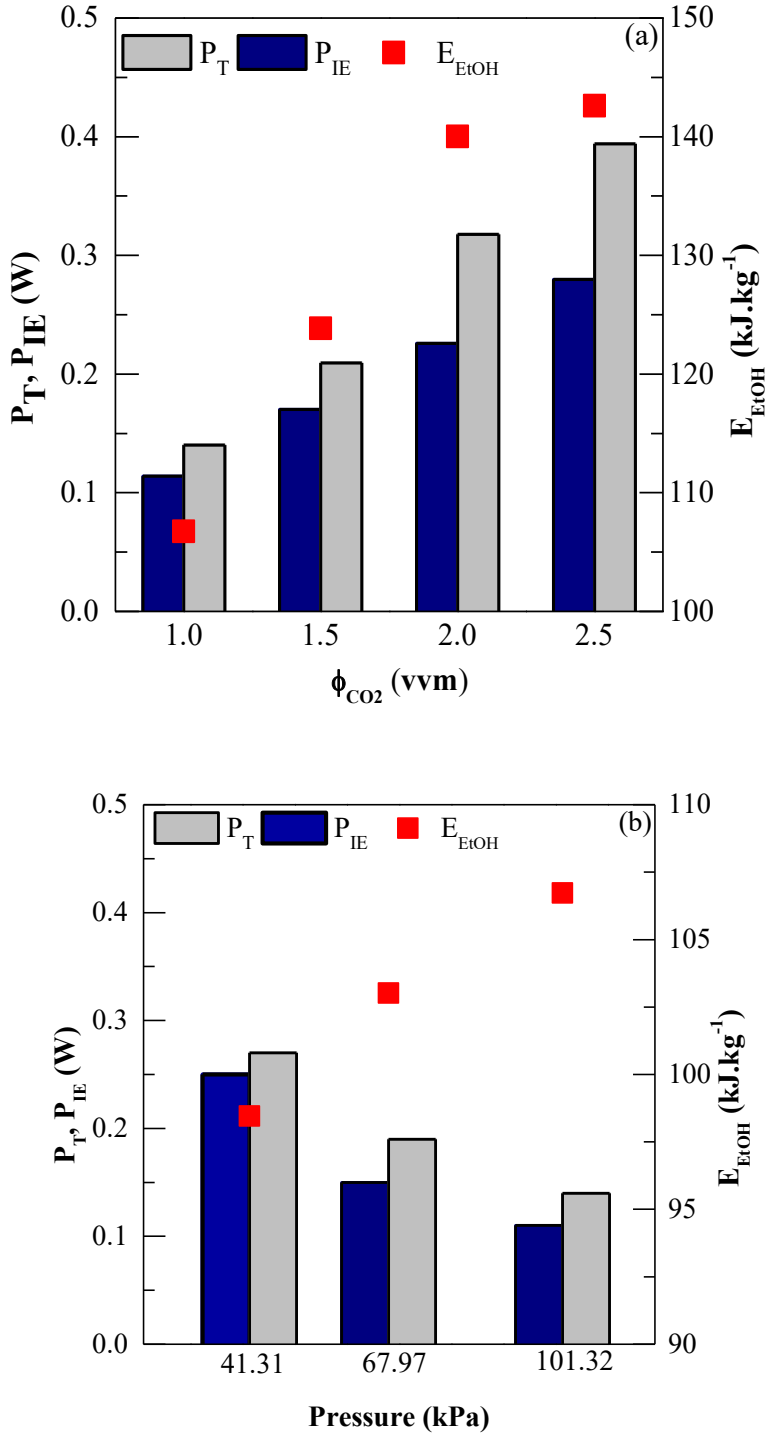

To facilitate a clearer observation of energy savings in the bioreactor, it is interesting to compare experimental conditions with comparable ethanol removal rates. For instance, comparing the operating conditions of 2.5 vvm at 101.32 kPa (Figure 3.7(a)) with 1.0 vvm at

41.31 kPa (Figure 3.7(b)), it is observed that the energy requirement in the vacuum-assisted condition was 30.9% lower than at atmospheric pressure. This difference can be attributed to the fact that the total bioreactor power input (P_T) required for ethanol removal was lower under vacuum conditions. However, it is important to highlight that the energy analysis approach adopted here considered only the bioreactor as the control volume in which ethanol removal occurred. The evaluation was not made of the total energy requirement for the overall process, including the work for gas compression**,** the vacuum pump, and subsequent ethanol recovery. Further studies could focus on technical and economic analyses to establish the feasibility of applying the vacuum-stripping technique on an industrial scale.

3.4. Conclusions

For vacuum-assisted gas stripping, the specific CO_2 flow rate was the most significant variable and presented a positive effect on the entrainment factor (F_E). An increase in the specific CO_2 flow rate increased the contribution of liquid entrainment to ethanol removal, promoting greater ethanol removal. The concentration factor (F_C) and ethanol/water selectivity ($\alpha_{E/W}$) were positively influenced by the CO_2 flow rate, because higher ϕ_{CO2} increased ethanol vaporization, due to the higher volatility of ethanol than water. Furthermore, the highest ethanol content (60 % v v^{-1}) in the gas stream leaving the bioreactor was higher than in the phlegm stream (40~50 % v v^{-1}) obtained in the distillation columns. The developed model was able to accurately describe the ethanol removal during the vacuum-assisted gas stripping operation, with low residual standard deviation values obtained for the mols of ethanol and water. The energy analyses using the bioreactor as control volume revealed that, despite higher power input associated with vacuum conditions in certain scenarios, they generally resulted in greater ethanol removal. Consequently, this led to a reduced energy demand for ethanol removal, which was 30.9% lower compared to the conventional gas stripping method.

CHAPTER 4

4. EXTRACTIVE ETHANOL FERMENTATION FROM SACCHARINE FEEDSTOCK USING VACUUM-ASSISTED GAS STRIPPING

Abstract

The conventional fermentation process is limited by the inhibitory effects of ethanol on yeast cells. Addressing this challenge, extractive fermentation can overcome the ethanol inhibition by removing the product as it is produced. This study investigates extractive fermentation from saccharine feedstock using vacuum-assisted gas stripping, a promising method for improving fermentation performance compared to conventional gas stripping. Extractive fermentation assays were performed using a 2-L bubble column, with monitoring of the gas phase by FT-MIR spectroscopy. The hybrid Andrews–Levenspiel model provided excellent fits to the experimental data from conventional fermentation. In vacuum-stripping fermentation, earlier substrate depletion resulted in an ethanol productivity of 12.03 g L^{-1} h^{-1}, which was 14.35% higher than that of the control. In addition, the vacuum-stripping process led to a 31.3% reduction in the energy requirement for ethanol production compared to conventional gas stripping.

Keywords: Extractive fermentation; ethanol; gas stripping; vacuum; integrated process.

4.1. Introduction

In Brazil, ethanol is produced by a consolidated industrial alcoholic fermentation process. Despite this, ethanol content at the end of fermentation usually reaches 8-11 % v v^{-1}. As a result of this low concentration value, vinasse is obtained in a proportion of 12 L of vinasse per liter of ethanol during the distillation process. Besides, the presence of ethanol also implies inhibitory effects on yeast cells, which affects ethanol production.

Two major strategies have been used to achieve higher ethanol production in fermentation processes: changes in fermentation temperature (Veloso et al., 2019), which result in higher ethanol content at the end of the fermentation; and extractive ethanol fermentation, which diminishes the inhibitory effect of ethanol on yeast cell.

Among the several techniques used to conduct extractive ethanol fermentation, gas stripping emerges as the most suitable technique for this purpose. Its operation includes the use

of a fermentation product (carbon dioxide) and can be conducted in the same vessel used for the fermentation. The application of gas stripping for extractive ethanol fermentation resulted in higher ethanol productivity, allowing the use of higher substrate content (Sonego et al., 2016) and enabling cooling water savings (Almeida et al., 2021; Campos et al., 2025; Veloso et al., 2023)

Several parameters have been studied to increase ethanol productivity using gas stripping extractive fermentation. Using fluid models (such as hydroalcoholic solutions) to evaluate ethanol entrainment during gas stripping, different operating conditions (gas flow rate, gas temperature, fermentation temperature, pressure) , vessel geometries and scales (Silva et al., 2015; Martins et al., 2023) and operation modes (batch, fed-batch and continuous) (Sonego et al. 2014; Sonego et al. 2016; Rodrigues et al., 2018; Almeida et al., 2021) were studied. In addition, the impact of reduced-size bubbles in ethanol entrainment was also evaluated (Pereira et al., 2024).

Based on these findings, several authors performed gas stripping extractive ethanol fermentations and compared them to conventional ethanol fermentations (Sonego et al. 2014; Sonego et al. 2016; Rodrigues et al., 2018; Almeida et al., 2021; Veloso et al., 2023). The results showed increases in ethanol production and productivity using extractive ethanol fermentation. In general, the higher values were found using higher gas flow rates.

Almeida et al. (2024) conducted vacuum-assisted gas stripping assays and evaluated the effects of carbon dioxide flow rate (ϕ_{CO2}), temperature (T), and pressure (P) on ethanol removal performance. Bench scale assays at 34 ◦C and atmospheric pressure exhibited the highest entrainment factor (FE) value with a specific CO_2 flow rate of 2.5 vvm. Similar ethanol removal rates were observed for the assays under vacuum pressure in two different conditions: at 67.97 kPa and 1.5 vvm, and at 41.31 kPa and 1.0 vvm. The results indicated that vacuum-assisted gas stripping could allow the use of reduced gas flow rates, keeping similar ethanol removal rates.

Therefore, the present work aimed to evaluate the use of vacuum-assisted gas stripping for extractive ethanol fermentation from saccharine feedstock. Fourier transform mid-infrared spectroscopy (FT-MIR) was employed to monitor the gas phase compositions.

4.2. Materials and Methods

4.2.1. Microorganism and culture medium

Fermentations were performed using the yeast *Saccharomyces cerevisiae* Y-904 (AB Brasil Indústria e Comércio de Alimentos Ltda, Brazil). The culture medium, simulated sugarcane molasses diluted for use in the industrial process, had the following composition (g L^{-1}): sucrose (171.0), urea (5.32), yeast extract (6.8), $MgSO_4$ $7H_2O$ (1.4), and KH_2PO_4 (5.6). The pH was adjusted to 4.6 using a 5.0 M HCl solution.

4.2.2. Experimental procedure for conventional and extractive fermentations

Conventional and extractive fermentations were conducted in a pneumatic bubble column bioreactor with a working volume of 2 L (liquid height: 33.8 cm; total height: 56.2 cm; internal diameter: 9.7 cm). The yeast (30 g) was pre-hydrated in 600 mL of distilled water (inoculum, representing 30% of the working volume) for 20 minutes. After acclimatization, 1.4 L of must was added to initiate fermentation. A commercial antifoaming agent (SQ 2005, Serquímica) was added (diluted 1:10 m m^{-1}) to prevent excessive foam formation. The temperature was maintained at 34 °C by recirculating water from a thermostatic bath through the bioreactor jacket. Samples of 5 mL were withdrawn every hour to quantify cell, sugar, and ethanol concentration.

Extractive ethanol fermentations (EF) followed the same initial procedure as conventional ethanol fermentation for the first 3 hours. Subsequently, CO_2 was injected into the bottom of the bioreactor through a crosshead sparger, and the bioreactor pressure was regulated using a vacuum pump (Figure 4.1). Three EF experiments were performed under different operational conditions. The first experiment (EFVS) was conducted under reduced pressure (40.1 kPa) with a specific gas flow rate of 1.0 vvm. The remaining two experiments, EFS1 and EFS2, were carried out under atmospheric pressure, with 2.5 and 1.0 vvm specific gas flow rates, respectively.

Figure 4.1 – Schematic illustration of the equipment used in the extractive fermentation experiments: (1) mass flow controller, (2) CO_2 cylinder, (3) bioreactor, (4) vacuum pump, (5) thermostatic bath, (6) gas sampling chamber, (7) spectrometer, and (8) data acquisition.

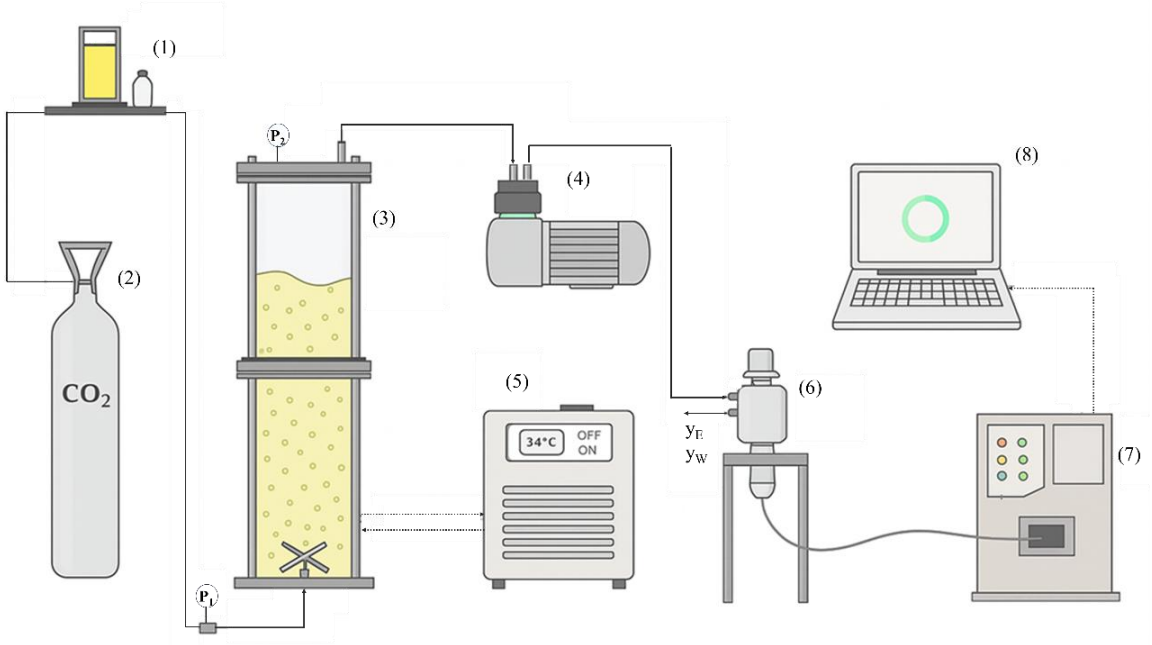

4.2.3. Gas phase concentration analysis

For extractive fermentations, the ethanol concentration in the gas phase was determined by Fourier-transform mid-infrared spectroscopy (FT-MIR). Online measurements were acquired by a gas cell (DST Fiber to Gas Cell, Mettler-Toledo) connected to a spectrometer. Before the analysis, a purge system with nitrogen gas was employed to remove CO_2 and water from the compartment. Spectra were collected from 3335 to 15411 nm (256 scans per sample), at a resolution of 4.2 nm. To cover a wide calibration range, 44 samples with various combinations of ethanol and water molar fractions were used in the calibration procedure, as described by Santos et al. (2022).

4.2.4. Performance parameters

The extractive fermentations were evaluated in terms of concentration factor (F_C) and ethanol/water selectivity ($\alpha_{E/W}$), Eqs. (4.1) and (4.2), respectively.

$$F_C\,(-) = \frac{y_E}{x_E} \tag{4.1}$$

$$\alpha_{E/W}(-)=\frac{y_E/y_W}{x_E/x_W} \quad (4.2)$$

where x_E and x_W are the mass fractions of ethanol and water in the liquid phase, and y_E and y_W are the mass fractions of ethanol and water in the gas phase.

The molar fraction of ethanol in the liquid phase (x_E) was determined using an experimental correlation (Eq. (4.3)), which was developed for alcoholic solutions with ethanol concentrations (C_E) ranging from 0 to 88.6 g L^{-1} at a temperature of 34 °C. The sum of molar fractions of ethanol and water in the liquid phase was determined using Eq. (4.4).

$$x_E=\frac{C_E}{2418.5} \quad (4.3)$$

$$x_E+x_W=1 \quad (4.4)$$

4.2.5. Modeling of conventional and extractive fermentations

The mathematical model describes the fermentation process based on mass balance equations for cell, substrate, and ethanol (Eqs. (4.5)–(4.8)), considering the volume variation due to mass removal rates of ethanol and water by stripping (Rodrigues et al., 2018).

$$\frac{dC_X}{dt}=\mu\cdot C_x-\frac{C_X}{V}\cdot\frac{dV}{dt} \quad (4.5)$$

$$\frac{dC_S}{dt}=-\frac{1}{Y_{X/S}}\mu\cdot C_x-\frac{C_S}{V}\cdot\frac{dV}{dt} \quad (4.6)$$

$$\frac{dC_E}{dt}=\frac{Y_{E/S}}{Y_{X/S}}\mu\cdot C_x-k_E\cdot C_E-\frac{C_E}{V}\cdot\frac{dV}{dt} \quad (4.7)$$

$$\frac{dV}{dt}=-\frac{\left(k_E\cdot C_E+k_W\cdot(\rho_L-C_E)\right)\cdot V}{\rho_W} \quad (4.8)$$

where μ is the specific cell growth rate (h^{-1}), C_X is the total cell concentration (g L^{-1}), C_S is the substrate concentration (g L^{-1}), C_E is the ethanol concentration (g L^{-1}), $Y_{X/S}$ is the cell yield coefficient (g_X g_S^{-1}), $Y_{E/S}$ is the ethanol yield coefficient (g_E g_S^{-1}), ρ_L is the specific mass of solution (g L^{-1}), and k_E and k_W are the removal rate constants for ethanol and water, respectively (h^{-1}).

The specific cell growth rate (μ) was described using the hybrid Andrews-Levenspiel kinetic model (Andrews, 1968; Levenspiel, 1980), which considers inhibition by substrate and ethanol:

$$\mu=\mu_{max}\cdot\frac{C_S}{K_S+C_S+\frac{C_S^2}{K_{IS}}}\cdot\left(1-\frac{C_E}{C_{Emax}}\right)^n \quad (4.9)$$

where μ_{max} is the maximum specific cell growth rate (h^{-1}), K_S is the saturation constant (g L^{-1}), K_{IS} is the substrate inhibition constant (g L^{-1}), C_{Emax} is the ethanol concentration causing cell growth to cease (g L^{-1}), and n is a dimensionless parameter related to the ethanol toxic potential.

According to Eq. (4.10), the specific mass of the solution (ρ_L) was calculated as a function of the ethanol concentration at each time

$$\rho_L=994.42+19.98\cdot10^{-2}\cdot C_E+1.55\cdot10^{-4}\cdot C_E^2 \quad (4.10)$$

The cell ($Y_{X/S}$) and ethanol yield coefficients ($Y_{E/S}$) were determined using Eqs. (4.11) and (4.12).

$$Y_{X/S}=\frac{C_{Xf}-C_{X0}}{C_{S0}-C_{Sf}} \quad (4.11)$$

$$Y_{E/S}=\frac{C_{Ef}-C_{E0}}{C_{S0}-C_{Sf}} \quad (4.12)$$

where the subscripts “0” and “f” represent the initial and final times of the culture, respectively.

In conventional fermentations, the constants k_E and k_W were equal to zero ($k_E=k_W=0$) because there was no removal of ethanol or water. For the extractive fermentations, k_E and k_W were calculated using equations obtained from mass balance for ethanol and water, according to the methodology proposed by Rodrigues et al. (2018). The experiments were carried out using an ethanol solution with an initial ethanol concentration of 80 g L^{-1}.

The mathematical model described in this work was implemented using Scilab v. 6.0.1 software, and the Runge-Kutta algorithm was employed for the numerical solution of the differential equations system. The prediction quality of the model was assessed using the statistical criterion of residual standard deviation (RSD) proposed by Cleran et al. (Cleran et al., 1991) and defined by Eq. (4.13).

$$RSD(\%)=\frac{\sqrt{\frac{1}{N_p}\sum_{j=1}^{N_p}\left(C_{exp}(t_j)-C_{sim}(t_j)\right)^2}}{\overline{C}_{exp}}\times 10 \tag{4.13}$$

where $C_{exp}(t_j)$ is the experimental concentration at time t_j, $C_{sim}(t_j)$ is the simulated concentration predicted by the model at time t_j, $\overline{C}_{exp}$ is the average of the experimental concentrations, and Np is the number of experimental points.

4.2.6. Energy analysis for ethanol production

The extractive fermentations were also analyzed based on the energy required for ethanol production (E_{EtOH}). This performance parameter was calculated as the ratio of the power input (P_T) to the ethanol production rate (R_{EtOH}), representing the energy cost of ethanol production, as shown in Eq. (4.14).

$$E_{EtOH}=\frac{P_T}{R_{EtOH}} \tag{4.14}$$

where E_{EtOH} is the energy required for ethanol production (J g_E^{-1}), and R_{EtOH} is the ethanol production rate (g s^{-1}).

The total power input in the extractive fermentations was calculated using Eq. (4.15), considering the gas streams at bioreactor inlet (1) and outlet (2) (Figure 4.1).

$$P_T=Q_m\cdot R\cdot T\cdot \ln\left(\frac{P_1}{P_2}\right) \tag{4.15}$$

where P_T (W≡J s^{-1}) is the total power input, Q_m is the molar gas flow rate (kmol s^{-1}), R is the

gas constant (8314 J $kmol^{-1}$ K^{-1}), P_1 is the pressure in the inlet gas stream (Pa), and P_2 is the pressure in the outlet gas stream (Pa).

4.2.7. Analytical methods

The cell concentration, on a dry basis, was determined using the gravimetric method. Samples were centrifuged at 9000 rpm and 4°C for 10 min. The precipitate was washed twice with distilled water and then dried at 80°C for 24 h. The viable cell percentage was determined using the methylene blue staining method (Lee et al., 1981), and cell counting was performed with an optical microscope (BX 50F-3, Olympus, Tokyo, Japan) and a Neubauer chamber. The viable cell concentration (C_{XV}) was calculated by multiplying the cell concentration by the percentage of viable cells. The concentrations of sucrose, glucose, fructose, and ethanol in the supernatant were determined using an HPLC system (Waters, U.S.A.) equipped with a refractive index detector and a Sugar-Pak I column (300 × 6.5 mm, 10 μm, Waters) maintained at 80 °C. The eluent was ultrapure water containing 50 mg L^{-1} of calcium EDTA (calcium disodium ethylenediaminetetraacetate hydrate) at a flow rate of 0.5 mL min^{-1}. The standards were sucrose, glucose, fructose, and ethanol solutions at concentrations ranging from 0.1 to 10.0 g L^{-1}.

4.3. Results and discussion

4.3.1. Conventional fermentation

Figure 4.2 shows the experimental and simulated time-course profile for viable cells (C_{VX}), substrate (C_S), and ethanol (C_E) in conventional fermentation. The total substrate consumption occurred within 8 hours, achieving a total ethanol concentration of 84.22 g L^{-1} (10.7% v v^{-1}) and ethanol productivity (P_E) of 10.53 g L^{-1} h^{-1}. The yield coefficients for cell ($Y_{X/S}$) and ethanol ($Y_{E/S}$) were calculated from experimental data of C_{VX}, C_S, and C_E, as described in Eqs. (4.8) and (4.9). The ethanol yield coefficient ($Y_{E/S}$) was 0.468 g_E g_S^{-1}, corresponding to 90% of the theoretical maximum yield (0.511 g_E g_S^{-1}). The cell yield coefficient ($Y_{X/S}$) was 0.04 g_X g_S^{-1}. These values agree with those typically observed in industrial fermentations, which generally achieve final ethanol concentrations of 8–11% v v^{-1} and ethanol yields of 90–92% of the theoretical maximum (Basso et al., 2011).

Figure 4.2 – Simulated (lines) and experimental data (points) in conventional fermentation experiments for viable cells (triangles), substrate (circles), and ethanol (squares) concentration. Error bars correspond to the standard deviation.

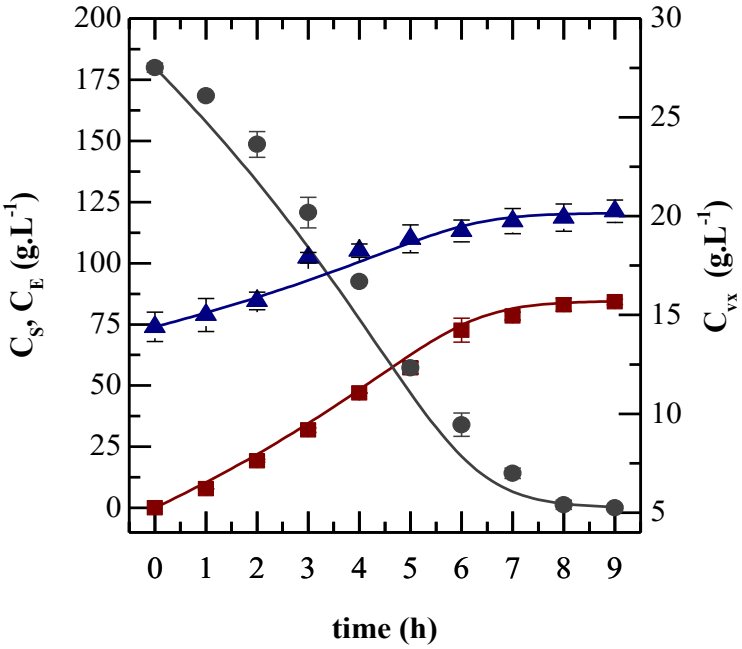

Moreover, the model accurately fits the experimental data (Figure 4.2). These results indicate that the hybrid Andrews–Levenspiel kinetic model effectively describes the behavior of ethanol fermentation. Table 4.1 shows the estimated kinetic parameters, which are consistent with values reported in the literature for similar experimental conditions (Rodrigues et al., 2025; Silva et al., 2024). Mathematical modeling is a fundamental tool for optimizing fermentation processes. It enables the prediction of cell growth dynamics, substrate consumption, and ethanol production, thereby supporting the design of efficient ethanol fermentation process configurations.

Table 4.1 – Values of kinetic and yield parameters from conventional fermentation.

Estimated parameter	**Value**	**Unit**
$\mu_{máx}$	0.152	h^{-1}
K_S	45.17	$g\ L^{-1}$
K_{IS}	91.09	$g\ L^{-1}$
C_{Emax}	99.98	$g\ L^{-1}$
n	0.201	–
Fixed parameter	**Value**	**Unit**
$Y_{X/S}$	0.032	$g_X\ g_S^{-1}$
$Y_{E/S}$	0.467	$g_E\ g_S^{-1}$

4.3.2. Extractive fermentation

Ethanol extractive fermentation was investigated under different operating conditions for specific gas flow rates and pressure. Figure 4.3 presents experimental and simulated data for viable cells (C_{VX}), substrate (C_S), and ethanol (C_E) in the EFVS (Figure 4.3a), EFS1 (Figure 4.3b), and EFS2 (Figure 4.3c) fermentations. Complete substrate depletion occurred within 7 hours in the extractive fermentations EFVS and EFS1, earlier than in the conventional process (Figure 4.2). This behavior was attributed to the reduced ethanol inhibition in yeast due to the lower ethanol concentrations in the fermentation broth.

Ethanol productivities (Table 4.2) for EFVS and EFS1 were calculated as 12.02 $g\ L^{-1}\ h^{-1}$, based on the total ethanol concentration (C_{ET}) ratio to the time required for complete substrate depletion. C_{ET} values were determined considering the ethanol yield coefficient relative to the total substrate concentration (C_S). Thus, similar C_{ET} values were expected for both extractive and conventional fermentations, as all were performed with an initial substrate concentration of 180.0 $g\ L^{-1}$. Moreover, the extractive fermentations EFVS and EFS1 achieved a 14.35% increase in ethanol volumetric productivity compared to conventional fermentation, highlighting the effectiveness of *in situ* ethanol removal in enhancing overall fermentation performance. These findings align with the results reported by Sonego et al. (2016), who observed a 13.20% increase in ethanol productivity for fed-batch extractive fermentation performed at a specific flow rate of 2.5 vvm and substrate concentration of 180.0 gL^{-1}.

Figure 4.3 – Simulated (lines) and experimental data (points) for viable cells (triangles), substrate (circles), and ethanol (squares) concentration in the extractive fermentations (a) EFVS, (b) EFS1, and (c) EFS2. Error bars correspond to the standard deviation.

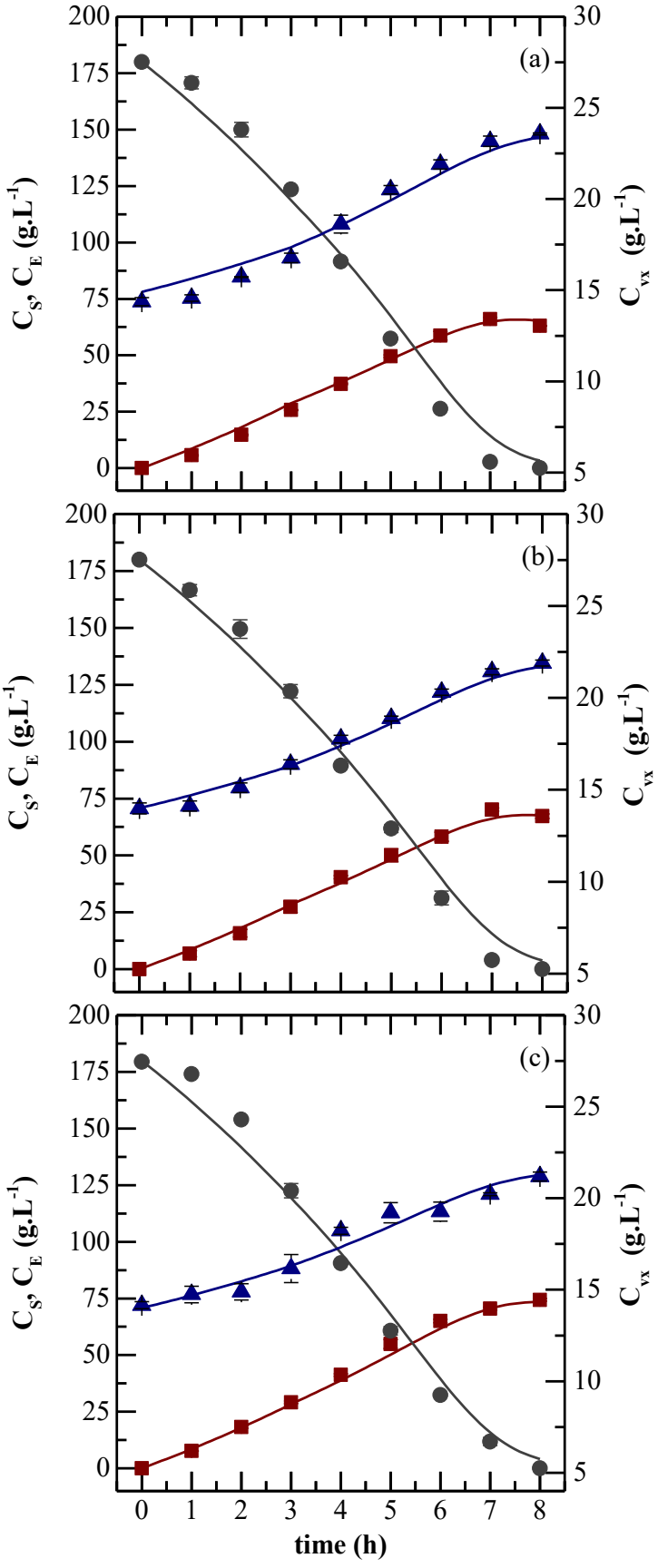

It is important to highlight that the similar performance between the extractive fermentations EFVS and EFS1 resulted from both operating at an equivalent ethanol removal rate. However, extractive fermentation using vacuum-stripping (EFVS) achieved this performance with less than half the specific gas flow rate required by conventional gas stripping at 2.5 vvm (EFS1). As reported by Almeida et al. (2024), applying vacuum conditions leads to a higher composition of ethanol and water in the gas phase, as the reduced pressure decreases the saturation temperature. Consequently, the removal of ethanol and water is enhanced, allowing effective extraction with a lower gas flow rate.

Table 4.2 – Performance comparison of conventional and extractive fermentations.

Variable	**Unit**	**Fermentation**			
		CF	EFVS	EFS1	EFS2
Total C_G consumed	g L^{-1}	179.96	180.01	179.65	180.00
Maximum C_E in the broth	g L^{-1}	84.22	63.02	66.32	74.90
Total C_E at the end of fermentation	g L^{-1}	84.22	84.24[a]	84.07[a]	84.24[a]
Ethanol productivity (P_E)	g L^{-1} h^{-1}	10.52	12.03	12.02	10.53
k_E	h^{-1}	-	0.071	0.074	0.034
k_W	h^{-1}	-	0.008	0.009	0.003

[a] Calculated considering $Y_{E/G}$ ($g_E \cdot g_S^{-1}$) = 0.467.

Regarding the results for EFS2 (Figure 4.3c), the fermentation profile closely resembled the conventional process. Complete substrate consumption was achieved within 8 hours, with an ethanol productivity of 10.52 g L^{-1} h^{-1} and a final ethanol concentration (C_E) of 74.90 g L^{-1} in the fermentation broth. The amount of ethanol removed at 1 vvm was insufficient to reduce the product inhibitory effects, which explains the EFS2 fermentation behavior similar to that observed under conventional conditions. These findings highlight the significance of applying vacuum-stripping in fermentation. This strategy enables efficient ethanol removal at reduced CO_2 flow rates, enhancing process intensification and facilitating industrial-scale implementation.

4.3.3. Model predictive performance

The predictive performance of the mathematical model was evaluated using the coefficient of determination (R^2) and the residual standard deviation (RSD) for viable cells (C_{VX}), substrate (C_S), and ethanol (C_E). As shown in Figure 4.4, low RSD values were obtained for ethanol (<4%), and viable cells (<6%), while the substrate presented slightly higher values (<14%). In bioprocess modeling, RSD values below 10% are considered acceptable (Atala, 2001). The RSD values for the substrate were slightly above 10%. Nevertheless, such deviations are commonly observed in simulation studies of fermentation processes (Veloso et al., 2019; Silva et al., 2024).

Across all fermentation experiments, the model demonstrated consistently high R^2 values (>0.96), confirming its ability to represent the dynamic behavior of the process with high accuracy. These statistical indicators reinforce the robustness of the proposed kinetic approach in simulating ethanol fermentation under different operational scenarios, including extractive configurations with *in situ* ethanol removal.

Figure 4.4 – RSD values for the kinetic model predictions of cells (C_X, red), substrate (C_S, gray), and ethanol (C_E, blue) concentrations in conventional and extractive fermentation processes.

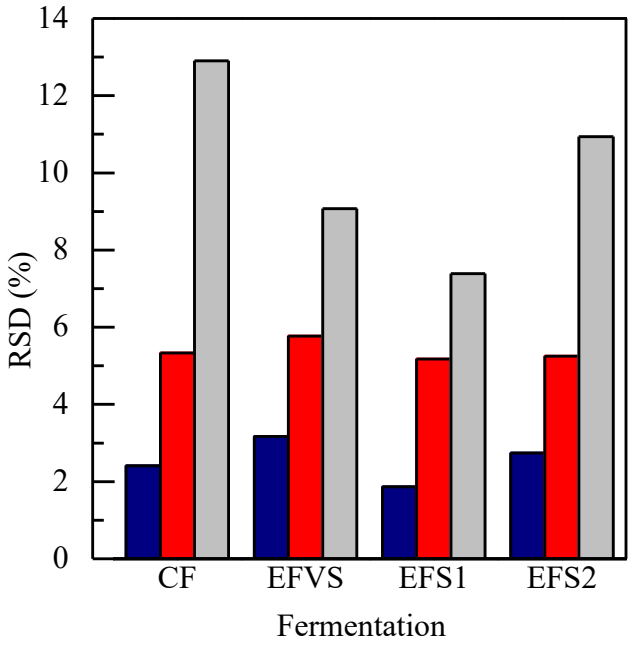

4.3.4. Evaluation of performance parameters in the extractive fermentations

The extractive fermentations EFVS, EFS1, and EFS2 were evaluated based on the

performance parameters ethanol concentration factor (F_C) and ethanol/water selectivity ($\alpha_{E/W}$), using data from monitoring the liquid and gas phases. As shown in Figure 4.5, similar values of F_C and $\alpha_{E/W\ were}$ obtained for EFVS and EFS1. These results suggest that the vacuum application did not influence ethanol enrichment in the gas stream nor its preferential separation over water. This behavior is consistent with the findings reported previously by Almeida et al. (2024), in which the vacuum condition had no significant effect on F_C or $\alpha_{E/W}$. Although vacuum promotes higher volatilization of ethanol by reducing its boiling point, it also increases the evaporation of water. As a result, both components are transferred from liquid to gas phase in similar proportions, which limits an improvement in F_C or $\alpha_{E/W}$.

Figure 4.5 – Concentration factor (F_C, blue) and ethanol/water selectivity ($\alpha_{E/W}$, red) for EFVS, EFS1, and EFS2.

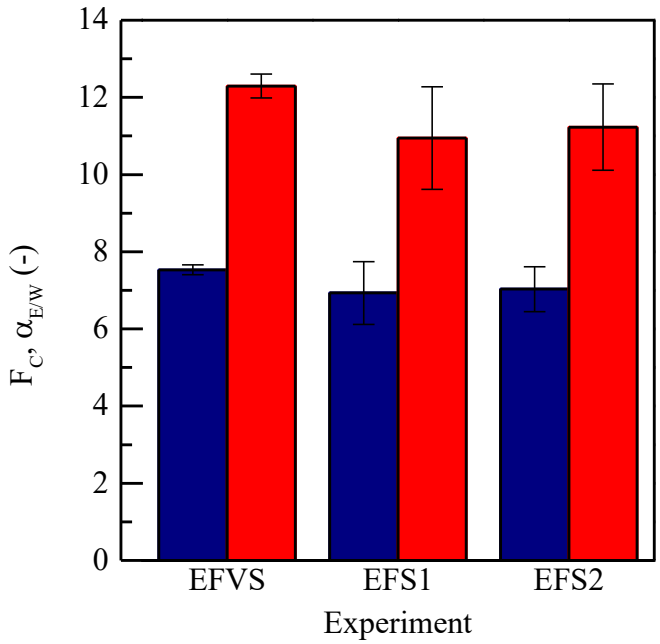

Notably, the values of F_C and $\alpha_{E/W}$ obtained during extractive fermentation were higher than those reported by Almeida et al. (2024) under similar operating conditions using ethanol solutions. This enhancement may be attributed to the thermodynamic effects of the sugars, glucose and fructose in the fermentation broth. According to Dias et al. (2017), the addition of fructose modified the vapor-liquid equilibrium of ethanol-water mixtures, increasing the activity coefficient of ethanol and decreasing that of water. This effect enhanced the volatility of ethanol relative to water, shifting the phase equilibrium toward a more ethanol-enriched

vapor composition.

4.3.5. Energy requirements for ethanol production by extractive fermentation

The energy requirement for ethanol production (E_{EtOH}) was calculated using the experimental values of power input (P_T) and ethanol production rate (R_{EtOH}). Based on the previous productivity results, only the EFSV and EFS1 experiments were considered in the energy analysis, as ethanol productivity could not be improved under the EFS2 operating conditions.

Table 4.3 presents the E_{EtOH} values calculated for the extractive fermentation experiments. For the vacuum-assisted gas stripping (EFVS), the E_{EtOH} was 40.6 J g_E^{-1}, whereas the conventional extractive fermentation (EFS1) required 59.1 J g_E^{-1}. The values obtained in this study are in agreement with those reported in the literature. Martins et al. (2023) simulated extractive fermentations in a 10.0 L bubble column bioreactor and reported E_{EtOH} values ranging from 12.9 to 77.2 J g_E^{-1}, depending on the operating conditions and geometric configurations.

Table 4.3 – Values of total power input (P_T), and energy requirement for ethanol production (E_{EtOH}) in the extractive fermentations.

Fermentation	P_T (W≡J s^{-1})	E_{EtOH} (J g_E^{-1}),
EFVS	0.27	40.60
EFS1	0.39	59.10

These results indicate that the energy required to produce 1 g of ethanol was 31.30% lower in the EFVS process, since the total power input (P_T) into the bioreactor was lower in vacuum conditions. Under the conventional gas stripping condition at 2.5 vvm (EFS1), the high specific gas flow rate results in a substantial molar gas flow Q_m, which strongly influences the total power input (P_T), as defined in Eq. (15). Therefore, the conventional stripping process exhibits a higher energy demand (E_{EtOH}) than the vacuum-stripping fermentation.

4.4. Conclusions

The Andrews–Levenspiel hybrid kinetic model provided an excellent fit to the experimental data obtained from conventional ethanol fermentation, allowing accurate estimation of the kinetic parameters. Extractive ethanol fermentations (EFVS and EFS1)

demonstrated a 14.35% higher volumetric ethanol productivity compared to conventional fermentation. It is important to highlight that EFVS achieved this performance with less than half the specific gas flow rate required by EFS1. Furthermore, vacuum-assisted gas stripping significantly reduced the energy requirement for ethanol production in extractive fermentation, resulting in a 31.3% decrease compared to conventional gas stripping.

CHAPTER 5

5. BIOETHANOL PRODUCTION FROM SORGHUM VIA EXTRACTIVE FERMENTATION WITH VACUUM-ASSISTED GAS STRIPPING: EXPERIMENTAL AND MODELING

Abstract

Extractive fermentation can mitigate the inhibitory effects of ethanol on yeast cells by continuously removing ethanol as it is produced, which can significantly enhance ethanol productivity during the fermentation of sorghum hydrolysates. The present study describes the modeling and experimental validation of ethanol production in separate hydrolysis and fermentation (SHF) and simultaneous saccharification and fermentation (SSF) processes, utilizing vacuum-assisted gas stripping for ethanol removal. Initially, kinetic parameters for saccharification and fermentation were determined separately. Subsequently, SSF experiments were conducted to evaluate the predictive capability of the proposed model. Finally, both SHF and SSF processes with ethanol removal were carried out in a 2–liter bubble column bioreactor utilizing vacuum-assisted gas stripping. The proposed model for SHF and SSF processes, based on mass balances for liquefied starch (St), glucose (G), and ethanol (E), and considering both kinetics of saccharification and fermentation with product inhibition, demonstrated excellent fit to the experimental data for both conventional and extractive fermentations. Furthermore, the extractive fermentations demonstrated superior performance compared to conventional methods, achieving ethanol productivity (P_E) values up to 60% higher.

Keywords: Bioethanol from sorghum; extractive fermentation; gas stripping; vacuum; integrated process.

5.1. Introduction

Concerns about climate change, driven by greenhouse gas emissions and the depletion of fossil fuel-based energy sources such as oil, coal, and natural gas, have led to an increased demand for renewable energy solutions (Joyia et al., 2024; Yeboah and Shaik, 2021). Among them, bioenergy is a sustainable alternative to conventional energy sources. It is derived from biomass and enables the production of various products, including biohydrogen, biogas, bio-

oil, biochar, bioethanol, biodiesel, and syngas (Agarwal and Kumar, 2018; Ahmad et al., 2016; Stamenković et al., 2020). Bioethanol is the most widely used transportation biofuel due to its high-octane number. It can be blended with gasoline or used as stand-alone vehicle fuel (Prasad et al., 2007). The United States is the largest ethanol producer, contributing 52% of global output, followed by Brazil with 28%. In the 2024 harvest, global ethanol production reached a total of 118.17 billion liters (Renewable fuel association, 2024.).

Conventional crops such as sugarcane, corn, cassava, sorghum, and other grains can be used as feedstock to produce bioethanol through microbial fermentation (Arif et al., 2024). Grain sorghum is a starch-rich cereal similar to corn and well-suited for bioethanol production. It offers agronomic advantages, including adaptability to various soils and climates, efficient water use, and drought tolerance (Ramírez et al., 2016). Currently, 8.07 million tons of sorghum are produced in the U.S., with around one-third of the total sorghum being used for ethanol production (U.S. Department of Agriculture, 2024). Due to its potential for biofuel applications, several studies have been investigated ethanol production from sorghum (Ai et al., 2011; Appiah-Nkansah et al., 2018; Weiss et al., 2025). Weiss et al. (2022) evaluated different sorghum varieties and yeast strains to assess their effects on ethanol concentration and yield during the fermentation process. According to the authors, waxy sorghum and Ethanol Red yeast achieved the highest average ethanol concentration and yield.

The dry-grind process is the most common method for producing sorghum ethanol, and plants typically operate with a solid slurry concentration of 25–32% w w^{-1}. The process includes size reduction, liquefaction, saccharification, fermentation, distillation, and coproduct recovery, yielding dried distiller's grain with solubles (DDGS) and wet distiller's grain with solubles (WDGS) (Kumar et al., 2018). The fermentation process can be performed either sequentially to saccharification, known as separated hydrolysis and fermentation (SHF), or through simultaneous saccharification and fermentation (SSF), in which the hydrolysis is carried out progressively throughout the process. The released glucose is directly metabolized, avoiding osmotic stress and the cellular growth inhibition (Ishizaki and Hasumi, 2014; Marulanda et al., 2019; Taylor et al., 2010). At the end of the fermentation process, the ethanol content reaches around 12–15% v v^{-1}. Ethanol accumulation in the fermentative broth is a critical factor that can affect fermentation due to its inhibitory effect on yeast metabolism. One approach to overcome the inhibitory effects is extractive fermentation, which includes several techniques (such as gas stripping, liquid-liquid extraction) that have been investigated for ethanol recovery from the broth during its production (Kumar et al., 2018; Lemos et al., 2020;

Martins et al., 2020; Pereira et al., 2024).

Vacuum-assisted gas stripping is a promising technique for removing ethanol from fermentation broth and offers advantages such as simple operation and high ethanol selectivity. Almeida et al. (2024) successfully applied vacuum-stripping for ethanol removal in preliminary tests using hydroalcoholic solutions. The authors achieved a gas stream six times more concentrated in ethanol than the liquid phase. However, to the best of our knowledge, vacuum-assisted gas stripping has not yet been applied in extractive fermentation processes such as SHF and SSF. Moreover, developing a suitable model to express the behavior of the extractive fermentation process would be very useful for supporting scale-up studies.

This study investigates ethanol removal from the SHF and SSF processes using vacuum-assisted gas stripping. A fermentation model was developed, and kinetic parameters were determined through a model-based optimization algorithm. First, the kinetic parameters of saccharification and fermentation were determined individually. Then, SSF experiments were conducted to evaluate the predictive capacity of the proposed model. Finally, applying vacuum and gas stripping, SHF and SSF experiments with ethanol removal were carried out. The findings of this study contribute to the development of a reliable mathematical model for both conventional and extractive SHF and SSF processes.

5.2. Materials and methods

5.2.1. Sorghum, enzymes and microorganism

Grain sorghum was obtained from a commercial seed company (MBS Seed, Denton, TX, USA). The enzymes α-amylase (Liquozyme®) and glucoamylase (Spirizyme®) were sourced from Novonesis (Bagsvaerd, Denmark). Commercial dried *Saccharomyces cerevisiae* strain (Ethanol Red, Fermentis-Lessaffre Yeast Corporation, Marquette-lez-Lille, France) was used as the ethanol-producing microorganism.

5.2.2. Liquefaction

Grain sorghum was ground using a cyclone sample mill (Model 3010, Udy Corporation, Fort Collins, CO, USA) equipped with a 1.0-mm screen. A sorghum slurry with 25% w w^{-1} solid content (dry basis) was prepared in 250 mL Erlenmeyer flasks, each containing 100 mL working volume. Then, 20 μL of α-amylase enzyme was added in each flask.

Liquefaction was carried out in a water-bath shaker (Model 939XL, Amerex Instruments, Concord, CA, USA) at 170 rpm. The temperature was gradually increased from 70 to 90°C over 30 min, then reduced to 85°C and maintained for 60 min (Weiss et al., 2023).

5.2.3. Saccharification

5.2.3.1. Experimental procedure

Following liquefaction with α-amylase, saccharification was carried out in the same Erlenmeyer flasks at 32 °C and pH 4.2 for 12 hours in a shaker incubator set at 150 rpm. Each flask (run in duplicate) received 100 µL of glucoamylase enzyme. Samples were collected every 2 h to measure glucose concentration, and glucoamylase was deactivated by immersing samples in boiling water for 10 min. The activity of glucoamylase was defined as the amount of enzyme required to release 1 µmol of glucose per min, calculated based on the initial reaction rate.

5.2.3.2. Mathematical modeling of saccharification

The saccharification model was developed based on the mass balances for liquefied starch (St) (Eq. (5.1)) and glucose (G) (Eq. (5.2)). The hydrolysis kinetics catalyzed by glucoamylase was described using Michaelis–Menten kinetics with competitive glucose inhibition.

$$\frac{dC_{St}}{dt} = -\frac{k_1 \cdot C_{Enz} \cdot C_{St}}{K_m\left(1+\frac{C_G}{K_i^G}\right)+C_{St}} \tag{5.1}$$

$$\frac{dC_G}{dt} = 1.11 \cdot \frac{k_1 \cdot C_{Enz} \cdot C_{St}}{K_m\left(1+\frac{C_G}{K_i^G}\right)+C_{St}} \tag{5.2}$$

where k_1 is the hydrolysis rate constant (g $U^{-1}h^{-1}$), K_m is the Michaelis-Menten constant (g L^{-1}), K_i^G is the inhibition constant of glucoamylase by glucose (g L^{-1}), C_{enz} is the enzyme concentration (U L^{-1}), C_{St} is the liquified starch concentration (g L^{-1}), and C_G is the glucose concentration (g L^{-1}). The constant "1.11" included in Eq. (2) represents the theoretical yield coefficient ($Y_{Gl/St}$=1.11 g_{Gl} g_{St}^{-1}). It was derived from the stoichiometric equation for the

hydrolysis of starch into glucose in water (Kroumov et al., 2006).

5.2.4. SHF and SSF

In the SHF assays, the pH of the liquefied sorghum slurry was first adjusted to 5.5 with 1M HCl. Then, 100 μL of glucoamylase enzyme was added, and saccharification was performed at 65°C for 12 h using a water-bath shaker at 170 rpm. After saccharification, the pH was adjusted to 4.2 with 1 M HCl. Next, 1 mL of activated yeast culture, 0.1 g of KH_2PO_4, and 0.3 g of yeast extract were added to each flask. Ethanol fermentations were carried out (in duplicate) at 32°C for 72 h in a shaker incubator set at 150 rpm. The yeast culture was prepared by dispersing 1.0 g of dry yeast in 19 mL of culture medium, followed by incubation in a shaking incubator at 38°C for 30 min with agitation set at 150 rpm. The culture medium consisted of 20 g L^{-1} glucose, 5.0 g L^{-1} peptone, 3.0 g L^{-1} yeast extract, 1.0 g L^{-1} KH_2PO_4, and 0.5 g L^{-1} $MgSO_4 \cdot 7H_2O$.

For SSF assays, yeast and glucoamylase enzyme were added at the same time to the liquefied sorghum slurry in the same amounts used for SHF assays. SSF assays were carried out (in duplicate) at 32°C and pH 4.2 for 72 h in a shaker incubator set at 150 rpm. Samples (2 mL) were collected at various time intervals to monitor the fermentation process.

5.2.5. Extractive ethanol fermentations

Extractive ethanol fermentations for both SHF and SSF methods were performed in a bubble column pneumatic bioreactor (2–L working volume, 9.7 cm internal diameter, 33.8 cm liquid height, and 56.2 cm total height). The bioreactor pressure (at vacuum conditions) was maintained at 41.3 kPa by a vacuum pump, and CO_2 was injected at 1.0 vvm through a perforated cross-sparger at the base of the bioreactor. The fermentation temperature was kept at 32°C using a thermostatic bath connected to a water jacket on the bioreactor. Figure 5.1 shows the experimental apparatus used in the extractive fermentations.

Figure 5.1 – Schematic illustration of the experimental apparatus used in the extractive fermentations: (a) CO_2 cylinder, (b) mass flow controller, (c) bioreactor, (d) vacuum pump, and (e) thermostatic bath.

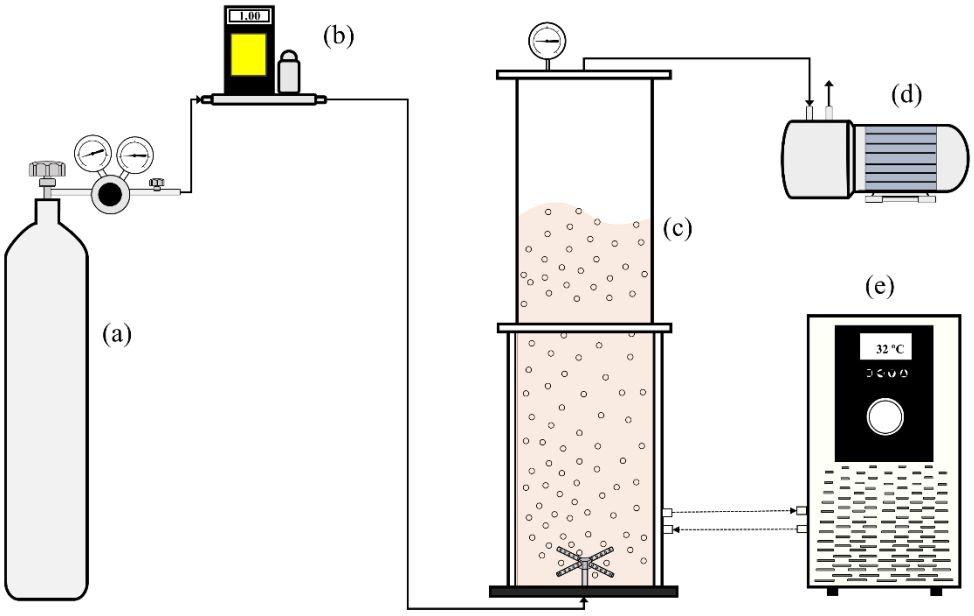

5.2.6. Analytical methods

The moisture content of sorghum was determined using the AOAC 930.15 standard method. Starch content was analyzed with the Megazyme Total Starch Assay Kit, following AACC method 79-13. Glucose and ethanol concentrations were measured by high-performance liquid chromatography (HPLC) using an Agilent system (1200 series, Santa Clara, CA, USA) equipped with a refractive index detector operated at 45 °C, and an HPX-87H organic acid column (7.8 × 300 mm) maintained at 60 °C. The mobile phase consisted of 5 mM H_2SO_4 at a flow rate of 0.60 mL min^{-1}.

5.2.7. Mathematical modeling of conventional and extractive ethanol fermentation

Mathematical models were developed to describe conventional and extractive fermentation for SHF and SSF processes.

5.2.7.1. SHF

The extractive SHF model was developed based on the mass balances for total cells (X)

(Eq. (5.3)), glucose (G) (Eq. (5.4)), and ethanol (E) (Eq. (5.5)), while also accounting for changes in broth volume (Eq. (5.6)).

$$\frac{dC_X}{dt} = \mu \cdot C_X - \frac{C_X}{V} \cdot \frac{dV}{dt} \tag{5.3}$$

$$\frac{dC_G}{dt} = -\frac{1}{Y_{X/G}} \mu \cdot C_X - \frac{C_G}{V} \cdot \frac{dV}{dt} \tag{5.4}$$

$$\frac{dC_E}{dt} = \frac{Y_{E/G}}{Y_{X/G}} \cdot \mu \cdot C_X - k_E \cdot C_E - \frac{C_E}{V} \cdot \frac{dV}{dt} \tag{5.5}$$

$$\frac{dV}{dt} = -\frac{\left(k_E \cdot C_E + k_W \cdot (\rho_W - C_E)\right) \cdot V}{\rho_W} \tag{5.6}$$

where μ is the specific cell growth rate (h^{-1}), C_X is the total cell concentration (g L^{-1}), C_G is the glucose concentration (g L^{-1}), C_E is the ethanol concentration (g L^{-1}), $Y_{X/G}$ represents the cell yield coefficient ($g_X\ g_G^{-1}$), $Y_{E/G}$ denotes the ethanol yield coefficient ($g_E\ g_G^{-1}$), ρ_W is the specific mass of water (g L^{-1}), and k_E and k_W are the removal rate constants for ethanol and water, respectively (h^{-1}).

The specific cell growth rate (μ) was modeled using the hybrid Andrews-Levenspiel kinetic equation (Andrews, 1968; Levenspiel, 1980), which accounts for inhibition by substrate (glucose) and product (ethanol):

$$\mu = \mu_{max} \cdot \frac{C_G}{K_S + C_G + \frac{C_G^2}{K_{IG}}} \cdot \left(1 - \frac{C_E}{C_{Emax}}\right)^n \tag{5.7}$$

where μ_{max} is the maximum specific cell growth rate (h^{-1}), K_S is the saturation constant (g L^{-1}), K_{IG} is the glucose inhibition constant (g L^{-1}), C_{Emax} is the ethanol concentration at which cell growth ceases (g L^{-1}), and n is a dimensionless parameter related to the ethanol's toxic potential.

The cell and ethanol yield coefficients, $Y_{X/G}$ and $Y_{E/G}$, were determined using the following equations:

$$Y_{X/G}=\frac{C_{Xf}-C_{X0}}{C_{G0}-C_{Gf}} \tag{5.8}$$

$$Y_{E/G}=\frac{C_{Ef}-C_{E0}}{C_{G0}-C_{Gf}} \tag{5.9}$$

where the subscripts “0” and “f” denote the initial and final times of the culture, respectively.

In the conventional SHF modeling, the constants k_E and k_W were set to zero (k_E=k_W=0) because there was no removal of ethanol and water. For the extractive fermentations, k_E and k_W were calculated using equations proposed by Rodrigues et al. (2018).

5.2.7.2. SSF

The model for extractive SSF was developed based on mass balances for total cells (Eq. (5.10)), liquefied starch (St) (Eq. (5.11)), glucose (Eq. (5.12)), and ethanol (Eq. (5.13)), while accounting for changes in the broth volume (Eq. (5.14)).

$$\frac{dC_X}{dt}=\mu\cdot C_X-\frac{C_X}{V}\cdot\frac{dV}{dt} \tag{5.10}$$

$$\frac{dC_{St}}{dt}=-\frac{k_1\cdot C_{Enz}\cdot C_{St}}{K_m\left(1+\frac{C_G}{K_i^G}\right)+C_{St}}-\frac{C_{St}}{V}\cdot\frac{dV}{dt} \tag{5.11}$$

$$\frac{dC_G}{dt}=1.11\cdot\frac{k_1\cdot C_{Enz}\cdot C_{St}}{K_m\left(1+\frac{C_G}{K_i^G}\right)+C_{St}}-\frac{1}{Y_{X/G}}\cdot\mu\cdot C_X-\frac{C_G}{V}\cdot\frac{dV}{dt} \tag{5.12}$$

$$\frac{dC_E}{dt}=\frac{Y_{E/G}}{Y_{X/G}}\cdot\mu\cdot C_X-k_E\cdot C_E-\frac{C_E}{V}\cdot\frac{dV}{dt} \tag{5.13}$$

$$\frac{dV}{dt}=-\frac{\left(k_E\cdot C_E+k_W\cdot(\rho_W-C_E)\right)\cdot V}{\rho_W} \tag{5.14}$$

In conventional SSF modeling, the constants k_E and k_W were set to zero (k_E=k_W=0) because there was no removal of ethanol and water.

5.2.8. Parameters estimation and model validation

Modeling and simulation were implemented using Scilab software (version 6.0.2). The Runge-Kutta algorithm was employed to numerically solve the system of differential equations system, while the kinetic parameters of the model were estimated using a genetic algorithm (GA). Initial values were assigned to all variables for parameter estimation, including the parameters to be estimated (k_1, K_i^G, K_M, μ_{max}, K_G, K_{IG}, C_{Emax}, n, and p) as well as the fixed initial and operating conditions (C_{Enz}, C_{St0}, C_{G0}, C_{E0}, C_{X0}, $Y_{X/G}$, $Y_{E/G}$, k_E, and k_W). Thus, the optimization process aims to determine θ by minimizing the objective function (E(θ), Eq. (5.15)) to achieve the best fit between experimental and simulated data.

$$E(\theta)=\sum_{k=1}^{N_P}\left[\sum_{i=1}^{n}\left(\frac{C_{i,k}-\widehat{C}_{i,k}}{C_{i,h}}\right)^2\right] \tag{5.15}$$

where θ is the vector of parameters to be estimated, N_P is the number of experimental data collected in each assay, n is the number of variables considered, $C_{i,k}$, is the experimental concentration for the k^{th} sample, $\widehat{C}_{i,k}$ is simulated concentration for the k^{th} sample , and $C_{i,h}$ is the highest experimental concentration values.

5.3. Results and discussion

5.3.1. Estimation of kinetic parameters for the saccharification

The Michaelis–Menten equation is the fundamental model used to understanding enzyme kinetics in the absence of inhibition mechanisms. When inhibitors are present, additional terms must be incorporated into the Michaelis–Menten model to accurately represent the process. Numerous studies have examined enzyme inhibition caused by high product concentrations during saccharification (Matsumura et al., 1988; Presečki et al., 2013; Wang et al., 2006). Among these, glucose competitive inhibition has been identified as the predominant mechanism (Cepeda et al., 2001; Nagy et al., 1992; Polakovič and Bryjak, 2004), although other mechanisms, such as non-competitive and uncompetitive inhibition, have also been explored.

In this study, the kinetics of saccharification catalyzed by the glucoamylase enzyme were modeled using an unstructured mathematical model (Eqs. (1)–(2)) based on Michaelis–

Menten kinetics and incorporating competitive glucose inhibition. Figure 5.2 presents the time-course profile of glucose generated from the hydrolysis of liquefied starch. The correlation coefficient (R^2) obtained was 0.990, indicating that the model predictions of glucose profile are in good agreement with experimental data.

Figure 5.2 – Simulated (lines) and experimental (points) glucose concentration profiles in the saccharification assay. Error bars correspond to the standard deviation.

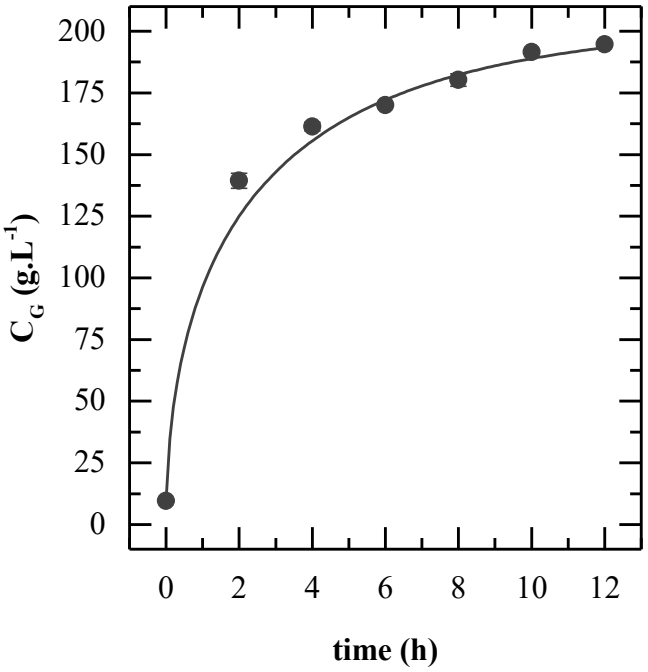

Table 5.1 shows the kinetic parameters obtained for the saccharification model. The values of K_m, k_1, and K_i^G were in good agreement with data previously reported in the literature (Nagy et al., 1992; Polakovič and Bryjak, 2004). The low value of glucose inhibition constant ($K_i^G = 0.31$ g L^{-1}) indicates that the glucoamylase enzymatic reaction was strongly inhibited by glucose. Similar findings were reported by Polakovič and Bryjak (2004), who studied the hydrolysis kinetics of soluble potato starch catalyzed by glucoamylase.

Table 5.1 – Values of kinetic parameters for saccharification, fermentation, yield coefficients and vacuum-stripping parameters.

Estimated parameter	**Value**	**Unit**
k_1	0.85	$g \cdot U^{-1} \cdot h^{-1}$
K_m	19.01	$g \cdot L^{-1}$
K_i^G	0.31	$g \cdot L^{-1}$
$\mu_{máx}$	0.16	h^{-1}
K_S	73.58	$g \cdot L^{-1}$
K_{IG}	167.11	$g \cdot L^{-1}$
C_{Emax}	94.34	$g \cdot L^{-1}$
n	0.81	–
Fixed parameter	**Value**	**Unit**
C_{Enz}	2552.24	$U \cdot L^{-1}$
$Y_{X/G}$	0.027	$g_X \cdot g_G^{-1}$
$Y_{E/G}$	0.404	$g_E \cdot g_G^{-1}$
k_E	0.0672	h^{-1}
k_W	0.0088	h^{-1}

5.3.2. Conventional fermentations

5.3.2.1. Modeling of separate hydrolysis and fermentation (SHF)

The cell yield coefficient ($Y_{X/G}$) and ethanol yield coefficient ($Y_{E/G}$) were calculated from experimental data for cell (C_X), glucose (C_G), and ethanol (C_E) concentrations using Eqs. (8) and (9). The kinetic parameters of the Andrews-Levenspiel model (μ_{max}, K_S, K_{IS}, C_{Emax}, and n) were estimated using a genetic algorithm in conjunction with the Runge-Kutta method for numerically solving the set of differential equations (Eqs. (3)–(6)), assuming $k_E = k_W = 0$. The criteria for obtaining kinetic parameters involved minimizing the sum of squared residuals (Eq. (5.15)). The estimated kinetic parameter values that provided the best fit between the calculated and experimental data are shown in Table 1. The kinetic parameters are in close agreement with the range of values reported in the literature for processes conducted under experimental

conditions similar to those used in this study (Sonego et al., 2018; Veloso et al., 2019).

Figure 5.3 presents the time-course profile of glucose (C_G) and ethanol (C_E) concentrations during the SHF process. The comparison between simulated and experimental data demonstrated that the model provided an excellent fit to the experimental data, with an R^2 values of 0.991 for C_G and 0.990 for C_E. These results indicate that the hybrid Andrews–Levenspiel model is well-suited to describe the kinetics of the process.

Figure 5.3 – Simulated (lines) and experimental (points) concentration profiles in SHF experiments for glucose (circles) and ethanol (squares). Error bars correspond to the standard deviation.

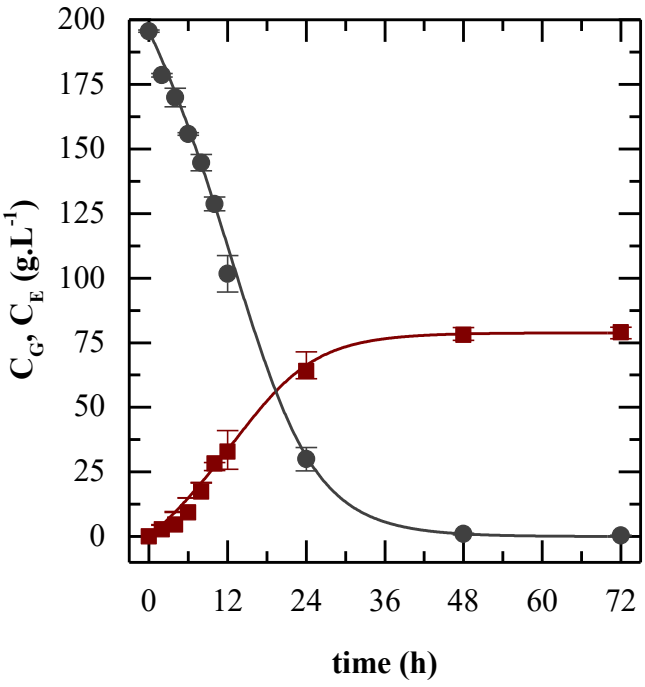

As can be seen from Figure 5.3, the initial glucose concentration was 195.60 ± 0.46 g/L and was completely depleted within 48 h. Ethanol production reached a final concentration of 78.90±1.85 g/L and a productivity of 1.64 ± 0.03 g L^{-1} h^{-1} by the end of the fermentation process. The ethanol yield coefficient ($Y_{E/G}$) was 0.404 ± 0.020 g_E/g_G based on total available sugars, corresponding to 79.10% of the theoretical yield. These results are consistent with findings from Weiss et al. (2022), who reported ethanol concentration values ranging from 79.81 to 89.47 g/L for similar ethanol fermentations from sorghum.

5.3.2.2. Modeling of simultaneous saccharification and fermentation (SSF)

The development of mathematical models is a useful tool to simulate different strategies for design of efficient SSF process configurations (Philippidis et al., 1992; Unrean et al., 2016). The kinetic parameters of the SSF model were determined through saccharification and SHF experiments, each of which individually investigates the kinetics of a specific step in the SSF process. Therefore, the kinetic parameters and yield parameters from saccharification (K_m, k_1, K_{IG}) and fermentation ($\mu_{máx}$, K_S, K_{IS}, C_{Emax}, n, $Y_{X/G}$, and $Y_{E/G}$) processes were incorporated into the SSF model, along with the mass balance equations (Eqs. (5.10)–(5.14)).

Figure 5.4 shows the experimental and simulated concentration profiles of glucose (C_G) and ethanol (C_E) for simultaneous saccharification and fermentation (SSF). The model demonstrates a good fit with the experimental data, with R^2 value of 0.995 for C_G and 0.990 for C_E. The results could potentially be improved by directly fitting the parameters to the SSF experimental data. However, this study aimed to model the SSF process using kinetic parameters that were previously determined from batch experiments.

Figure 5.4 – Simulated (lines) and experimental (points) concentration profiles in SSF experiments for glucose (circles) and ethanol (squares). Error bars correspond to the standard deviation.

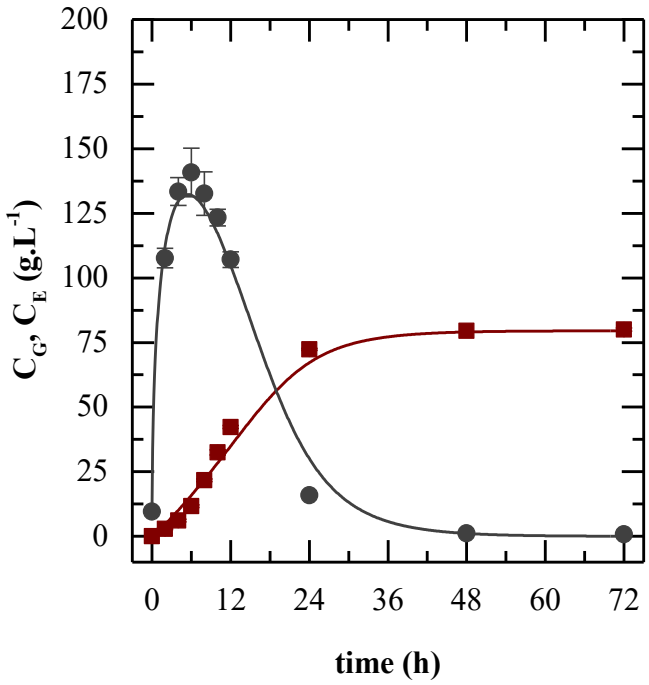

As shown in Figure 5.4, glucose concentration (C_G) was completely depleted within 48 h, the ethanol concentration (C_E) reached 79.54 ± 0.64 g L^{-1}, and volumetric ethanol

productivity (Pr_E) was 1.66 ± 0.01 g $L^{-1}h^{-1}$.

5.3.3. Modeling of extractive SHF and SSF processes

The SHF and SSF models with ethanol removal by CO_2 stripping were applied to evaluate the effect of ethanol removal on the dynamics of the extractive separate hydrolysis and fermentation (ESHF) and extractive simultaneous saccharification and fermentation (ESSF), using the values of removal rate constants for ethanol (k_E) and water (k_W) and the kinetic parameters for saccharification and fermentation. It is important to note that the k_E and k_W parameters used in the simulations were determined through vacuum-assisted stripping experiments conducted using an ethanol solution and provide a good approximation of ethanol removal in fermentation broth.

In the subsequent step, ESHF and ESSF experiments were performed to assess whether the model accurately represented the dynamics of extractive fermentation. Figure 5.5 (a)–(b) compares the experimental (symbols) and simulated (lines) concentration profiles of C_G and C_E obtained from the extractive experiments conducted in a 2–L bubble bioreactor. As shown, the proposed model could accurately predict the behavior of both fermentations using the kinetic parameters obtained in experiments performed at a smaller scale (100 mL) without ethanol removal. The correlation coefficient (R^2) obtained in the ESHF was 0.999 for C_G and 0.997 for C_E, while in the ESSF, the R^2 values were 0.992 for C_G and 0.990 for C_E.

Ethanol removal using vacuum stripping was initiated once the ethanol concentrations (C_E) reached approximately 40.0 g L^{-1} (~ 12 h), preventing the ethanol inhibitory effect from impacting yeast cell growth. According to Aiba et al. (1968), yeast inhibition by ethanol becomes more pronounced once the ethanol concentration rises above 40.0 g L^{-1}. Lemos et al. (2020) reported similar ethanol concentration in the fermentation broth (~40.0 g L^{-1}) for initiating ethanol removal in liquid–liquid extractive fed-batch ethanol fermentation. Additionally, Sonego et al. (2014) also reported a similar value (C_E=35.0 g L^{-1}) for beginning ethanol removal in fed-batch fermentations using CO_2 stripping, with the ethanol concentration determined through an optimization algorithm.

Figure 5.5 – Simulated (lines) and experimental (points) concentration profiles for glucose (circles) and ethanol (squares) with ethanol removal using vacuum-stripping: (a) ESHF and (b) ESSF. Error bars correspond to the standard deviation.

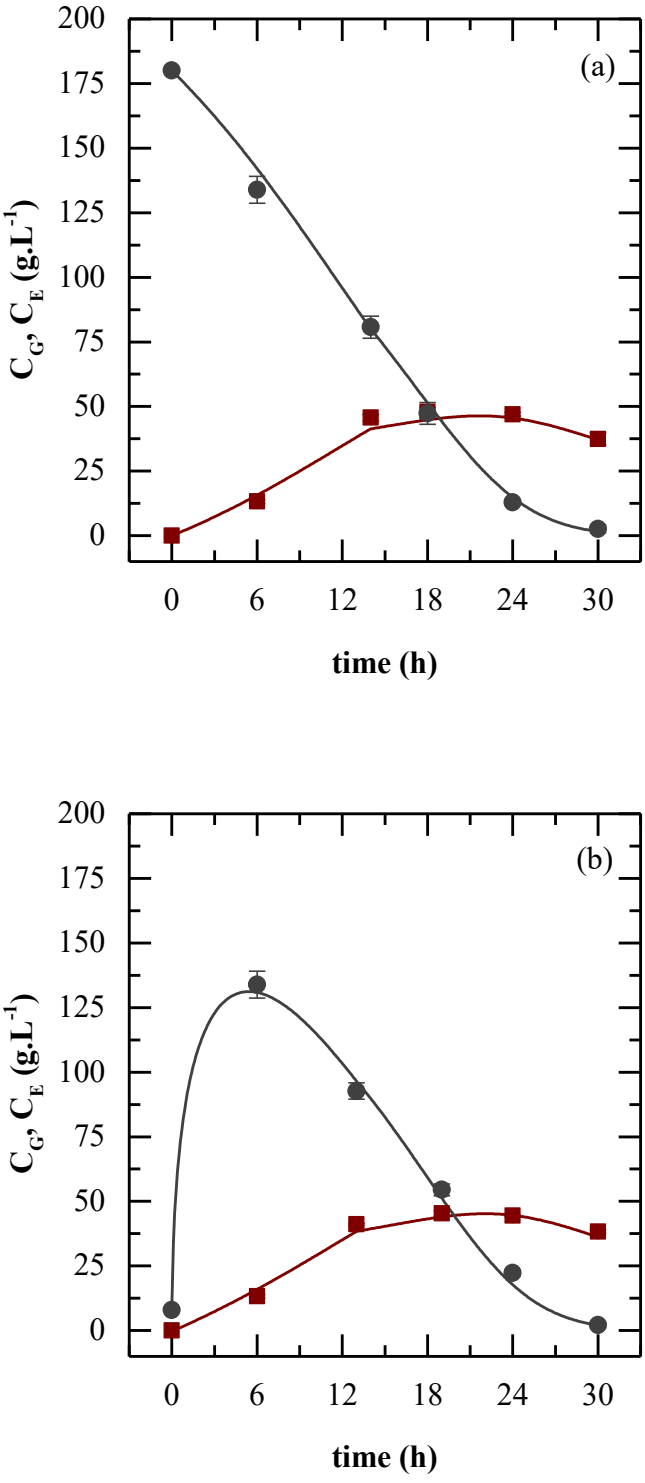

In the extractive fermentations (ESHF and ESSF), glucose consumption occurred earlier than in the conventional fermentations (SHF and SSF). Glucose exhaustion was observed within 30 h for ESHF and ESSF, whereas in the conventional fermentations (SHF and SSF), depletion occurred at 48 h. This behavior can be attributed to the reduced inhibition of yeast activity caused by ethanol accumulation, as ethanol was removed throughout the fermentation process via vacuum stripping. In this technique, the gas phase is sparged in fermentation broth, and ethanol is transferred from the liquid to the gas phase until carbon dioxide bubbles become ethanol-saturated (Pereira et al., 2024). Under vacuum conditions, the gas phase is richer in ethanol and water, as the vacuum lowers the saturation temperature, allowing for greater removal of ethanol and water (Nguyen et al., 2009).

As shown in Table 5.2, the maximum ethanol concentrations in the liquid phase for ESHF and ESSF remained below 50.0 g L^{-1}, highlighting the effective removal of ethanol. The ethanol productivities for ESHF and ESSF were up to 2.4 g L^{-1} h^{-1} as obtained by the ratio of the total final C_E and the time for substrate depletion. Therefore, the extractive fermentations had ethanol productivity (P_E) values of around 60% higher than the conventional methods (SHF and SSF). Previous studies on ethanol extractive fermentation from corn starch have demonstrated high ethanol productivity and effective conversion of concentrated glucose feedstocks, using gas stripping (Taylor et al., 1996) or vacuum (Kumar et al., 2018) for ethanol removal. Although variability in process conditions limits direct comparisons, these findings support the results obtained in the present study.

Table 5.2 – Performance comparison of conventional and extractive fermentations.

Variable	**Unit**	**Fermentation**			
		SHF	SSF	ESHF	ESSF
Total C_G consumed	$g \cdot L^{-1}$	195.29	195.00[a]	180.01	195.00[a]
Maximum C_E in the broth	$g \cdot L^{-1}$	78.90	79.08	47.30	45.29
Total C_E at the end of fermentation	$g \cdot L^{-1}$	78.90	79.08	73.12[b]	78.78[b]
Ethanol productivity (P_E)	$g \cdot L^{-1} \cdot h^{-1}$	1.64	1.65	2.43	2.62

[a] Calculated considering starch content of 70.27%.

[b] Calculated considering $Y_{E/G}$ ($g_E \cdot g_G^{-1}$) = 0.404.

According to the results, conventional (SHF and SSF) and extractive (ESHF and ESSF) experiments achieved similar ethanol productivities (Table 5.2) at the end of fermentations. However, the SSF method offers an advantage by reducing the number of required vessels, which can lower the initial investment costs. Moreover, heating costs are minimized since the maintenance of slurry temperatures during an independent saccharification stage is not required. Additionally, SSF prevents substrate inhibition caused by high glucose concentration, as the yeast immediately converts the glucose generated during saccharification into ethanol (Marulanda et al., 2019).

It is important to highlight that ethanol concentration in the broth is lower in extractive fermentations due to the ethanol removal by vacuum stripping. Nonetheless, the vaporized ethanol fraction can be recovered through techniques such as condensation (Farias and Maugeri-Filho, 2021; Huang et al., 2015), absorption (Rodrigues et al., 2025, 2019), and adsorption (Hashi et al., 2010). Although this study does not address ethanol recovery techniques, they are critical for improving ethanol production efficiency.

5.4. Conclusions

This study modeled the saccharification of liquefied starch and fermentation processes in different configurations, including conventional and extractive separate hydrolysis and fermentation (SHF) as well as conventional and extractive simultaneous saccharification and fermentation (SSF). The proposed model, based on mass balance equations, effectively described the behavior of the bench-scale conventional and extractive fermentations. Therefore, the model provides a reliable alternative for optimizing strategies and could contribute to overcoming the challenges that hinder the industrial-scale application of extractive fermentation.

Moreover, applying the vacuum stripping technique in both SHF and SSF processes resulted in up to 60% higher ethanol productivity compared to conventional fermentation. These findings highlight the feasibility of extractive fermentation with ethanol removal by vacuum-stripping, indicating its potential for industrial-scale applications. However, further studies on economic viability are necessary to evaluate its suitability for large-scale implementation.

CHAPTER 6

6. FINAL CONSIDERATIONS AND SUGGESTIONS FOR FUTURE INVESTIGATIONS

From the present results, it can be concluded that:

- ✓ The operating variables — specific CO_2 flow rate, temperature, and pressure — had a significant effect on ethanol and water removal within the experimental range studied. Among them, the specific CO_2 flow rate had the most significant effect, with a positive impact on the entrainment factor (F_E).

- ✓ The concentration factor (F_C), which indicates how much more concentrated ethanol is in the gas phase leaving the reactor compared to the liquid solution, increased with higher specific CO_2 flow rates. The ethanol content in the gas phase was six times greater than in the liquid phase.

- ✓ Monitoring of the gas stream during extractive fermentation experiments showed that the ethanol concentration in the outlet stream was six times greater than in the liquid phase, demonstrating the potential of the technique to reduce costs in the ethanol recovery stage.

- ✓ In the extractive fermentations using saccharine feedstock, vacuum-assisted gas stripping reduced the energy requirement for ethanol production by 31.3% compared to conventional gas stripping.

- ✓ The proposed model, which encompasses saccharification, fermentation, and the kinetics of ethanol and water removal, provided an excellent fit to the experimental data from SHF and SSF processes, accurately describing the observed behavior of the system.

- ✓ The application of the vacuum-assisted gas stripping technique in both SHF and SSF processes resulted in up to 60% higher ethanol productivity compared to conventional fermentation.

- ✓ These findings demonstrated that extractive fermentation with ethanol removal via vacuum-assisted gas stripping is a viable approach, with potential for industrial-scale application.

Suggestions for further investigations:

- ✓ To optimize the application time of vacuum-assisted gas stripping, comparing continuous and intermittent modes.

- ✓ To evaluate the technical and economic feasibility of extractive fermentation via vacuum-assisted gas stripping.

- ✓ To investigate the performance of vacuum-assisted gas stripping at elevated temperatures using thermotolerant yeast strains.

REFERENCES

ABDEHAGH, N.; TEZEL, F. H.; THIBAULT, J. Separation techniques in butanol production: challenges and developments. *Biomass and Bioenergy*, v. 60, p. 222–246, 2014. DOI: https://doi.org/10.1016/j.biombioe.2013.10.003.

ABDULRAZZAQ, N.; AL-SABBAGH, B. H.; REES, J. M.; ZIMMERMAN, W. B. Purification of bioethanol using microbubbles generated by fluidic oscillation: a dynamical evaporation model. *Industrial & Engineering Chemistry Research*, v. 55, p. 12909–12918, 2016. DOI: https://doi.org/10.1021/acs.iecr.6b01666.

ABRAMS, D. S.; PRAUSNITZ, J. M. Statistical thermodynamics of liquid mixtures: a new expression for the excess Gibbs energy of partly or completely miscible systems. *AIChE Journal*, v. 21, p. 116–128, 1975. DOI: https://doi.org/10.1002/aic.690210115.

AGARWAL, S.; KUMAR, A. Historical development of biofuels. In: KUMAR, A.; DHINGRA, S. *Biofuels: greenhouse gas mitigation and global warming*. New Delhi: Springer India, 2018. p. 17–45. DOI: https://doi.org/10.1007/978-81-322-3763-1_2.

AHMAD, A.; BUANG, A.; BHAT, A. H. Renewable and sustainable bioenergy production from microalgal co-cultivation with palm oil mill effluent (POME): a review. *Renewable and Sustainable Energy Reviews*, v. 65, p. 214–234, 2016. DOI: https://doi.org/10.1016/j.rser.2016.06.084.

AIBA, S.; SHODA, M.; NAGATANI, M. Kinetics of product inhibition in alcohol fermentation. *Biotechnology and Bioengineering*, v. 10, p. 845–864, 1968. DOI: https://doi.org/10.1002/bit.260100610.

AI, Y.; MEDIC, J.; JIANG, H.; WANG, D.; JANE, J. Starch characterization and ethanol production of sorghum. *Journal of Agricultural and Food Chemistry*, v. 59, p. 7385–7392, 2011. DOI: https://doi.org/10.1021/jf2007584.

ALMEIDA, L. P.; BUFFO, M. M.; PEREIRA, R. D.; CRUZ, A. J. G.; ESPERANÇA, M. N.; BADINO, A. C. Ethanol removal by vacuum-assisted gas stripping: influence of operating conditions. *Chemical Engineering and Processing - Process Intensification*, v. 203, p. 109873, 2024. DOI: https://doi.org/10.1016/j.cep.2024.109873.

ALMEIDA, L. P.; SILVA, C. R.; MARTINS, T. B.; PEREIRA, R. D.; ESPERANÇA, M. N.; CRUZ, A. J. G.; BADINO, A. C. Heat transfer evaluation for conventional and extractive ethanol fermentations: saving cooling water. *Journal of Cleaner Production*, v. 304, 2021. DOI: https://doi.org/10.1016/j.jclepro.2021.127063.

ALPER, H.; MOXLEY, J.; NEVOIGT, E.; FINK, G. R.; STEPHANOPOULOS, G. Engineering yeast transcription machinery for improved ethanol tolerance and production. *Science*, v. 314, p. 1565–1568, 2006. DOI: https://doi.org/10.1126/science.1131969.

AMORIM, H. V.; LOPES, M. L.; DE CASTRO OLIVEIRA, J. V.; BUCKERIDGE, M. S.; GOLDMAN, G. H. Scientific challenges of bioethanol production in Brazil. *Applied Microbiology and Biotechnology*, v. 91, p. 1267–1275, 2011. DOI: https://doi.org/10.1007/s00253-011-3437-6.

AMORIM, H. V. de. *Fermentação alcoólica: ciência e tecnologia*. Piracicaba: Fermentec, 2005. 448 p.

ANDLAR, M.; OROS, D.; REZIĆ, T.; LUDWIG, R.; ŠANTEK, B. In-situ vacuum assisted gas stripping recovery system for ethanol removal from a column bioreactor. *Fibers*, v. 6, 2018. DOI: https://doi.org/10.3390/fib6040088.

ANDREWS, J. F. A mathematical model for the continuous culture of microorganisms utilizing inhibitory substrates. *Biotechnology and Bioengineering*, v. 10, p. 707–723, 1968. DOI: https://doi.org/10.1002/bit.260100602.

APPIAH-NKANSAH, N. B.; ZHANG, K.; ROONEY, W.; WANG, D. Ethanol production from mixtures of sweet sorghum juice and sorghum starch using very high gravity fermentation with urea supplementation. *Industrial Crops and Products*, v. 111, p. 247–253, 2018. DOI: https://doi.org/10.1016/j.indcrop.2017.10.028.

ARIF, S.; MUDASSIR, M. A.; KOUSAR, S.; RAHIM, U.; MAKAREM, M. A.; KIANI, P. Upgrading bioenergy materials to chemicals. In: SAYIGH, A. *Encyclopedia of Renewable Energy, Sustainability and the Environment*. Amsterdam: Elsevier, 2024. p. 849–860. DOI: https://doi.org/10.1016/B978-0-323-93940-9.00018-9.

ATASOY, M.; OWUSU-AGYEMAN, I.; PLAZA, E.; CETECIOGLU, Z. Bio-based volatile fatty acid production and recovery from waste streams: current status and future challenges. *Bioresource Technology*, v. 268, p. 773–786, 2018. DOI: https://doi.org/10.1016/j.biortech.2018.07.042.

BADINO, A. C.; CRUZ, A. J. G. *Reatores químicos e bioquímicos*. São Carlos: Coleção UAB-UFSCar, 2012.

BAGUL, R. K.; PILKHWAL, D. S.; VIJAYAN, P. K.; JOSHI, J. B. Entrainment phenomenon in gas-liquid two-phase flow: a review. *Sādhanā: Academy Proceedings in Engineering Sciences*, v. 38, p. 1173–1217, 2013.

BAI, F. W.; ANDERSON, W. A.; MOO-YOUNG, M. Ethanol fermentation technologies from sugar and starch feedstocks. *Biotechnology Advances*, v. 26, p. 89–105, 2008. DOI: https://doi.org/10.1016/j.biotechadv.2007.09.002.

BASSO, L. C.; BASSO, T. O.; ROCHA, S. N. Ethanol production in Brazil: the industrial process and its impact on yeast fermentation. In: BERNARDES M. A. S. *Biofuel production – recent developments and prospects*. London: IntechOpen, 2011. p. 85–100. DOI: https://doi.org/10.5772/17047.

BHARATHIRAJA, B.; JAYAMUTHUNAGAI, J.; SUDHARSANAA, T.; BHARGHAVI, A.; PRAVEENKUMAR, R.; CHAKRAVARTHY, M.; YUVARAJ, D. Biobutanol – an impending biofuel for future: a review on upstream and downstream processing techniques. *Renewable and Sustainable Energy Reviews*, v. 68, p. 788–807, 2017. DOI: https://doi.org/10.1016/j.rser.2016.10.017.

BOKHARY, A.; LEITCH, M.; LIAO, B. Q. Liquid–liquid extraction technology for resource recovery: applications, potential, and perspectives. *Journal of Water Process Engineering*, v. 40, p. 101762, 2021. DOI: https://doi.org/10.1016/j.jwpe.2020.101762.

BOTHAST, R. J.; SCHLICHER, M. A. Biotechnological processes for conversion of corn into ethanol. *Applied Microbiology and Biotechnology*, v. 67, p. 19–25, 2005. DOI: https://doi.org/10.1007/s00253-004-1819-8.

CAI, D.; CHEN, H.; SI, Z.; WEN, J.; QIN, P. Alcohol production: downstream processes. In: QIN, P. (ed.). *Higher alcohols production platforms*. Amsterdam: Elsevier, 2024. p. 183–235. DOI: https://doi.org/10.1016/B978-0-323-91756-8.00001-3.

CAI, D.; WEN, J.; ZHUANG, Y.; HUANG, T.; SI, Z.; QIN, P.; CHEN, H. Review of alternative technologies for acetone-butanol-ethanol separation: principles, state-of-the-art, and development trends. *Separation and Purification Technology*, v. 298, p. 121244, 2022. DOI: https://doi.org/10.1016/j.seppur.2022.121244.

CALVERLEY, J.; ZIMMERMAN, W. B.; LEAK, D. J.; BANDULASENA, H. C. H. Hot microbubble air stripping of dilute ethanol–water mixtures. *Industrial & Engineering Chemistry Research*, v. 59, p. 19392–19405, 2020. DOI: https://doi.org/10.1021/acs.iecr.0c03250.

CALVERLEY, J.; ZIMMERMAN, W. B.; LEAK, D. J.; BANDULASENA, H. C. H. Continuous removal of ethanol from dilute ethanol-water mixtures using hot microbubbles. *Chemical Engineering Journal*, v. 424, p. 130511, 2021. DOI: https://doi.org/10.1016/j.cej.2021.130511.

CAMPOS, B. G.; VELOSO, I. I. K.; RIBEIRO, M. P. A.; BADINO, A. C.; CRUZ, A. J. G. Thermal analysis of extractive fed-batch ethanol fermentation with CO_2 stripping: modeling and simulation. *Chemical Engineering and Processing - Process Intensification*, v. 182, p. 109185, 2022. DOI: https://doi.org/10.1016/j.cep.2022.109185.

CAMPOS, B. G.; VELOSO, I. I. K.; DA SILVA, M. M.; BADINO, A. C.; CRUZ, A. J. G. A novel approach to heat removal and temperature control in fed-batch extractive ethanol fermentation using CO_2. *Chemical Engineering and Processing - Process Intensification*, v. 210, p. 110212, 2025. DOI: https://doi.org/10.1016/j.cep.2025.110212.

CEPEDA, E.; HERMOSA, M.; BALLESTEROS, A. Optimization of maltodextrin hydrolysis by glucoamylase in a batch reactor. *Biotechnology and Bioengineering*, v. 76, p. 70–76, 2001. DOI: https://doi.org/10.1002/bit.1027.

CHISTI, Y. *Airlift bioreactors*. New York: Elsevier, 1989.

CLERAN, Y.; THIBAULT, J.; CHERUY, A.; CORRIEU, G. Comparison of prediction performances between models obtained by the group method of data handling and neural networks for the alcoholic fermentation rate in enology. *Journal of Fermentation and Bioengineering*, v. 71, p. 356–362, 1991. DOI: https://doi.org/10.1016/0922-338X(91)90350-P.

CONAB - Companhia Nacional de Abastecimento. Boletim da safra de cana-de-açúcar. 2025.Available at: https://www.conab.gov.br/info-agro/safras/cana/boletim-da-safra-de-cana-de-acucar. Accessed on: July 2, 2025.

CUSSLER, E. L. *Diffusion: mass transfer in fluid systems*. 3. ed. Cambridge: Cambridge University Press, 2009.

CYSEWSKI, G. R.; WILKE, C. R. Rapid ethanol fermentations using vacuum and cell recycle.

Biotechnology and Bioengineering, v. 19, p. 1125–1143, 1977. DOI: https://doi.org/10.1002/bit.260190804.

DALMOLIN, I.; SKOVROINSKI, E.; BIASI, A.; CORAZZA, M. L.; DARIVA, C.; OLIVEIRA, J. V. Solubility of carbon dioxide in binary and ternary mixtures with ethanol and water. *Fluid Phase Equilibria*, v. 245, p. 193–200, 2006. DOI: https://doi.org/10.1016/j.fluid.2006.04.017.

DEED, R. C.; DEED, N. K.; GARDNER, R. C. Transcriptional response of *Saccharomyces cerevisiae* to low temperature during wine fermentation. *Antonie van Leeuwenhoek*, v. 107, p. 1029–1048, 2015. DOI: https://doi.org/10.1007/s10482-015-0395-5.

DESAI, P. D.; TURLEY, M.; ROBINSON, R.; ZIMMERMAN, W. B. Hot microbubble injection in thin liquid film layers for ammonia separation from ammonia rich-wastewater. *Chemical Engineering and Processing - Process Intensification*, v. 180, p. 108693, 2022. DOI: https://doi.org/10.1016/j.cep.2021.108693.

DESAI, P. D.; ZIMMERMAN, W. B. Microbubble intensification of bioprocessing. *Johnson Matthey Technology Review*, v. 67, p. 371–401, 2023. DOI: https://doi.org/10.1595/205651323X16778518231554.

DIAS, M. O. de S.; MACIEL FILHO, R.; MANTELATTO, P. E.; CAVALETT, O.; ROSSELL, C. E. V.; BONOMI, A.; LEAL, M. L. R. V. Sugarcane processing for ethanol and sugar in Brazil. *Environmental Development*, v. 15, p. 35–51, 2015. DOI: https://doi.org/10.1016/j.envdev.2015.03.004.

DIAS, R. M.; CHIAVONE-FILHO, O.; BERNARDO, A.; GIULIETTI, M. Vapour-liquid equilibria for (water + ethanol + fructose): experimental data and thermodynamic modelling. *Journal of Chemical Thermodynamics*, v. 115, p. 27–33, 2017. DOI: https://doi.org/10.1016/j.jct.2017.07.021.

DING, W.; XIAO, Z.; TANG, X.; DENG, K.; FU, S.; JIANG, Y.; YUAN, L. Evolutionary engineering of yeast for closed-circulating ethanol fermentation in PDMS membrane bioreactor. *Biochemical Engineering Journal*, v. 60, p. 56–61, 2012. DOI: https://doi.org/10.1016/j.bej.2011.09.019.

ENSINAS, A. V.; NEBRA, S. A.; LOZANO, M. A.; SERRA, L. M. Analysis of process steam demand reduction and electricity generation in sugar and ethanol production from sugarcane. *Energy Conversion and Management*, v. 48, p. 2978–2987, 2007. DOI:

https://doi.org/10.1016/j.enconman.2007.06.038.

EZEJI, T. C.; KARCHER, P. M.; QURESHI, N.; BLASCHEK, H. P. Improving performance of a gas stripping-based recovery system to remove butanol from *Clostridium beijerinckii* fermentation. *Bioprocess and Biosystems Engineering*, v. 27, p. 207–214, 2005. DOI: https://doi.org/10.1007/s00449-005-0403-7.

EZEJI, T. C.; QURESHI, N.; BLASCHEK, H. P. Production of acetone, butanol and ethanol by *Clostridium beijerinckii* BA101 and in situ recovery by gas stripping. *World Journal of Microbiology and Biotechnology*, v. 19, p. 595–603, 2003. DOI: https://doi.org/10.1023/A:1025103011923.

FADAVI, A.; CHISTI, Y. Gas holdup and mixing characteristics of a novel forced circulation loop reactor. *Chemical Engineering Journal*, v. 131, p. 105–111, 2007. DOI: https://doi.org/10.1016/j.cej.2006.12.037.

FAN, S.; LIU, J.; TANG, X.; WANG, W.; XIAO, Z.; QIU, B.; WANG, Y; JIAN, S.; QIN, Y.; WANG, Y. Process operation performance of PDMS membrane pervaporation coupled with fermentation for efficient bioethanol production. *Chinese Journal of Chemical Engineering*, v. 27, p. 1339–1347, 2019. DOI: https://doi.org/10.1016/j.cjche.2018.12.005.

FAN, S.; XIAO, Z.; LI, M. Energy efficient of ethanol recovery in pervaporation membrane bioreactor with mechanical vapor compression eliminating the cold traps. *Bioresource Technology*, v. 211, p. 24–30, 2016. DOI: https://doi.org/10.1016/j.biortech.2016.03.063.

FARIAS, D.; MAUGERI-FILHO, F. Sequential fed batch extractive fermentation for enhanced bioethanol production using recycled *Spathaspora passalidarum* and mixed sugar composition. *Fuel*, v. 288, 2021. DOI: https://doi.org/10.1016/j.fuel.2020.119673.

GHAZALI, M. F. S. M.; MUSTAFA, M. Bioethanol as an alternative fuels: a review on production strategies and technique for analysis. *Energy Conversion and Management: X*, v. 26, p. 100933, 2025. DOI: https://doi.org/10.1016/j.ecmx.2025.100933.

GIL, I. D.; GÓMEZ, J. M.; RODRÍGUEZ, G. Control of an extractive distillation process to dehydrate ethanol using glycerol as entrainer. *Computers and Chemical Engineering*, v. 39, p. 129–142, 2012. DOI: https://doi.org/10.1016/j.compchemeng.2012.01.006.

GILMOUR, D. J.; ZIMMERMAN, W. B. Microbubble intensification of bioprocessing. *Advances in Microbial Physiology*, v. 77, p. 1–35, 2020. DOI: https://doi.org/10.1016/BS.AMPBS.2020.07.001.

GRUNDTVIG, I. P. R.; HEINTZ, S.; KRÜHNE, U.; GERNAEY, K. V.; ADLERCREUTZ, P.; HAYLER, J. D.; WELLS, A. S.; WOODLEY, J. M. Screening of organic solvents for bioprocesses using aqueous-organic two-phase systems. *Biotechnology Advances*, v. 36, p. 1801–1814, 2018. DOI: https://doi.org/10.1016/j.biotechadv.2018.05.007.

GUIJARRO, J. M.; LAGUNAS, R. *Saccharomyces cerevisiae* does not accumulate ethanol against a concentration gradient. *Journal of Bacteriology*, v. 160, p. 874–878, 1984. DOI: https://doi.org/10.1128/jb.160.3.874-878.1984.

HAN, K.; LEVENSPIEL, O. Extended Monod kinetics for substrate, product, and cell inhibition. *Biotechnology and Bioengineering*, v. 32, p. 430–447, 1988. DOI: https://doi.org/10.1002/bit.260320404.

HASHI, M.; TEZEL, F. H.; THIBAULT, J. Ethanol recovery from fermentation broth via carbon dioxide stripping and adsorption. *Energy & Fuels*, v. 24, p. 4628–4637, 2010. DOI: https://doi.org/10.1021/ef901130q.

HIMMELBLAU, D. M.; RIGGS, J. B. *Basic principles and calculations in chemical engineering*. 8. ed. Upper Saddle River, NJ: Prentice Hall, 2012.

HUANG, H.; QURESHI, N.; CHEN, M.-H.; LIU, W.; SINGH, V. Ethanol production from food waste at high solids content with vacuum recovery technology. *Journal of Agricultural and Food Chemistry*, v. 63, p. 2760–2766, 2015. DOI: https://doi.org/10.1021/jf5054029.

HUANG, H. J.; RAMASWAMY, S.; TSCHIRNER, U. W.; RAMARAO, B. V. A review of separation technologies in current and future biorefineries. *Separation and Purification Technology*, v. 62, p. 1–21, 2008. DOI: https://doi.org/10.1016/j.seppur.2007.12.011.

INTERNATIONAL ENERGY AGENCY. *World energy outlook 2024*. Paris: IEA, 2024. Available at: https://www.iea.org/reports/world-energy-outlook-2024. Accessed on: July 9, 2025.

ISHIZAKI, H.; HASUMI, K. Ethanol production from biomass. In: BROWN, R. C. (ed.). *Research approaches to sustainable biomass systems*. Amsterdam: Elsevier, 2014. p. 243–258. DOI: https://doi.org/10.1016/B978-0-12-404609-2.00010-6.

JOYIA, M. A. K.; AHMAD, M.; CHEN, Y.-F.; MUSTAQEEM, M.; ALI, A.; ABBAS, A.; GONDAL, M. A. Trends and advances in sustainable bioethanol production technologies from first to fourth generation: a critical review. *Energy Conversion and Management*, v. 321, p. 119037, 2024. DOI: https://doi.org/10.1016/j.enconman.2024.119037.

KAMELIAN, F. S.; MOHAMMADI, T.; NAEIMPOOR, F. Fast, facile and scalable fabrication of novel microporous silicalite-1/PDMS mixed matrix membranes for efficient ethanol separation by pervaporation. *Separation and Purification Technology*, v. 229, p. 115820, 2019. DOI: https://doi.org/10.1016/j.seppur.2019.115820.

KHAN, M. Z. A.; KHAN, H. A.; RAVI, S. S.; TURNER, J. W.; AZIZ, M. Potential of clean liquid fuels in decarbonizing transportation – an overlooked net-zero pathway? *Renewable and Sustainable Energy Reviews*, v. 183, p. 113483, 2023. DOI: https://doi.org/10.1016/j.rser.2023.113483.

KHANNA, M.; CRAGO, C. L.; BLACK, M. Can biofuels be a solution to climate change? The implications of land use change-related emissions for policy. *Interface Focus*, v. 1, p. 233–247, 2011. DOI: https://doi.org/10.1098/rsfs.2010.0016.

KOLLERUP, F.; DAUGULIS, A. J. A mathematical model for ethanol production by extractive fermentation in a continuous stirred tank fermentor. *Biotechnology and Bioengineering*, v. 27, p. 1335–1346, 1985. DOI: https://doi.org/10.1002/bit.260270910.

KROUMOV, A. D.; MÓDENES, A. N.; TAIT, M. C. de A. Development of new unstructured model for simultaneous saccharification and fermentation of starch to ethanol by recombinant strain. *Biochemical Engineering Journal*, v. 28, p. 243–255, 2006. DOI: https://doi.org/10.1016/j.bej.2005.11.008.

KUJAWSKA, A.; KUJAWSKI, J.; BRYJAK, M.; KUJAWSKI, W. ABE fermentation products recovery methods — a review. *Renewable and Sustainable Energy Reviews*, v. 48, p. 648–661, 2015. DOI: https://doi.org/10.1016/j.rser.2015.04.028.

KUMAR, D.; JUNEJA, A.; SINGH, V. Fermentation technology to improve productivity in dry grind corn process for bioethanol production. *Fuel Processing Technology*, v. 173, p. 66–74, 2018. DOI: https://doi.org/10.1016/j.fuproc.2018.01.014.

KUMAR, D.; SINGH, V. Bioethanol production from corn. In: SERNA-SALDÍVAR, S. O. (ed.). *Corn*. Amsterdam: Elsevier, 2019. p. 615–631. DOI: https://doi.org/10.1016/B978-0-12-811971-6.00022-X.

KOWSKI, J. R.; McALOON, A. J.; TAYLOR, F.; JOHNSTON, D. B. Modeling the process and costs of fuel ethanol production by the corn dry-grind process. *Industrial Crops and Products*, v. 23, p. 288–296, 2006. DOI: https://doi.org/10.1016/j.indcrop.2005.08.004.

LEE, S. S.; ROBINSON, F. M.; WANG, H. Y. Rapid determination of yeast viability.

Biotechnology and Bioengineering Symposium, v. 11: University of Michigan, Ann Arbor, 1981.

LEMOS, D. A.; SONEGO, J. L. S.; BOSCHIERO, M. V.; ARAUJO, E. C. C.; CRUZ, A. J. G.; BADINO, A. C. Selection and application of nontoxic solvents in extractive ethanol fermentation. *Biochemical Engineering Journal*, v. 127, p. 128–135, 2017. DOI: https://doi.org/10.1016/j.bej.2017.08.003.

LEMOS, D. A.; SONEGO, J. L. S.; CRUZ, A. J. G.; BADINO, A. C. Improvement of ethanol production by extractive fed-batch fermentation in a drop column bioreactor. *Bioprocess and Biosystems Engineering*, v. 43, p. 2295–2303, 2020. DOI: https://doi.org/10.1007/s00449-020-02414-5.

LEVENSPIEL, O. The Monod equation: a revisit and a generalization to product inhibition situations. *Biotechnology and Bioengineering*, v. 22, p. 1671–1687, 1980. DOI: https://doi.org/10.1002/bit.260220810.

LIU, C.-G.; XUE, C.; LIN, Y.-H.; BAI, F.-W. Redox potential control and applications in microaerobic and anaerobic fermentations. *Biotechnology Advances*, v. 31, p. 257–265, 2013. DOI: https://doi.org/10.1016/j.biotechadv.2012.11.005.

LIU, R.-S.; TANG, Y.-J. *Tuber melanosporum* fermentation medium optimization by Plackett–Burman design coupled with Draper–Lin small composite design and desirability function. *Bioresource Technology*, v. 101, p. 3139–3146, 2010. DOI: https://doi.org/10.1016/j.biortech.2009.12.022.

LOUREIRO, V.; FERREIRA, H. G. On the intracellular accumulation of ethanol in yeast. *Biotechnology and Bioengineering*, v. 25, p. 2263–2269, 1983. DOI: https://doi.org/10.1002/bit.260250911.

MAIORELLA, B.; BLANCH, H. W.; WILKE, C. R. By-product inhibition effects on ethanolic fermentation by *Saccharomyces cerevisiae*. *Biotechnology and Bioengineering*, v. 25, p. 103–121, 1983. DOI: https://doi.org/10.1002/bit.260250109.

MARIANO, A. P.; FILHO, R. M.; EZEJI, T. C. Energy requirements during butanol production and in situ recovery by cyclic vacuum. *Renewable Energy*, v. 47, p. 183–187, 2012. DOI: https://doi.org/10.1016/j.renene.2012.04.041.

MARTINS, T. B.; ALMEIDA, L. P.; CERRI, M. O.; BADINO, A. C. Mass transfer performance of ethanol removal by CO_2 stripping in different pneumatic bioreactors. *Industrial*

Biotechnology, v. 16, p. 81–90, 2020. DOI: https://doi.org/10.1089/ind.2019.0035.

MARTINS, T. B.; SANTOS, M. V.; VELOSO, I. I. K.; RODRIGUES, K. C. S.; ESPERANÇA, M. N.; CERRI, M. O.; BADINO, A. C Effects of operational and geometric variables of a bubble column bioreactor on ethanol stripping with CO_2: liquid and gas-phase monitoring. *Industrial & Engineering Chemistry Research*, 2023. DOI: https://doi.org/10.1021/acs.iecr.3c01903.

MARULANDA, V. A.; GUTIERREZ, C. D. B.; ALZATE, C. A. C. Thermochemical, biological, biochemical, and hybrid conversion methods of bio-derived molecules into renewable fuels. In: PANDEY, A.; LARROCHE, C.; RICKE, S. C.; DUSSAP, C.-G.; GNANSOUNOU, E. (ed.). *Advanced bioprocessing for alternative fuels, biobased chemicals, and bioproducts*. Amsterdam: Elsevier, 2019. p. 59–81. DOI: https://doi.org/10.1016/B978-0-12-817941-3.00004-8.

MATSUMURA, M.; HIRATA, J.; ISHII, S.; KOBAYASHI, J. Kinetics of saccharification of raw starch by glucoamylase. *Journal of Chemical Technology and Biotechnology*, v. 42, p. 51–67, 1988. DOI: https://doi.org/10.1002/jctb.280420107.

MAVROMMATI, M.; PAPANIKOLAOU, S.; AGGELIS, G. Improving ethanol tolerance of *Saccharomyces cerevisiae* through adaptive laboratory evolution using high ethanol concentrations as a selective pressure. *Process Biochemistry*, v. 124, p. 280–289, 2023. DOI: https://doi.org/10.1016/j.procbio.2022.11.027.

MAYANK, R.; RANJAN, A.; MOHOLKAR, V. S. Mathematical models of ABE fermentation: review and analysis. *Critical Reviews in Biotechnology*, v. 33, p. 419–447, 2013. DOI: https://doi.org/10.3109/07388551.2012.726208.

MOON, M. H.; RYU, J.; CHOENG, Y.-H.; HONG, S.-K.; KANG, H. A.; CHANG, Y. K. Enhancement of stress tolerance and ethanol production in *Saccharomyces cerevisiae* by heterologous expression of a trehalose biosynthetic gene from *Streptomyces albus*. *Biotechnology and Bioprocess Engineering*, v. 17, p. 986–996, 2012. DOI: https://doi.org/10.1007/s12257-012-0148-5.

NAGASAWA, H.; TSURU, T. Silica membrane application for pervaporation process. In: ISMAIL, A. F.; KHULBE, K. C. (ed.). *Current trends and future developments on (bio-)membranes*. Amsterdam: Elsevier, 2017. p. 217–241. DOI: https://doi.org/10.1016/B978-0-444-63866-3.00009-1.

NAGODAWITHANA, T. W.; STEINKRAUS, K. H. Influence of the rate of ethanol production and accumulation on the viability of *Saccharomyces cerevisiae* in “rapid fermentation.” *Applied and Environmental Microbiology*, v. 31, p. 158–162, 1976. DOI: https://doi.org/10.1128/aem.31.2.158-162.1976.

NAIK, S. N.; GOUD, V. V.; ROUT, P. K.; DALAI, A. K. Production of first and second generation biofuels: a comprehensive review. *Renewable and Sustainable Energy Reviews*, v. 14, p. 578–597, 2010. DOI: https://doi.org/10.1016/j.rser.2009.10.003.

NAGY, E.; BÉLAFI-BAKÓ, K.; SZABÓ, L. A kinetic study of the hydrolysis of maltodextrin by soluble glucoamylase. *Starch – Stärke*, v. 44, p. 145–149, 1992. DOI: https://doi.org/10.1002/star.19920440407.

NGUYEN, V. D.; KOSUGE, H.; AURESENIA, J.; TAN, R.; BRONDIAL, Y. Effect of vacuum pressure on ethanol fermentation. *Journal of Applied Sciences*, v. 9, p. 3020–3026, 2009. DOI: https://doi.org/10.3923/jas.2009.3020.3026.

NOSRATI-GHODS, N.; HARRISON, S. T. L.; ISAFIADE, A. J.; LENG TAI, S. Mathematical modelling of bioethanol fermentation from glucose, xylose or their combination – a review. *ChemBioEng Reviews*, v. 7, p. 68–88, 2020. DOI: https://doi.org/10.1002/cben.201900024.

O’BRIEN, D. J.; ROTH, L. H.; McALOON, A. J. Ethanol production by continuous fermentation–pervaporation: a preliminary economic analysis. *Journal of Membrane Science*, v. 166, p. 105–111, 2000. DOI: https://doi.org/10.1016/S0376-7388(99)00255-0.

OFFEMAN, R. D.; FRANQUI-ESPIET, D.; CLINE, J. L.; ROBERTSON, G. H.; ORTS, W. J. Extraction of ethanol with higher carboxylic acid solvents and their toxicity to yeast. *Separation and Purification Technology*, v. 72, p. 180–185, 2010. DOI: https://doi.org/10.1016/j.seppur.2010.02.004.

OUTRAM, V.; LALANDER, C.; LEE, J. G. M.; DAVIES, E. T.; HARVEY, A. P. Applied in situ product recovery in ABE fermentation. *Biotechnology Progress*, v. 33, p. 563–579, 2017. DOI: https://doi.org/10.1002/btpr.2446.

PEREIRA, R. D.; ALMEIDA, L. P.; SOUSA, M. D. B.; BUFFO, M. M.; VELOSO, I. I. K.; SILVA, K. C. R.; CRUZ, A. J. G.; BADINO, A. Ethanol removal by stripping with CO_2 reduced-size bubbles: mechanical and thermodynamic entrainments. *Chemical Engineering and Processing - Process Intensification*, v. 205, p. 110011, 2024. DOI: https://doi.org/10.1016/j.cep.2024.110011.

PEREIRA, R. D.; RODRIGUES, K. C. S.; SONEGO, J. L. S.; CRUZ, A. J. G.; BADINO, A. C. A new methodology to calculate the ethanol fermentation efficiency at bench and industrial scales. *Industrial & Engineering Chemistry Research*, v. 57, p. 16182–16191, 2018. DOI: https://doi.org/10.1021/acs.iecr.8b03943.

PHILIPPIDIS, G. P.; SPINDLER, D. D.; WYMAN, C. E. Mathematical modeling of cellulose conversion to ethanol by the simultaneous saccharification and fermentation process. *Applied Biochemistry and Biotechnology*, v. 34–35, p. 543–556, 1992. DOI: https://doi.org/10.1007/BF02920577.

POLAKOVIČ, M.; BRYJAK, J. Modelling of potato starch saccharification by an *Aspergillus niger* glucoamylase. *Biochemical Engineering Journal*, v. 18, p. 57–63, 2004. DOI: https://doi.org/10.1016/S1369-703X(03)00164-5.

PERRY, R. H.; GREEN, D. W.; MALONEY, J. O. *Perry's chemical engineers' handbook*. 7. ed. New York: McGraw-Hill, 1997.

PRASAD, S.; SINGH, A.; JOSHI, H. C. Ethanol as an alternative fuel from agricultural, industrial and urban residues. *Resources, Conservation and Recycling*, v. 50, p. 1–39, 2007. DOI: https://doi.org/10.1016/j.resconrec.2006.05.007.

PRESEČKI, A. V.; BLAŽEVIĆ, Z. F.; VASIĆ-RAČKI, Đ. Complete starch hydrolysis by the synergistic action of amylase and glucoamylase: impact of calcium ions. *Bioprocess and Biosystems Engineering*, v. 36, p. 1555–1562, 2013. DOI: https://doi.org/10.1007/s00449-013-0926-2.

QURESHI, N. Integrated processes for product recovery. In: PANDEY, A. et al. (ed.). *Biorefineries*. Amsterdam: Elsevier, 2014. p. 101–118. DOI: https://doi.org/10.1016/B978-0-444-59498-3.00005-1.

RAMÍREZ, M. B.; FERRARI, M. D.; LAREO, C. Fuel ethanol production from commercial grain sorghum cultivars with different tannin content. *Journal of Cereal Science*, v. 69, p. 125–131, 2016. DOI: https://doi.org/10.1016/j.jcs.2016.02.019.

REID, R. C.; PRAUSNITZ, J. M.; SHERWOOD, T. K. *The properties of gases and liquids*. 4. ed. New York: McGraw-Hill, 1987.

RENEWABLE FUELS ASSOCIATION. *Annual world fuel ethanol production 2022*. Available at: https://ethanolrfa.org/markets-and-statistics/annual-ethanol-production. Accessed on: Apryl 3, 2023.

RENEWABLE FUELS ASSOCIATION. *Annual world fuel ethanol production 2024*. Available at: https://ethanolrfa.org/markets-and-statistics/annual-ethanol-production. Accessed on: July 13, 2025.

RODRIGUES, K. C. S.; VELOSO, I. I. K.; LEMOS, D. A.; CRUZ, A. J. G.; BADINO, A. C. Extractive ethanol fermentation with ethanol recovery by absorption in open and closed systems. *Fermentation*, v. 11, p. 12, 2025. DOI: https://doi.org/10.3390/fermentation11010012.

RODRIGUES, K. C. S.; SONEGO, J. L. S.; BERNARDO, A.; RIBEIRO, M. P. A.; CRUZ, A. J. G.; BADINO, A. C. Real-time monitoring of bioethanol fermentation with industrial musts using mid-infrared spectroscopy. *Industrial & Engineering Chemistry Research*, v. 57, p. 10823–10831, 2018. DOI: https://doi.org/10.1021/acs.iecr.8b01181.

RODRIGUES, K. C. S.; SONEGO, J. L. S.; CRUZ, A. J. G.; BERNARDO, A.; BADINO, A. C. Modeling and simulation of continuous extractive fermentation with CO_2 stripping for bioethanol production. *Chemical Engineering Research and Design*, v. 132, p. 77–88, 2018. DOI: https://doi.org/10.1016/j.cherd.2017.12.024.

SAMANTA, H. S.; RAY, S. K. Separation of ethanol from water by pervaporation using mixed matrix copolymer membranes. *Separation and Purification Technology*, v. 146, p. 176–186, 2015. DOI: https://doi.org/10.1016/j.seppur.2015.03.006.

SÁNCHEZ, Ó. J.; CARDONA, C. A. Trends in biotechnological production of fuel ethanol from different feedstocks. *Bioresource Technology*, v. 99, p. 5270–5295, 2008. DOI: https://doi.org/10.1016/j.biortech.2007.11.013.

SANTOS, M. V.; RODRIGUES, K. C. S.; VELOSO, I. I. K.; BADINO, A. C.; CRUZ, A. J. G. Real-time monitoring of ethanol fermentation using mid-infrared spectroscopy analysis of the gas phase. *Industrial & Engineering Chemistry Research*, v. 61, p. 7225–7234, 2022. DOI: https://doi.org/10.1021/acs.iecr.2c00325.

SHEKHAR, C.; AHMAD, A.; SINGH, D. K. A comprehensive review on bioethanol production from diverse lignocellulosic biomass and its usability in SI engines: recent advances, scientometric analysis, and future perspectives. *Journal of Thermal Analysis and Calorimetry*, 2025. DOI: https://doi.org/10.1007/s10973-025-14391-6.

SHIHADEH, J. K.; HUANG, H.; RAUSCH, K. D.; TUMBLESON, M. E.; SINGH, V. Vacuum stripping of ethanol during high solids fermentation of corn. *Applied Biochemistry and Biotechnology*, v. 173, p. 486–500, 2014. DOI: https://doi.org/10.1007/s12010-014-0855-9.

SHULER, M. L.; KARGI, F. *Bioprocess engineering: basic concepts*. 2. ed. Upper Saddle River, NJ: Prentice Hall, 2002. DOI: https://doi.org/10.1016/0168-3659(92)90106-2.

SI, Z.; SHAN, H.; HU, S.; CAI, D.; QIN, P. Recovery of ethanol via vapor phase by polydimethylsiloxane membrane with excellent performance. *Chemical Engineering Research and Design*, v. 136, p. 324–333, 2018. DOI: https://doi.org/10.1016/j.cherd.2018.06.003.

SILVA, C. R.; ESPERANÇA, M. N.; CRUZ, A. J. G.; MOURA, L. F.; BADINO, A. C. Stripping of ethanol with CO_2 in bubble columns: effects of operating conditions and modeling. *Chemical Engineering Research and Design*, v. 102, p. 150–160, 2015. DOI: https://doi.org/10.1016/j.cherd.2015.06.022.

SILVA, E. H.; LEMOS, D. A.; CRUZ, A. J. G.; BADINO, A. C.; SILVA, R. G.; SONEGO, J. L. S. Bioethanol production using mixtures of sorghum juice and sugarcane molasses: experimental data and kinetic modeling. *Sugar Tech*, v. 26, p. 799–808, 2024. DOI: https://doi.org/10.1007/s12355-024-01393-1.

SMITH, J. M.; VAN NESS, H. C.; ABBOTT, M. M. *Introduction to chemical engineering thermodynamics*. 7. ed. New York: McGraw-Hill, 2005.

SONEGO, J. L. S.; LEMOS, D. A.; CRUZ, A. J. G.; BADINO, A. C. Optimization of fed-batch fermentation with in situ ethanol removal by CO_2 stripping. *Energy & Fuels*, v. 32, p. 954–960, 2018. DOI: https://doi.org/10.1021/acs.energyfuels.7b02979.

SONEGO, J. L. S.; LEMOS, D. A.; PINTO, C. E. M.; CRUZ, A. J. G.; BADINO, A. C. Extractive fed-batch ethanol fermentation with CO_2 stripping in a bubble column bioreactor: experiment and modeling. *Energy & Fuels*, v. 30, p. 748–757, 2016. DOI: https://doi.org/10.1021/acs.energyfuels.5b02320.

SONEGO, J. L. S.; LEMOS, D. A.; RODRIGUEZ, G. Y.; CRUZ, A. J. G.; BADINO, A. C. Extractive batch fermentation with CO_2 stripping for ethanol production in a bubble column bioreactor: experimental and modeling. *Energy & Fuels*, v. 28, 2014.

STAMENKOVIĆ, O. S.; SILIVERU, K.; VELJKOVIĆ, V. B.; BANKOVIĆ-ILIĆ, I. B.; TASIĆ, M. B.; CIAMPITTI, I. A.; ĐALOVIĆ, I. G.; MITROVIĆ, P. M.; SIKORA, V. Š.; PRASAD, P. V. V. Production of biofuels from sorghum. *Renewable and Sustainable Energy Reviews*, v. 124, p. 109769, 2020. DOI: https://doi.org/10.1016/j.rser.2020.109769.

TAVARES, B.; FELIPE, M. das G. de A.; DOS SANTOS, J. C.; PEREIRA, F. M.; GOMES, S. D.; SENE, L. An experimental and modeling approach for ethanol production by

Kluyveromyces marxianus in stirred tank bioreactor using vacuum extraction as a strategy to overcome product inhibition. *Renewable Energy*, v. 131, p. 261–267, 2019. DOI: https://doi.org/10.1016/j.renene.2018.07.030.

TAYLOR, F.; KURANTZ, M. J.; GOLDBERG, N.; CRAIG, J. C. Kinetics of continuous fermentation and stripping of ethanol. *Biotechnology Letters*, v. 20, p. 67–72, 1998. DOI: https://doi.org/10.1023/A:1005339415979.

TAYLOR, F.; KURANTZ, M. J.; GOLDBERG, N.; CRAIG, J. C. Control of packed column fouling in the continuous fermentation and stripping of ethanol. *Biotechnology and Bioengineering*, v. 51, p. 33–39, 1996. DOI: https://doi.org/10.1002/(SICI)1097-0290(19960705)51:1<33::AID-BIT4>3.0.CO;2-1.

TAYLOR, F.; KURANTZ, M. J.; GOLDBERG, N.; CRAIG, J. C. Continuous fermentation and stripping of ethanol. *Biotechnology Progress*, v. 11, p. 693–698, 1995. DOI: https://doi.org/10.1021/bp00036a014.

TAYLOR, F.; MARQUEZ, M. A.; JOHNSTON, D. B.; GOLDBERG, N. M.; HICKS, K. B. Continuous high-solids corn liquefaction and fermentation with stripping of ethanol. *Bioresource Technology*, v. 101, p. 4403–4408, 2010. DOI: https://doi.org/10.1016/j.biortech.2010.01.092.

TRUONG, K. N.; BLACKBURN, J. W. The stripping of organic chemicals in biological treatment processes. *Environmental Progress*, v. 3, p. 143–152, 1984. DOI: https://doi.org/10.1002/ep.670030304.

UNREAN, P.; KHAJEERAM, S.; LAOTENG, K. Systematic optimization of fed-batch simultaneous saccharification and fermentation at high-solid loading based on enzymatic hydrolysis and dynamic metabolic modeling of *Saccharomyces cerevisiae*. *Applied Microbiology and Biotechnology*, v. 100, p. 2459–2470, 2016. DOI: https://doi.org/10.1007/s00253-015-7173-1.

U.S. DEPARTMENT OF AGRICULTURE. United States sorghum area, yield and production. 2024. Available at: https://ipad.fas.usda.gov/countrysummary/Default.aspx?id=US&crop=Sorghum. Accessed on: January 8, 2025.

U.S. DEPARTMENT OF ENERGY. Alternative fuels data center. 2024. Available at: https://afdc.energy.gov/data. Accessed on: July 13, 2025.

VAN DER BRUGGEN, B.; LUIS, P. Pervaporation as a tool in chemical engineering: a new era? *Current Opinion in Chemical Engineering*, v. 4, p. 47–53, 2014. DOI: https://doi.org/10.1016/j.coche.2014.01.005.

VAN HECKE, W.; KAUR, G.; DE WEVER, H. Advances in in-situ product recovery (ISPR) in whole cell biotechnology during the last decade. *Biotechnology Advances*, v. 32, p. 1245–1255, 2014. DOI: https://doi.org/10.1016/j.biotechadv.2014.07.003.

VARIZE, C. S.; BÜCKER, A.; LOPES, L. D.; CHRISTOFOLETI-FURLAN, R. M.; RAPOSO, M. S.; BASSO, L. C.; et al. Increasing ethanol tolerance and ethanol production in an industrial fuel ethanol *Saccharomyces cerevisiae* strain. *Fermentation*, v. 8, p. 470, 2022. DOI: https://doi.org/10.3390/fermentation8100470.

VELOSO, I. I. K.; CAMPOS, B. G.; ESPERANÇA, M. N.; CRUZ, A. J. G.; BADINO, A. C. Thermal analysis of conventional and extractive fed-batch ethanol fermentation at different temperatures. *Bioenergy Research*, v. 16, p. 2093–2104, 2023. DOI: https://doi.org/10.1007/s12155-023-10586-7.

VELOSO, I. I. K.; RODRIGUES, K. C. S.; ESPERANÇA, M. N.; BATISTA, G.; CRUZ, A. J. G.; BADINO, A. C. A more accurate modeling for fed-batch ethanol fermentation with high cell density. *Biochemical Engineering Journal*, v. 193, p. 108855, 2023. DOI: https://doi.org/10.1016/j.bej.2023.108855.

VELOSO, I. I. K.; RODRIGUES, K. C. S.; SONEGO, J. L. S.; CRUZ, A. J. G.; BADINO, A. C. Fed-batch ethanol fermentation at low temperature as a way to obtain highly concentrated alcoholic wines: modeling and optimization. *Biochemical Engineering Journal*, v. 141, p. 60–70, 2019. DOI: https://doi.org/10.1016/j.bej.2018.10.005.

VOLODKO, O. I.; IVANOVA, T. S.; KULICHKOVA, G. I.; LUKASHEVYCH, K. M.; BLUME, Y. B.; TSYGANKOV, S. P. Fermentation of sweet sorghum syrup under reduced pressure for bioethanol production. *Open Agriculture Journal*, v. 14, p. 235–245, 2020. DOI: https://doi.org/10.2174/1874331502014010235.

DE VRIJE, T.; BUDDE, M.; VAN DER WAL, H.; CLAASSEN, P. A. M.; LÓPEZ-CONTRERAS, A. M. “In situ” removal of isopropanol, butanol and ethanol from fermentation broth by gas stripping. *Bioresource Technology*, v. 137, p. 153–159, 2013. DOI: https://doi.org/10.1016/j.biortech.2013.03.098.

WANG, J.; ZENG, A.; LIU, Z.; YUAN, X. Kinetics of glucoamylase hydrolysis of corn starch. *Journal of Chemical Technology and Biotechnology*, v. 81, p. 727–729, 2006. DOI: https://doi.org/10.1002/jctb.1435.

WAN, Z.; HU, H.; LIU, K.; QIAO, Y.; GUO, F.; WANG, C.; XIN, F.; ZHANG, W.; JIAN, M. Engineering industrial yeast for improved tolerance and robustness. *Critical Reviews in Biotechnology*, v. 44, p. 1461–1477, 2024. DOI: https://doi.org/10.1080/07388551.2024.2326677.

WEI, W.; XIA, S.; LIU, G.; DONG, X.; JIN, W.; XU, N. Effects of polydimethylsiloxane (PDMS) molecular weight on performance of PDMS/ceramic composite membranes. *Journal of Membrane Science*, v. 375, p. 334–344, 2011. DOI: https://doi.org/10.1016/j.memsci.2011.03.059.

WEISS, T.; BARRETTO, R.; CHEN, G.; HONG, S.; LI, Y.; ZHENG, Y.; SUN, X. S.; WANG, D. Blue, red and white maize as a sustainable resource for production of distilled spirit. *Journal of Agricultural and Food Research*, v. 14, p. 100770, 2023. DOI: https://doi.org/10.1016/j.jafr.2023.100770.

WEISS, T.; HONG, S.; XIAO, R.; WU, X.; LI, Y.; TILLEY, M.; WANG, D. Assessment of granular starch hydrolysis enzyme on ethanol yield from partially swollen sorghum starch and analysis of extracted protein properties. *Journal of Agricultural and Food Research*, v. 19, p. 101621, 2025. DOI: https://doi.org/10.1016/j.jafr.2024.101621.

WEISS, T.; ZHAO, J.; HU, R.; LIU, M.; LI, Y.; ZHENG, Y.; SMITH, G.; WANG, D. Production of distilled spirits using grain sorghum through liquid fermentation. *Journal of Agricultural and Food Research*, v. 9, p. 100314, 2022. DOI: https://doi.org/10.1016/j.jafr.2022.100314.

WEILNHAMMER, C.; BLASS, E. Continuous fermentation with product recovery by in-situ extraction. *Chemical Engineering & Technology*, v. 17, p. 365–373, 1994. DOI: https://doi.org/10.1002/ceat.270170602.

WHEALS, A. E.; BASSO, L. C.; ALVES, D. M.; AMORIM, H. V. Fuel ethanol after 25 years. *Trends in Biotechnology*, v. 17, p. 482–487, 1999. DOI: https://doi.org/10.1016/S0167-7799(99)01384-0.

XIANGLI, F.; CHEN, Y.; JIN, W.; XU, N. Polydimethylsiloxane (PDMS)/ceramic composite membrane with high flux for pervaporation of ethanol–water mixtures. *Industrial &*

Engineering Chemistry Research, v. 46, p. 2224–2230, 2007. DOI: https://doi.org/10.1021/ie0610290.

XUE, C.; DU, G. Q.; SUN, J. X.; CHEN, L. J.; GAO, S. S.; YU, M. L.; YANG, S.-T.; BAI, F.-W. Characterization of gas stripping and its integration with acetone–butanol–ethanol fermentation for high-efficient butanol production and recovery. *Biochemical Engineering Journal*, v. 83, p. 55–61, 2014a. DOI: https://doi.org/10.1016/j.bej.2013.12.003.

XUE, C.; WANG, Z.-X.; DU, G.-Q.; FAN, L.-H.; MU, Y.; REN, J.-G.; BAI, F.-W. Integration of ethanol removal using carbon nanotube (CNT)-mixed membrane and ethanol fermentation by self-flocculating yeast for antifouling ethanol recovery. *Process Biochemistry*, v. 51, p. 1140–1146, 2016. DOI: https://doi.org/10.1016/j.procbio.2016.05.030.

XUE, C.; ZHAO, J.-B.; CHEN, L.-J.; BAI, F.-W.; YANG, S.-T.; SUN, J.-X. Integrated butanol recovery for an advanced biofuel: current state and prospects. *Applied Microbiology and Biotechnology*, v. 98, p. 3463–3474, 2014b. DOI: https://doi.org/10.1007/s00253-014-5561-6.

YANG, J.; TAVAZOIE, S. Regulatory and evolutionary adaptation of yeast to acute lethal ethanol stress. *PLoS ONE*, v. 15, e0239528, 2020. DOI: https://doi.org/10.1371/journal.pone.0239528.

YEBOAH, O.; SHAIK, S. The influence of climate change on the demand for ethanol. *Renewable Energy*, v. 164, p. 1559–1565, 2021. DOI: https://doi.org/10.1016/j.renene.2020.10.139.

ZENTOU, H.; ABIDIN, Z.; YUNUS, R.; AWANG BIAK, D.; KORELSKIY, D. Overview of alternative ethanol removal techniques for enhancing bioethanol recovery from fermentation broth. *Processes*, v. 7, p. 458, 2019. DOI: https://doi.org/10.3390/pr7070458.

ZHANG, J.; CHEN, J. J. J.; ZHOU, N. Characteristics of jet droplet produced by bubble bursting on the free liquid surface. *Chemical Engineering Science*, v. 68, p. 151–156, 2012. DOI: https://doi.org/10.1016/j.ces.2011.09.019.